THESIS / THÈSE

DOCTOR OF SCIENCES

Investigation of the replication and the role of (p)ppGpp in the pathogen Brucella abortus

VAN der HENST, Mathilde

Award date:
2019

Awarding institution:
University of Namur

Investigation of the replication and the role of (p)ppGpp in the pathogen *Brucella abortus*

Dissertation presented by Mathilde Van der Henst

in preparation of the degree of PhD in Sciences

Jury members

Prof. Justine Collier (Université de Lausanne, Suisse)

Prof. Laurence Van Melderen (Université de Bruxelles, Belgique)

Prof. Stephan Köhler (Institut de Recherche en Infectiologie de Montpellier, France)

Prof. Régis Hallez (Université de Namur, Belgique)

Prof. Xavier De Bolle (Université de Namur, Belgique)

2019

Remerciements

Je voudrais tout d'abord remercier les membres de mon jury, Pr. Justine Collier, Pr. Laurence Van Melderen, Pr. Stephan Köhler et le Pr. Régis Hallez, pour avoir accepté de faire partie de mon jury de thèse, d'avoir donné de leur temps pour la lecture de ce manuscrit, ainsi que pour les discussions, commentaires et conseils qui ont contribué à l'amélioration de cette thèse. Également, un grand merci à eux d'avoir fait le déplacement jusqu'à Namur ! Merci aux membres de mon comité d'accompagnement, Pr. Geraldine Laloux et Pr. Sébastien Rigali, également pour leur temps consacré et leurs commentaires à propos de ce projet.

Je voudrais ensuite dire un grand merci à mon promoteur, Xavier De Bolle, qui, en plus de m'avoir donné l'envie et l'opportunité de réaliser cette thèse, a toujours été disponible malgré un emploi du temps souvent surbooké (ou même en vacance...)! Merci pour toutes ces heures de discussion passées, ton état d'esprit toujours positif quoi qu'il arrive, et ta passion pour la science, que tu arrives à transmettre aux autres d'une manière incroyable.

Merci aux membres de la Xa Team, actuels et anciens, qui ont permis d'avoir une ambiance particulièrement joyeuse durant ces années... non une ambiance de folie en fait ! Merci à Vicky, ma biche, pour ton soutien, tes conseils, ton franc-parler, tu es une personne plus que sincère (tout le monde le sait ça :p). Merci à Katystrophe, désolé ce surnom est lourd, mais il t'est tellement bien adapté...Merci pour ton soutien aussi, toutes nos discussions sur le chemin du retour après labo... ah le bon vieux temps ! Merci à Pierre, Agnès et Caro pour tous ces délires passés dans le bureau, l'ambiance n'aurait pas été pareil sans vous ! (mes fesses non plus d'ailleurs, avec tout votre chocolat !). Merci pour la pêche aux moules Aurore, cela me restera gravé à jamais ! Qui l'aurait cru, on s'est connues au cercle et on se retrouve ensemble à faire une thèse... et du trampoline ! Manque plus qu'on se marie, et la boucle sera bouclée (faudra juste s'occuper de Cédric...). Plein de bonheur à vous deux ! Merci à Angy d'être également toujours disponible pour discuter et échanger, j'espère que tu garderas un bon souvenir de ton expérience chez les belges ! Merci Keke pour ta bonne humeur et ton humour sans limite. On te voit moins souvent, mais rien n'a changé lorsque tu es parmi nous et ça c'est top ! Merci Fra pour toutes nos discussions, et bagarres surtout (qui aime bien châtie bien !). Merci à Séverin pour toutes nos discussions, et de m'avoir mise sur la voie sacrée du (p)ppGpp. Merci à tous les habitués de la beer hour, ces petits (grands ?) moments du vendredi après-midi vont vraiment me manquer ! Merci aux techniciens, sans qui le labo

tournerait beaucoup moins bien, voire pas du tout en fait ! Merci à tous les autres membres d'URBM (anciens et actuels), et de GeMo, la liste est grande, ces années passées parmi vous étaient géniales ! Finalement, on peut résumer tout ça en disant que j'ai trouvé des collègues en entrant dans ce labo, et que j'en suis repartie avec des potes que je compte bien revoir et re-revoir dans le futur !

Un énorme merci à toi Popo, pour ton amitié, pour avoir toujours été présent pour moi et de m'avoir soutenue (et coachée !). Merci pour ton humour et ta joie de vivre, des comme toi, il y en a pas deux sur terre 👌 ! Nos beer hours avec Consti resteront gravées dans ma mémoire, quel trio infernal ! Je n'oublierai jamais non plus la rencontre avec mes *******, Eme, Doudou et Mel. Malgré les distances rien n'a changé, on peut toujours compter les unes sur les autres, et ça, ça n'a pas de prix ! Vivement la prochaine guindaille ! Et qui sait, peut-être qu'un jour on retravaillera ensemble ???

Merci à ma poulette de m'avoir supporté depuis maintenant presque 14ans ! En ce qui concerne les vraies amitiés, la distance ne change rien, et on en est une belle preuve !

Finalement, un immense merci à toute ma famille, Maman, Papa, Claude, Charly, Marie, Parrain et Marie-Claude, qui m'ont toujours soutenue quoi qu'il arrive et sur qui j'ai toujours pu compter. Merci Maman pour ta confiance, tous tes conseils, et de m'aider comme tu l'as toujours fait. Papa, de m'avoir appuyé et aidé pendant ces études. Qu'est-ce que je ferais sans mon Charly, tu es un frère en or. Merci d'être toujours là pour ta sœur unique et préférée, chérie adorée :D. Tous les deux, on sait qu'on pourra toujours compter l'un sur l'autre, car oui c'est un lien indestructible qu'il y a entre nous ! Merci à mes beaux-parents qui m'ont accueillie tout naturellement dans la famille, et qui m'ont également toujours soutenue.

Un merci tout particulier à mes anges gardiens, Pépé et Baby, qui ont été un modèle pour moi et le resteront pour toujours, je suis tellement fière d'avoir eu des grands-parents comme vous.

Enfin et surtout je voudrais remercier Seb, mon Nouni, qui m'a toujours motivée et supportée, (surtout pendant la rédaction :D), pendant plus de 12 années maintenant, quel courage :p ! Merci pour ton aide, et d'être ce que tu es, tu es le meilleur à mes yeux ☺.

“The most exciting phrase to hear in science,
the one that heralds new discoveries,
is not 'Eureka!' but 'That's funny...”
Isaac Asimov

Table of content

List of abbreviations

aBCV: autophagic Brucella Containing Vacuole
CFU: Colony Forming Unit
ChIP-seq: Chromatin Immunoprecipitation sequencing
ChrI: Chromosome I
ChrII: Chromosome II
COG: Conserved Oligomeric Golgi
Cori: replication origin of *C. crescentus* chromosome
dsDNA: double strand DNA
eBCV: endosomal Brucella Containing Vacuole
EEA1: Early Endosome Antigen 1
ER : Endoplasmic Reticulum
FACS: Fluorescence Activated Cell Sorting
LAMP1 : Lysosomal Associated Membrane Protein 1
MOI : Multiplicity Of Infection
OD: Optical Density
OMPs : Outer Membrane Proteins
oriC : replication origin of *E. coli* chromosome
oriI : origin of chromosome I in *B. abortus*
oriII: origin of chromosome II in *B. abortus*
p.i: post-infection
ppi: inorganic phosphate
(p)ppGpp: Guanosine pentaphosphate/tetraphosphate
rBCV: replicative Brucella Containing Vacuole
RNAP: RNA polymerase II
ssDNA: single strand DNA
T4SS: Type 4 Secretion System
ter: terminal region
TRSE: Texas Red Succinimidyl Ester

Summary

Brucella spp. are facultative intracellular bacteria responsible for Brucellosis, a worldwide anthropozoonosis. This neglected disease is found in a variety of mammals and humans are considered as accidental hosts. The genome of *B. abortus* is divided into two chromosomes, and several tools were developed to monitor the state of chromosomes replication throughout the cell cycle at the single cell level.

The study of chromosomes replication showed first that the chromosome I starts its replication before the chromosome II, indicating the existence of coordinated mechanisms regulating the initiation of replication of both chromosomes. Secondly, these investigations revealed that *B. abortus* presents a biphasic infection process, with a first non-proliferation phase characterized by a G1 arrest, and a second phase in which bacteria restart their cell cycle, and actively proliferate. Moreover, G1 bacteria were shown to be preferentially internalized inside host cells, and thus represented the infectious form of the pathogen. These results demonstrated that the cell cycle of *B. abortus* is intimately linked to its infection strategy.

Here, we investigated mechanisms potentially involved in the control of the cell cycle, especially in chromosomes replication regulation, focusing our researches on conserved actors already known to regulate DNA replication in *Escherichia coli* and *Caulobacter crescentus.* We notably found that the alarmone (p)ppGpp plays a role in this control. Indeed, the overproduction of (p)ppGpp in *B. abortus* led to growth and replication defects, reflecting a general cell cycle delay. The impact observed on replication could be explained, in part, by the alteration of the level of the replication initiator DnaA upon (p)ppGpp overproduction. Finally, we showed that (p)ppGpp is important for the establishment of a successful infection process, since mutants which cannot produce (p)ppGpp, or which are depleted for this alarmone were strongly attenuated during the infection.

Introduction

Introduction

I. Chapter 1: *Brucella*

I.1. Brucellosis

Brucellosis is a worldwide anthropozoonosis affecting many different mammals, including cattle, goats, sheep, swines, dogs as well as marine mammals. This infectious disease is also found in human, which is an accidental host, and is often called Malta fever or undulant fever. The designation "Malta fever" comes from the first discovery of the responsible pathogenic germ in Malta. *Micrococcus melitensis* was isolated for the first time in 1887 by David Bruce, from the spleen of a sick soldier in Malta. The bacterial genus was later renamed *Brucella* in honor of David Bruce. Symptoms related to the disease are diversified in animals, comprising severe arthritis, infertility in males and abortion in pregnant females. In humans the disease is characterized by different pathological manifestations and evolves by successive phases resulting in diverse symptoms including headache, weakness and undulant fever. In the long term and without treatment, infection leads to chronicity and more severe symptoms such as arthritis, muscular pain, endocarditis and can have a fatal outcome. In human, the disease can be eliminated with rifampicin and doxycycline antibiotic treatment (Moreno and Moriyon, 2006). Infection can be transmitted to humans through several ways, such as the ingestion of unpasteurized dairy products obtained from infected animals, or the inhalation of aerosols containing bacteria when abortion occurs for example (Figure 1). However, human-to-human transmission has not been reported whereas horizontal transmission widely occurs between animals through close contact and exchange of secretions (Moreno and Moriyon, 2006).

First preventive actions against brucellosis were milk pasteurization and systematic elimination of infected flocks when infection was diagnosed in order to eradicate the disease (Moreno and Moriyon, 2002). This implies important economic losses, especially in developing countries where the disease is still endemic. So far, no efficient human vaccine has been found. Some bovine vaccines, like *B. abortus* S19 and RB51 or *B. melitensis* Rev1 have been reported to be efficient if administered outside pregnancy periods, in countries where pregnancy is synchronized along the year. However, there are many countries in which pregnancy is not synchronized, making vaccination hazardous. *Brucella spp*. are considered as

class III bioterrorism agents because of their impact on both public health and economy (Moreno and Moriyon, 2002).

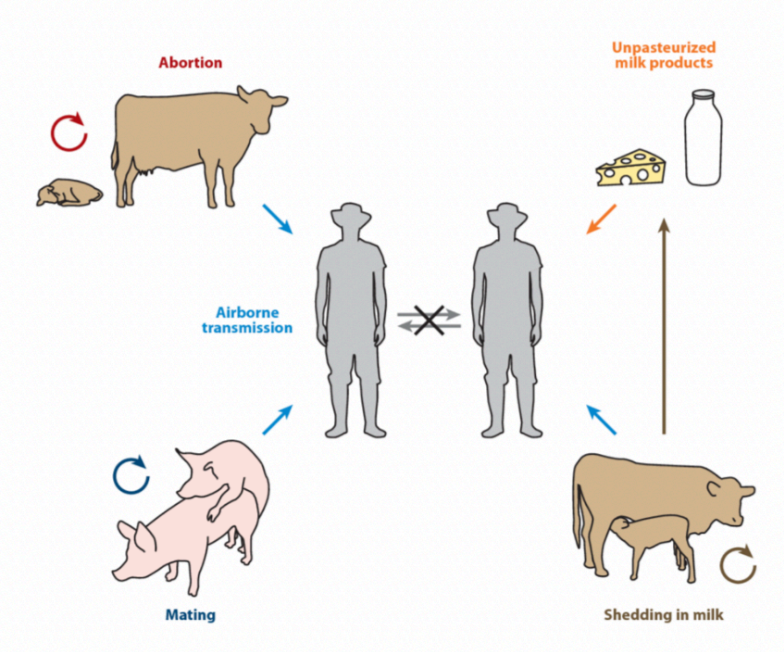

Figure 1: Transmission of brucellosis. *Brucella* can spread by different ways including aerosols, ingestion of unpasteurized milk products, and mating in animals. No case of transmission between humans has been reported so far. From Atluri *et al*., 2011.

I.2. The *Brucella* genus

Brucella spp. are intracellular bacteria responsible for Brucellosis. Another classification of the pathogen has emerged as "facultative extracellular, intracellular pathogen" (Moreno and Moriyon, 2006). Indeed, the term of intracellular pathogen would imply that bacteria need hosts to survive and multiply, however *Brucella* can grow in extracellular environments such as culture medium. Accordingly, the mostly intracellular nature of *B. abortus* means more that host cell environment provides favorable conditions for replication and expansion making it a preferential niche (Moreno and Moriyon, 2006).

This Gram-negative pathogen is non-motile (with an exception for *B. vulpis*) and presents a coccobacilli morphology from 0.5 to 1.5 µm long (Moreno and Moriyon, 2006; Al Dahouk *et al*., 2017). The genus *Brucella* is commonly divided into different species according to their tropism for host organism. For decades, six "classical" species were counted in the *Brucella* genus, *i.e. B. abortus, B. melitensis, B. suis, B. canis*, *B. neotomae* and *B. ovis* where the first three are known to be pathogenic for humans. However, with the improvement of detection methods, several "new" species have been found to belong to the genus *Brucella*,

such as *B. microti, B. ceti, B. pinnipedialis, B. papionis* and *B. vulpis, B. inopinata.* More recently, additional motile *Brucella* strains have been isolated from African bullfrogs (Al Dahouk *et al*., 2017). Despite host preference and several phenotypic variations, *Brucella* species are closely related at the genetic level, displaying more than 98 % of sequence identity between strains of different species (Mayer-Scholl *et al*., 2010).

I.3. *Brucella* is an α-proteobacterium

Brucella belongs to the α-proteobacteria class whose members are highly diversified. Indeed, this group ranges from soil bacteria like the plant pathogen *Agrobacterium* and plant symbiont *Rhizobium* to the intracellular pathogens Rickettsiales, or the non-pathogenic free-living *Caulobacter crescentus*, an aquatic bacterium. Despite these different lifestyles, several α-proteobacteria present common features, showing a unipolar growth (for Rhizobiales) and asymmetric division, sometimes leading to functional asymmetry (Brown *et al*., 2012). For example, *C. crescentus*, used as a model of bacterial differentiation, presents a morphologically and functional asymmetry since cell division generates two distinct daughter cells having different functional properties. Indeed, each division gives a motile non-replicating flagellated cell in the one hand and secondly a sessile stalked cell displaying an appendage with adherent properties (Curtis *et al*., 2010) (Figure 2). The flagellated cell named swarmer cell is able to find a suitable niche to differentiate into the stalked replicative-cell and initiate a new cell cycle. This adaptation in lifestyle allows the swarmer bacteria to explore their environment until they reach an appropriate environment for growth and colonization (Skerker and Laub, 2004).

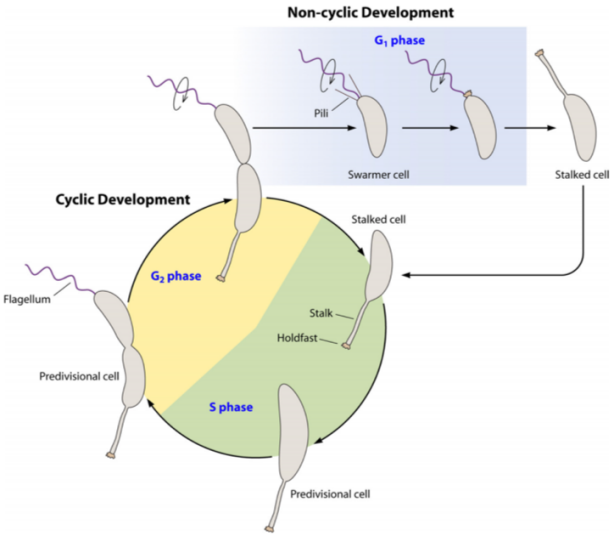

Figure 2: Cell cycle of *Caulobacter crescentus*. After cytokinesis, *C. crescentus* gives two distinct daughter cells, a non-motile stalked cell able to directly initiate DNA replication and a new cell cycle, and a motile swarmer cell, presenting flagellum and pili, which needs to differentiate into a stalked cell prior to initiating a new cell cycle.

I.4. The genome of *Brucella*

Brucella spp. is part of the 10% of bacterial species having a bipartite genome characterized by a chromosome I (ChrI) of 2.1 Mb, a chromosome II (ChrII) of 1.15 Mb, and the absence of plasmids in natural strains (Michaux-Charachon et al., 1993; Jumas-Bilak, 1998). An exception for *B. suis* biovar 3 has to be mentioned since this strain presents only one large chromosome of 3.1 Mb (Jumas-Bilak, 1998). The genomes of the different *Brucella* species are closely related since a genomic microarray study revealed that on 3.198 ORFs analysed from *B. melitensis*, more than 3.110 were present in the other *Brucella* strains (Rajashekara *et al*., 2004).

ChrII is probably the result of an ancestral plasmid domestication. Indeed, the ChrII contains the plasmidic replication and segregation system *repABC* which is typically found in plasmids that are widely distributed among Rhizobiales (Cevallos *et al*., 2008). Moreover, a recent Tn-seq study on *B. abortus* reveals a difference in essential genes distribution between both chromosomes (Sternon *et al*., 2018). Indeed, 19% of the genes present on the ChrI are essential for the growth on rich culture medium plates while the ChrII carries only 5% of essential genes. Finally, a study of chromosome replication and segregation highlighted important differences between ChrI and ChrII. The replication and segregation of the origin of ChrI occur before the corresponding events for ChrII origin indicating the existence of a process that allows the temporal coordination of these events. The replication origin of ChrI

displays an old pole localization before becoming bipolar after the initiation of the replication and segregation process, whereas the replication origin of ChrII does not show clear polar attachment (Deghelt *et al*., 2014), which would be expected for plasmids rather than chromosomes. Taken together, all these evidences support the hypothesis that the ChrII may originate from a megaplasmid acquired during evolution.

I.5. *Brucella* infection and trafficking

Brucella can infect mammalian hosts through oral route and aerosol. Once inside its host, bacteria can disseminate to specific tissues or organs for which *B. abortus* shows preferential tropism such as the placenta in pregnant females or the reproductive tract. This propagation is mediated by crossing the mucosal epithelium barrier and by entering and surviving inside professional and non-professional phagocytic cells, including macrophages and dendritic cells. In this context, different *in vitro* models for the study of host cell infection and trafficking have been used such as RAW 264.7 mouse macrophages, THP-1 human macrophages or HeLa epithelial cells. Once internalized in the mammalian cells, *B. abortus* resides in a vacuole named BCV for *Brucella* Containing Vacuole. This vacuole first acquires early trafficking markers such as Rab5 and EEA-1 by interacting with the endosomal pathway and is therefore named eBCV. This vacuole then maturates and rapidly acquires markers of late endosomal traffic such as the Lysosomal Associated Membrane Protein 1 (Lamp1). A fraction of the bacteria is able to avoid lysosomal degradation by preventing the fusion of the BCV with lysosomes, containing active hydrolases such as cathepsin D, although transient interactions between both compartments have been reported (Celli *et al*., 2003; Starr *et al*., 2008). Acidification of the BCV is required for the success of the intracellular trafficking (Porte *et al*., 1999) and it also triggers the expression of the *virB* virulence factor (Starr *et al*., 2008; Boschiroli *et al*., 2002). The *virB* operon, which is conserved among *Brucella* species, codes for a type IV secretion system (T4SS) homologous to the well described VirB system found in *A. tumefaciens*. The expression of *virB* genes constitutes a crucial step for the *Brucella* trafficking to a compartment derived from the endoplasmic reticulum (ER) where bacteria replicate and establish the proliferation niche therefore named rBCV. Indeed, a deletion mutant for *virB* cannot reach this ER-derived compartment and stays blocked in Lamp1-positive compartment (Boschiroli *et al*., 2002; Sedzicki *et al*., 2018). Some effectors secreted by the VirB system have been identified such as BspB which can interact with the conserved oligomeric Golgi (COG)

complex modifying the Golgi vesicles traffic and allowing the formation of the rBCV (Miller *et al*., 2017). Interestingly, bacterial growth is initiated in eBCVs while daughter cells are only detected in rBCVs, consistent with the initiation of growth of the *virB* mutant, which never generate daughter cells, showing that trafficking and cell cycle progression are intimately connected (Deghelt *et al*., 2014).

I.6. Cell cycle and virulence

The *B. abortus* intracellular trafficking can be separated in two steps that are well illustrated with a CFUs experiment: a first phase characterized by a constant CFUs number where bacteria reside in the BCV, and a second one showing an exponential increase of CFUs number over time, matching with the establishment of the replicative niche in the ER-derived compartment. Interestingly, during the first step of infection, bacteria do not present any growth (shown by TRSE labelling) and are blocked in the G1 phase of the cell cycle (shown by highlighting *oriI*, the replication origin of ChrI) reflecting the inability of bacteria to proliferate (Figure 3). Moreover, it was shown that G1 bacteria are more internalized, and thus, are more infectious than S or G2 bacteria (Figure 3). Indeed, since classical phagocytosis is expected to uptake bacteria at any stage of their cell cycle, the finding that G1 bacteria are internalized more efficiently suggests that they present feature(s) favoring their uptake, and thus that bacteria somehow control their invasion of the host cell. The duration of the non-proliferative phase differs according to the host cells model used ranging from 4 hours to 8 hours respectively for RAW 264.7 macrophages and HeLa epithelial cells. Then, bacteria resume their growth and start chromosomes replication just prior to the transition into rBCV, when they are still in Lamp1-positive compartments (Deghelt *et al*., 2014).

The non-proliferative phase observed at the beginning of the infection and the mechanisms involved in the cell cycle arrest remain to be elucidated. This global cell cycle arrest could represent a widespread strategy shared by pathogenic bacteria to face intracellular stresses such as oxydative/nitrosative stresses, diffusion sensing, acidic stress and/or nutrient limitation.

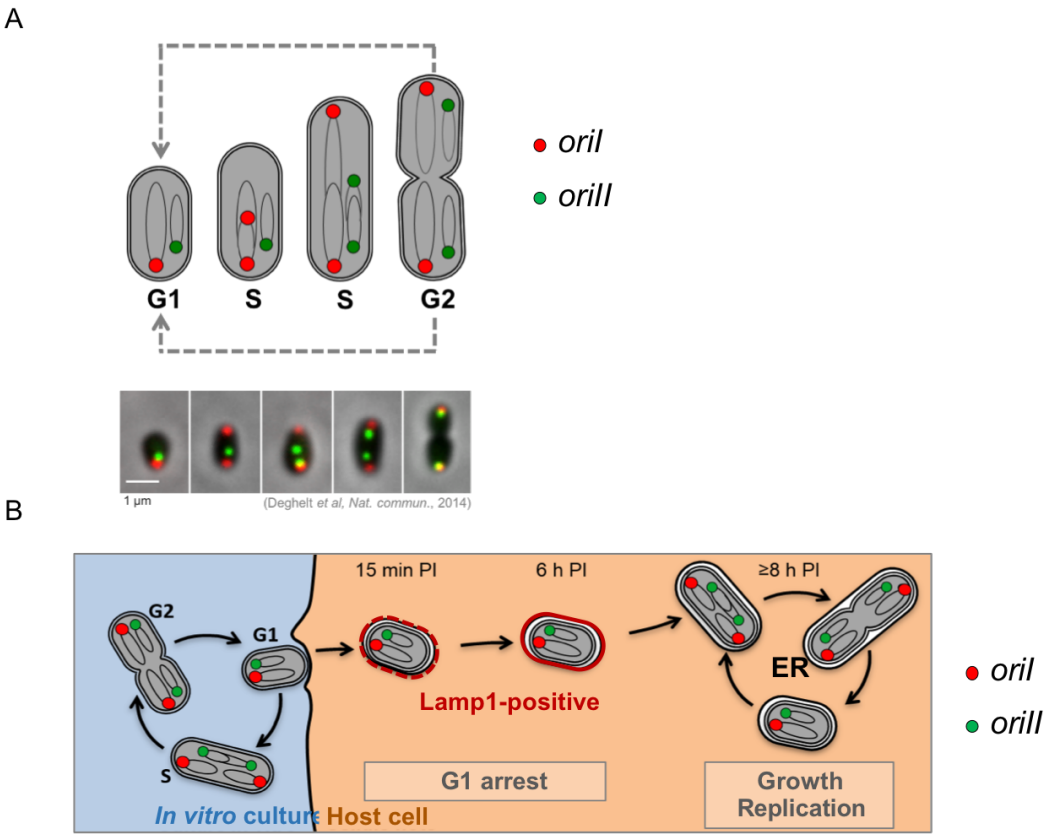

Figure 3: Cell cycle monitoring and infection of *Brucella abortus*. Bacteria expressing *mcherry-parB* and *yfp-repB* present only one focus of both fluorophores during the G1 phase, when chromosome replication has not started. Once the replication of chromosome I has started (S phase), two mCherry fluorescent foci are observed, resulting from the segregation of the duplicated origins. This event is followed by the replication of the chromosome II corresponding to the presence of two fluorescent YFP foci (A). In rich culture medium, the G1 bacteria represent approximately 25% of the population, however at 15 minutes post infection, this percentage increases to approximately 80%, indicating that G1 bacteria enter better than the other cells. After the entry, the vacuole containing *B. abortus* acquires successively early endosomal markers and then, late endosomal markers (Lamp1). Bacteria stay in G1 and present no growth during approximately 6 hours in HeLa cells. Bacteria then restart DNA replication and growth and reach the ER in order to proliferate extensively (B).

II. Chapter 2: Cell cycle in bacteria and regulation

Growth, DNA replication and cell division, which can be defined as cell cycle, are processes shared by all living cells whether they are eukaryotes or prokaryotes. However, the order in which these processes take place are relatively different in these two types of organisms. While the eukaryotic cell cycle phases are clearly divided temporally with the presence of check points between each step, the different phases of the cell cycle in prokaryotes can overlap during the time. Nevertheless, all bacteria have to coordinate growth, DNA replication and division in order to maintain the cell integrity and the correct inheritance of genome. Initially, the bacterial cell cycle phases were named B, C and D, corresponding to the period from cell birth to initiation of DNA synthesis (B phase), the period of DNA replication (C phase), and the period from DNA synthesis completion to cell division (D phase) (Figure 4). In fast-growing species, such as *Escherichia coli,* the B phase is absent and successive cell cycles can overlap over the time leading to several DNA replication initiation events before cell division completion. Thus, the time used to generate a new cell is shorter than the time used for one round of DNA replication. The cell cycle of slow-growing bacteria contains only one complete replication event before division. Subsequently, each cell cycle contains one B, one C and one D period. By extension, as compared with eukaryotic cells, these three phases are also named G1, S and G2 phases, respectively corresponding to the B, C and D phases.

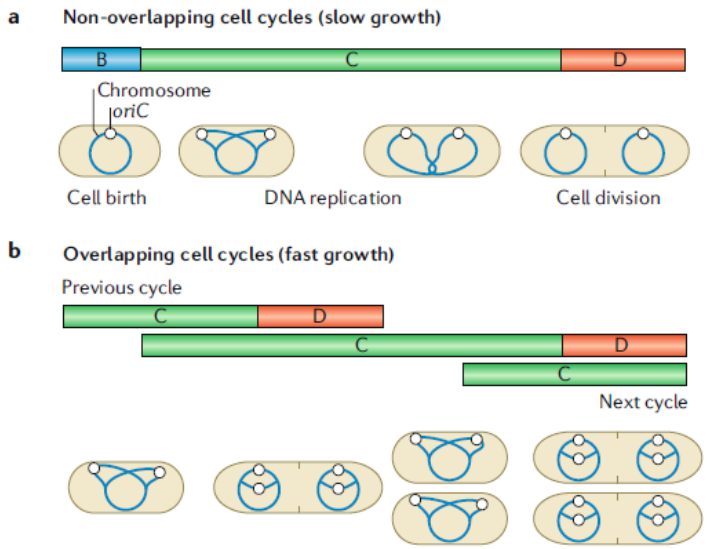

Figure 4: Cell cycle steps in slow growing bacteria compared to fast growing bacteria. The B period is characterized by the absence of chromosomal replication. The C period starts when bacteria have initiated their DNA replication and the D period begins when chromosome replication is finished and division occurs. Modified from Reyes-Lamothe and Sherratt, 2019

Whether slow-growing or fast-growing species, bacteria have to ensure that the correct number of replication initiation events occurs per cell cycle. This control is principally mediated through the regulation of the replication initiator DnaA which is highly conserved among bacteria. DnaA binds replication origin on chromosomes and induces the recruitment of other proteins involved in the replication process (Hirota *et al*., 1970; Fuller *et al*., 1984). These recruited factors form a complex that is commonly referred as the replisome (Box 1).

Box 1: Replisome assembly and DNA replication in *E. coli*

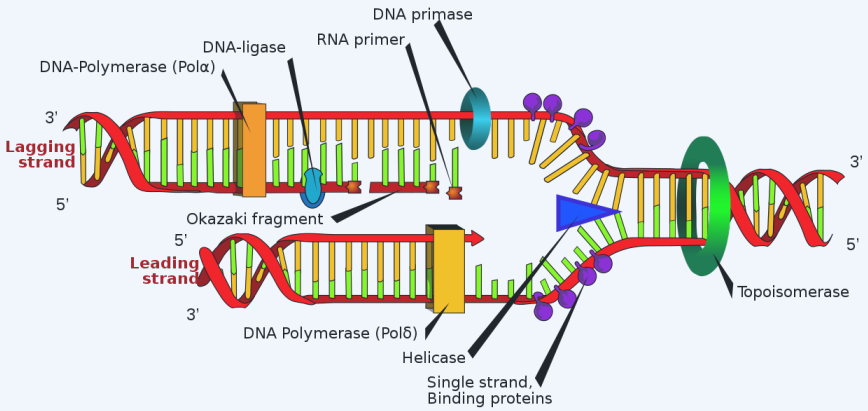

In prokaryotes, replication of the genome is mediated by the DNA polymerase III holoenzyme which is composed of several factors. The replisome is a molecular complex that includes the DNA polymerase III in addition to other factors essential for the replication process. The replisome is formed at the origin of replication (*oriC*), where DnaA-ATP recognizes and binds multiple DnaA boxes (Hirota et al., 1970; Fuller *et al*., 1970). DnaA bound to dsDNA can recruit DiaA which in turn facilitates the recruitment and the oligomer-organization of other DnaA proteins to the initiation site. The binding of IHF (Integration Host Factor) that stimulates a dsDNA bending at the *oriC* is also crucial to form a functional initiation complex (Swinger and Rice, 2004). Once the initiation complex is complete, DnaA can induce the denaturation of the dsDNA and an open complex is formed at the *oriC*. The DnaB helicase is subsequently recruited to the initiation complex with the help of DnaA and of the DnaC helicase loader (Masai *et al*., 1990). DnaB forms a hexamer with a ring shape structure that allows the opening of the replication fork along the chromosome during the replication process. The DnaG primase is then recruited and synthesizes RNA oligonucleotides that are used as starting points for DNA synthesis on both the leading and lagging strands. The presence of these RNA primers is crucial since the DNA polymerase can only add complementary nucleotides on a pre-existing 3'OH extremity. A clamp loader is then recruited at the replication fork and promotes the assembly of the β-clamp and of the DNA polymerase III. The leading strand is synthesized continuously because the polymerase moves in the same direction than the replication fork along the chromosome. However, in the case of the lagging strand, the DNA polymerase proceeds in the opposite direction compared with the replication fork because of the DNA strand polarity. This results in the synthesis of oligonucleotides called Okazaki fragments that are ligated afterwards by a DNA ligase to form a continuous strand. Because of the double-helical structure of the DNA, supercoils are formed in front of the DNA polymerase and are resolved by a type II topoisomerase, also named gyrase. During the replication process, single strand binding proteins (SSB proteins) are bound to the "temporary" ssDNA to stabilize the structure before addition of nucleotides to form dsDNA. The two replication forks proceed bidirectionnaly along the chromosome until they reach the *ter* region where completion of DNA replication and removal of catenation links by gyrases takes place.

II.1. The replication initiator DnaA

The DnaA protein is composed of four principal domains (Figure 5) (Messer *et al.*, 1999). Located at the N-terminal part of the protein, the domains I and II define respectively a protein-protein interaction domain and a flexible loop commonly thought to serve as a linker. Domain I is crucial for the function of the protein since amino acids substitutions in this part of DnaA lead to non-functional proteins (Weigel *et al.*, 1999). In addition, to mediate oligomerization of DnaA, domain I allows the binding of DnaB and DiaA that are crucial for the replication process (see Box 1). The domain III is an AAA+ ATPase domain responsible for the binding to ATP or ADP. Following its translation, DnaA binds to free ATP present in the cytosol leading to the formation of the active form DnaA-ATP. This form is able to recognize and bind three DnaA-binding sites in *oriC* and forms a super-helix composed of four monomers per turn. The initiation of replication takes place when approximately twenty DnaA monomers are bound to the *oriC*. This binding induces first the denaturation of the DUE complex (Duplex Unwinding Element) that contains the AT-rich region, and secondly the recruitment of replisome factors (Sekimizu *et al.*, 1987; Hwang and Kornberg, 1992; Margulies and Kaguni, 1996). Organization of the *oriC* is detailed in Figure 6. Finally, the domain IV contains three alpha-helix that are involved in the binding to DnaA-binding sites on the genome (Messer *et al.*, 1999). These sites, also called DnaA boxes, contain the conserved 9-mer consensus sequences $TT^{A}/_{T}TNCACA$ and were originally found in *E. coli* where 308 of these motifs are present on the genome (Schaper and Messer, 1995). Additional "non-conventional" 6-mer DnaA boxes have also been discovered carrying the sequence AGATCT but the binding to these sites is restricted to the DnaA-ATP form and the presence of a "conventional" DnaA-binding box close to this site is required (Speck *et al.*, 1999).

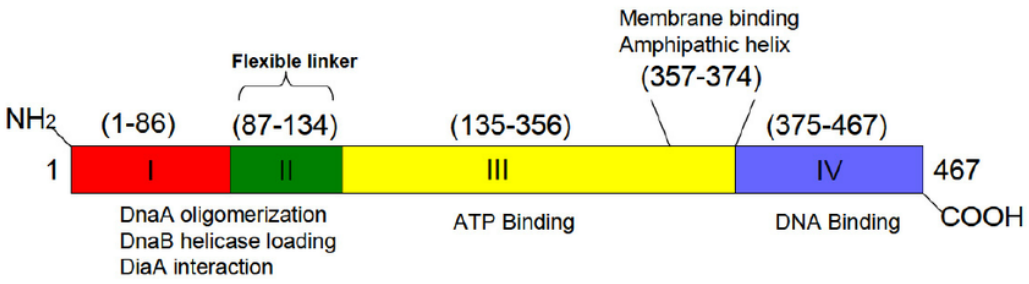

Figure 5: The DnaA protein presents four domains (I to IV). The domain I is involved in oligomerization, helicase loading and DiaA interaction. The domain II is a linker. The domain III is a AAA+ ATPase domain. The domain IV is involved in the binding to DNA. From Saxena *et al.*, 2013

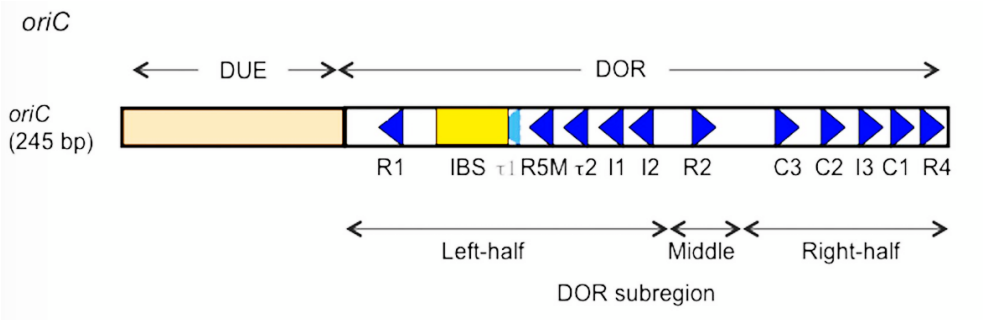

Figure 6: Organization of the *oriC* in *E. coli*. Representation of the *oriC* with the DUE (Duplex Unwinding Element) and the DOR (DnaA Oligomerization Region). The blue arrows represent DnaA boxes, IBS (IHF Binding Site) is in yellow. Modified from Sakiyama *et al*., 2018

II.2. Regulation of the replication initiation

This section highlights principally regulation processes known in the bacterial model *E. coli*. However, the mechanisms used by other bacterial species are mentioned as well when it is appropriate.

II.2.1. Transcriptional regulation

One major way to regulate the initiation of replication is the control of the abundance and the activity of the initiator DnaA itself. Studies using *dnaA*(Ts) mutants showed that the transcription of *dnaA* was increased 5-fold at non-permissive temperature, while the overproduction of the DnaA protein led to a decrease of *dnaA* transcription up to 5-fold. These results highlighted a mechanism of negative autoregulation of *dnaA* transcription where the DnaA protein is able to repress the *dnaA* promoter (Atlung *et al*., 1984, 1985; Braun *et al*., 1985). Sequencing of the *dnaA* locus has shown that the *dnaA* gene is controlled by two promoters, designed as p1 and p2, in between which one conserved DnaA box is present. Five "non-conventional" DnaA-boxes, named boxes 1, 2, a, b, and c, are also located in the promoter region (Figure 7) (Hansen *et al*., 1982; Atlung *et al*., 1984; Braun *et al*., 1985). One DnaA-binding box is also present in the coding sequence of the *dnaA* gene but has been shown to have no effect on *dnaA* transcription (Polaczek and Wright, 1990). Mutations in the perfectly conserved DnaA-box located in the *dnaA* promoter region induced a 5-fold increase of transcripts from the p1 but a decrease of transcription from p2 *in vitro,* suggesting that the binding of DnaA to this box inhibits the p1 and activates the p2 (Polaczek and Wright, 1990). However, these results were not confirmed *in vivo*, as a DnaA overproduction still induced an

inhibition of transcription in strains mutated for the DnaA-box and a derepression of *dnaA* promoters was not observed (Smith *et al*., 1997). Further studies showed that the p1 and p2 are differently regulated by DnaA whether the protein in linked to ATP or ADP. Indeed, frootprinting assays revealed that the six DnaA-boxes present in the *dnaA* promoters are present different affinities for DnaA-ATP or DnaA-ADP. The boxes 1, 2 and the conserved DnaA-box are protected by both DnaA-ATP and DnaA-ADP whereas the box a, b, and c are only bound by DnaA-ATP. Transcriptional studies indicated that DnaA-ATP represses *dnaA* transcription from p1 and p2 more efficiently than DnaA-ADP suggesting the existence of a molecular switch in gene regulation depending on the nucleotide-binding and hydrolysis state of DnaA (Speck *et al*., 1999).

Nine GATC methylation sites are also present in *dnaA* promoter region (Figure 7). The methylation of two of these sites located in the -10 and -35 sequences of the p2 induces an increase of transcription from this promoter (Braun and Wright, 1986). This suggests that *dnaA* transcription is also regulated during the cell cycle since methylation of the genome is directly dependent on replication/cell cycle progression.

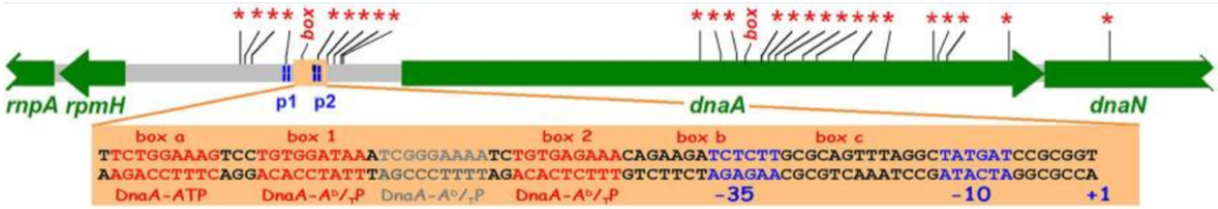

Figure 7: *dnaA* locus organization. Six DnaA boxes are present in the promoter region of *dnaA*. GATC methylation sites are highlighted by stars. The -35 and -10 regions are highlighted in blue. Hansen and Atlung, 2018.

II.2.2. DNA methylation and the SeqA protein

The *E. coli oriC* region contains 11 5'-GATC-3' sites which are methylated on the adenine by the Dam methylase (Waldminghaus and Skarstad, 2009). Because bacteria use semi-conservative DNA replication, the newly synthesized strand is unmethylated after replication whereas the parental strand is still methylated. As a consequence, the DNA molecule is in a hemi-methylated state during a certain period of time of the cell cycle (Lu *et al*., 1994). This hemi-methylated state allows the binding of the protein SeqA to the 5'-GATC-

3’ sites, including those located in *oriC*. This leads to a sequestration of the replication origin from DnaA and thus allows the inhibition of an untimely re-initiation event (Waldminghaus and Skarstad, 2009). Moreover, the SeqA-DNA binding competes with the Dam methylase for the 5’-GATC-3’ motifs in *oriC* which thus stay hemi-methylated longer than other chromosomal motifs (Kang *et al*., 2005). The spontaneous release of SeqA from DNA occurs approximately 10 minutes after initial binding, in *E. coli* cells, having a doubling time of 30 minutes (Kang *et al*., 2005). Moreover, evidences pointed out also SeqA as a negative regulator for *dnaA* transcription (Campbell and Kleckner, 1990). By these processes, SeqA prevents the replication of newly replicated *oriC* and plays a role in regulation of chromosome replication (Waldminghaus and Skarstad, 2009).

II.2.3. DnaA titration

DnaA intracellular levels and activity are also regulated post-translationally with a process named DDAH (*datA*-dependent DnaA-ATP hydrolysis). The *datA* locus contains a cluster of DnaA-boxes which are bound by DnaA and a IHF binding site which is bound by the IHF protein after the initiation of replication (Kitagawa *et al*., 1996). These bindings have two consequences. First, DnaA proteins undergo a titration effect meaning that less DnaA molecules are available to bind to the *oriC*. Secondly, the binding of DnaA-ATP and IHF to the *datA* site induces the hydrolysis of ATP into ADP leading to a DnaA form that is inactive for replication. Indeed, the deletion of the *datA* locus or the IHF gene leads to an increase of DnaA-ATP and inappropriate replication initiation events (Kitagawa *et al*., 1996; Kitagawa *et al*., 1998; Nozaki *et al*., 2009). The chromosomal position of the *datA* locus is relatively close to the *oriC* meaning that this region is duplicated soon after replication initiation and subsequently that a higher titration of DnaA-ATP occurs (Kitagawa *et al*., 1996). Indeed, a mutant where *datA* was translocated near the replication termination site showed untimely initiation events, and on the other hand, the presence of additional *datA* sites on a replicative plasmid induced a delay in replication initiation (Kitagawa *et al*., 1998; Morigen *et al*., 2003). These results demonstrated the important role of the DDAH mechanism in the timed control of replication initiation. The *datA* sites containing DnaA-boxes were found in *Bacillus subtilis* and *Streptomyces coelicolor,* and were also demonstrated to be involved in initiation control, indicating that this regulatory process could be conserved among bacteria (Smulczyk-Krawczyszyn *et al*., 2006; Okumura *et al*., 2012).

II.2.4. The RIDA process

The regulatory inactivation of DnaA (RIDA) system constitutes another way that controls the DNA replication initiation in different bacterial species. This mechanism involves the Hda (Homolog of DnaA) protein in *E. coli* and HdaA in *C. crescentus* (Kato and Katayama, 2001; Collier and Shapiro, 2009). Both Hda and HdaA possess an AAA+ domain that present strong homology with the domain III of DnaA. During DNA replication in *E. coli*, Hda is able to interact with the β-sliding clamp of the DNA polymerase III, also named DnaN. The recruitment of Hda to the replication fork stimulates the hydrolysis of DnaA-ATP into DnaA-ADP, and thus, the inactivation of the protein. RIDA mechanism has been shown to prevent over-initiation of chromosome replication in both *E. coli* and *C. crescentus* since the loss of Hda/HdaA led to an aberrant increase of chromosomes number (Kato and Katayama, 2001; Collier and Shapiro, 2009). HdaA colocalized with DnaN and induced conversion of DnaA-ATP into the non-active form DnaA-ADP in *C. crescentus* (Collier and Shapiro, 2009; Fernandez-Fernandez *et al*., 2011). But in addition to what is observed in *E. coli*, HdaA was demonstrated to be involved in the stability of DnaA protein since one consequence of HdaA depletion is a decrease of DnaA proteolysis (Wargachuk and Marczynski, 2015). Indeed, unlike in *E. coli*, in WT *C. crescentus* the DnaA pool undergoes a turnover during exponential phase of growth and this pool is completely removed during stationary phase or in nutrient-depleted condition (Wargachuk and Marczynski, 2015). It was suggested that this DnaA proteolysis could be mediated by the Lon protease, as Jonas *et al*. showed that during a proteotoxic stress, the increase of misfolded proteins stimulates Lon for degradation of DnaA (Jonas *et al*., 2013). Recently, it was reported that the protease ClpAP was directly involved in DnaA proteolysis during the stationary phase, and by this manner, was implicated in the control of chromosomes replication in *C. crescentus*. The DnaA degradation by ClpAP is inhibited by ClpS, suggesting a role for this later protein in inhibiting ClpAP during certain conditions (Liu *et al*., 2016).

II.2.5. DnaA-ATP regeneration

In order to reinitiate a new chromosomal replication, *E. coli* has to convert the DnaA-ADP pool into DnaA-ATP active for replication initiation. The DARS (DnaA Reactive Sequence) sites, containing three DnaA-boxes each, stimulate the releasing of ADP from DnaA leading to apo-DnaA that is free to bind ATP. These intergenic regions were shown to stimulate initiation of replication *in vitro* and *in vivo* and their loss supressed the overinitiation phenotype that is

observed in *seqA* and *datA* mutants (Fujimitsu and Katayama, 2004; Fujimitsu *et al*., 2009). In the same way, deletion of both DARS sites led to a strong decrease of the ratio DnaA-ATP/DnaA-ADP ratio (from 70% to 30%) in cells lacking *hda*, meaning that this mechanism plays a major role in DnaA-ATP regeneration.

Other studies highlighted the role of acidic phospholipids contained in *E. coli* cell membrane in promoting the conversion of DnaA-ADP into DnaA-ATP (Fingland *et al*., 2012; Saxena *et al*., 2013). The cardiolipin (CL) and phosphatidyl-glycerol (PG) induced nucleotides dissociation from DnaA *in vitro* and mutants presenting a decrease in acidic phospholipids membrane composition showed an inhibition of initiation events (Crooke *et al*., 1992; Saxena *et al*., 2013). However, the exact mechanism involved in this regulation is not yet understood so far.

II.3. Cell cycle regulation in *C. crescentus*

The alphaproteobacterium *Caulobacter crescentus* was extensively used as a model for cell cycle studies. As a reminder, this bacterium presents two distinct forms during its cell cycle: a swarmer cell and a stalked cell. In nutrient rich environments, the stalked cell can adhere to a surface through the holdfast, a polysaccharide-based adhesin, that is produced at the tip of the stalk (Merker and Smit, 1988). This cell is able to initiate DNA replication and a new cell cycle. *C. crescentus* divides asymmetrically, leading to two different daughter cells after cytokinesis: one large stalked cell and one small swarmer cell which present flagellum and pili. This later form is motile and is able to move and find favorable environments to colonize. In order to initiate DNA replication, the swarmer cell has to differentiate into a stalked cell through a complex reprogramming system named SwaPS (Swarmer Progeny Specific) program (Degnen and Newton, 1972; Matroule *et al*., 2004). This differentiation event has been shown to be regulated by a molecular mechanism involving different actors (detailed in Figure 8). DivK is an essential response regulator which is regulated through phosphorylation by two histidine kinases, PleC and DivJ, where PleC shows kinase and phosphatase activities on DivK, and DivJ presents only a kinase activity (Hecht and Newton, 1995; Ohta *et al*., 1992; Wang *et al*., 1993). In swarmer cells, PleC is localized at the flagellated pole and acts as a phosphatase on DivK, which results in the diffusion of dephosphorylated DivK in the cytoplasm. During the SwaPS, DivJ replaces progressively PleC at the old pole and phosphorylates DivK, which leads to DivK localization at the pole. This induces the loss of the flagellum and retraction of the pili at this pole, and the formation of the stalk (Wheeler and

Shapiro, 1999; Matroule *et al*., 2004). In predivisional cells, DivJ is localized at the stalked pole and PleC is localized at the new pole, which triggers a shuttling of DivK from pole to pole. Indeed, at the stalked pole DivK is phosphorylated by DivJ and at the flagellated pole DivK is dephosphorylated by PleC (Matroule *et al*., 2004). After septation, DivK remains phosphorylated in the stalked cell and dephosphorylated in the swarmer cell, and thus, the regulatory activity of DivK differs between both cell types (Figure 9). Thanks to the DivL intermediate, DivK modulates a phosphorelay composed of a histidine kinase CckA and a phosphotransferase ChpT which in turn controls the activation via phosphorylation or the proteolysis of the master cell cycle regulator CtrA (Figure 8). In the stalked cell, the presence of DivK-P inhibits DivL which normally stimulates the autophosphorylation of CckA which leads to inactivation and degradation of CtrA, this later process being mediated through the CpdR protein. On the opposite, in the swarmer cell, DivL is not inhibited and can stimulate the CckA/ChpT phosphorylation cascade that leads to the activation of CtrA (Iniesta *et al*., 2010). The arrest in G1 observed in swarmer cells is especially due to CtrA activation. This cell cycle regulator is a transcription factor regulating almost one hundred genes and is notably involved in the G1 arrest observed in swarmer cells by preventing initiation of DNA replication (Quon *et al*., 1998).

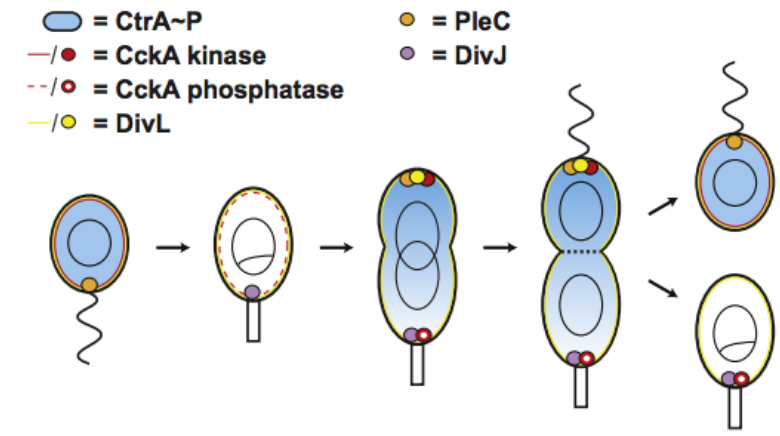

Figure 8: Localization of PleC/DivJ/DivK and DivL/CckA/CtrA during the cell cycle of *C. crescentus*. The PleC phosphatase is localized at the flagellated pole and leads to CtrA phosphorylated form (CtrA-P) in the swarmer cell. During the swarmer to stalked cell transition, DivK is phosphorylated through DivJ kinase, inhibits DivL, and subsequently induces the CckA phosphatase activity and proteolysis of CtrA. At the flagellated pole of the predivisional cell, PleC phosphatase dephosphorylates DivK and CckA autophosphorylation activity is then stimulated via DivL. The phosphorylation of CckA leads to phosphorylation of CtrA and its activation in swarmer cell after cytokinesis. From Tsokos *et al*., 2011.

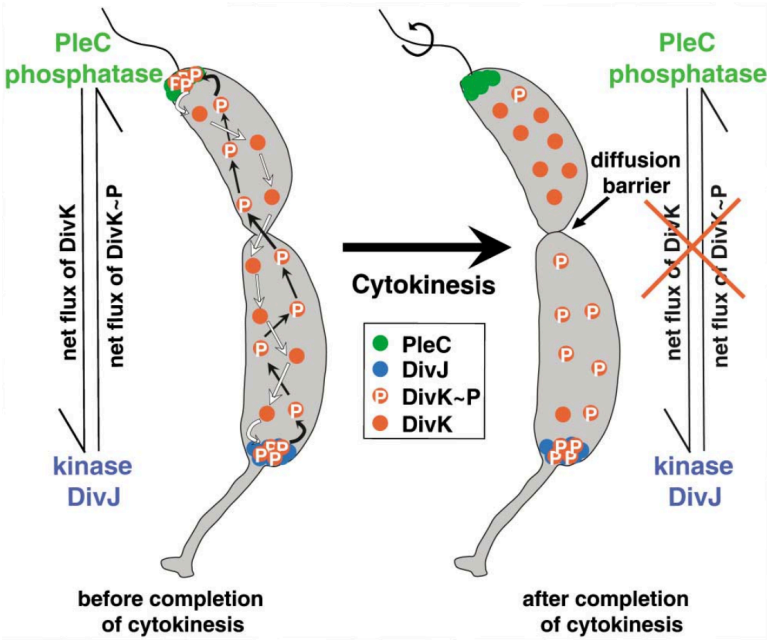

Figure 9: Schematic representation of the DivK shuttling in *C. crescentus*. In Predivisional cell, the PleC phosphatase is localized at the flagellated pole and dephosphorylates DivK, whereas DivJ is localized at the stalked pole and phosphorylates DivK. After completion of cytokinesis, DivK remains dephosphorylated in swarmer and phosphorylated in stalked cell. From Matroule *et al.*, 2004

II.4. The CtrA and GcrA cell cycle regulators

The master regulators CtrA and GcrA are both transcription factors conserved among alphaproteobacteria and are involved in the regulation of the cell cycle in *C. crescentus*. Their levels are out of phase during cell cycle progression, with CtrA being present and active in the swarmer cells, and GcrA starting to accumulate early in the S phase in stalked cells.

CtrA belongs to the OmpR family and presents a phosphorylatable aspartate residue at its the N-terminal part and a DNA binding domain at its C-terminal part. This factor is commonly defined as a master cell cycle regulator since it controls the transcription of hundreds of genes and regulates multiple cell cycle events such as DNA replication, DNA methylation, flagellum and pili biogenesis and division in *C. crescentus* (Quon *et al.*, 1996; Domian *et al.*, 1997). GcrA has been shown to bind GANTC motifs on DNA, which can be fully methylated or hemi-methylated on the adenine by the CcrM methyltransferase. Especially, it has been shown that GcrA can distinguish between both methylation states of the DNA and binds with more affinity fully methylated GANTC sequences *in vitro*. However, it has to be mentioned that not all the *in vivo* targets of GcrA contain GANTC sites, as shown by ChIP-seq experiment (Fioravanti *et al.*, 2013). Instead, GcrA is able to bind to the σ^{70} housekeeping factor and then, this complex preferentially interacts with GANTC sites on the DNA, which

promote the formation of an open complex and thus, transcription of the target gene (Haakonsen *et al*., 2015; Wu *et al*., 2018).

During the cell cycle, CtrA is regulated at transcriptional, post-translational and proteolysis levels. The initial transcription of *ctrA* during the S phase is governed by a control circuit involving DnaA, GcrA and DNA methylation state (Figure 10). At the beginning of a new cell cycle in swarmer cells, the fully methylated state of the *dnaA* promoter allows its transcription (Collier *et al*., 2007). The increase of intracellular DnaA induces first DNA replication and the entry in S phase, and secondly the expression of *gcrA.* GcrA has been shown to regulate cell cycle processes such as nucleotides synthesis, chromosome segregation, and cell division, suggesting that GcrA is involved in the gene expression pattern which governs the S phase and later steps of the cell cycle (Haakonsen *et al*., 2015). In addition, GcrA was shown to induce transcription from the P1 promoter of *ctrA* when this later is hemimethylated, *i.e.* when the replication fork has passed through this region (Collier *et al*., 2006). The GcrA-dependent increase of CtrA induces a positive feedback loop since CtrA is able to bind to its own P2 promoter leading to a strong transcription activation. At the end of the cell cycle, the expression of the CcrM methylase encoding gene is induced by CtrA, which allows the methylation of the chromosome (Figure 10). After septation, the stalked cell induces the proteolysis of CtrA by ClpXP and DNA replication can then occur (Iniesta *et al*., 2006). However, in swarmer cells where DivK is unphosphorylated due to the PleC phosphatase, the CtrA-P protein is still present and active, and can therefore prevent a new round of replication. CtrA is proteolyzed during the swarmer to stalked cell transition, which allows DNA replication initiation and cell cycle progression (Figure 11) (Domian *et al*., 1997).

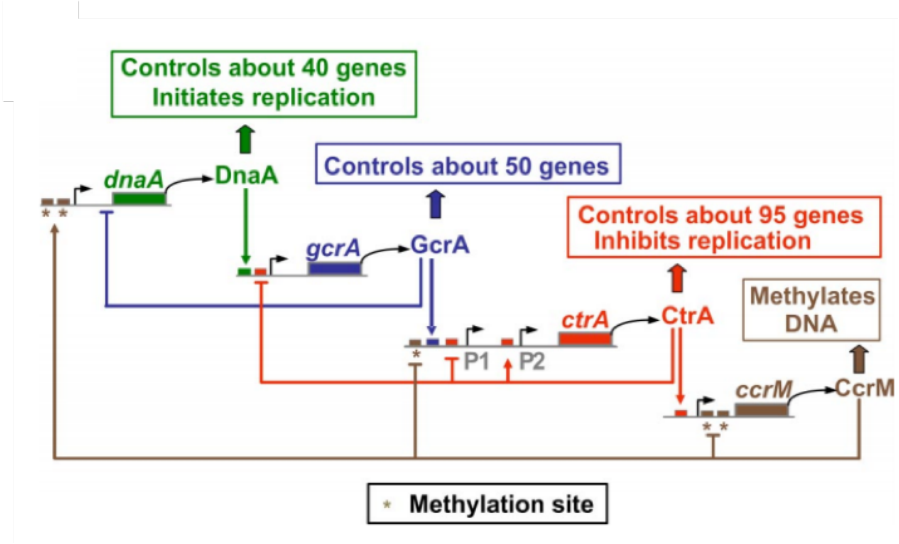

Figure 10: The DnaA/GcrA/CtrA/CcrM circuit in *C. crescentus*. The fully methylated state of the *dnaA* promoter region allows transcription. The production of DnaA leads to the expression of *gcrA* which in turn induces the expression of *ctrA* from its P1 promoter. CtrA exerts a positive feedback loop by activating its P2 promoter. At the end of the cell cycle, *ccrM* transcription is induced by CtrA leading to the fully methylated state of the chromosome. From Collier *et al*., 2007

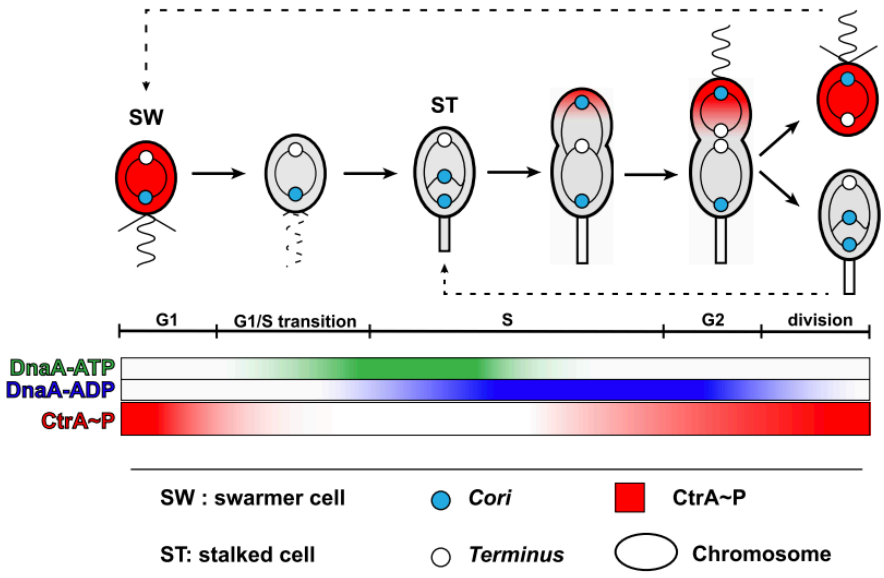

Figure 11: Regulation of CtrA and DnaA levels during the cell cycle of *C. crescentus*. CtrA-P is present in swarmer cells and prevents initiation of DNA replication. At the transition between swarmer cells and stalked cells, CtrA is proteolyzed and DnaA-ATP levels increase leading to DNA replication. After initiation of replication, DnaA-ATP is converted in DnaA-ADP. During late S phase, CtrA-P starts to increase, and after septation, it is present in the swarmer cell and absent in stalked cell due to its proteolysis. From Frandi and Collier, 2019.

CtrA was shown to inhibit replication initiation by directly binding to the *Cori* (Quon *et al*., 1996; Quon *et al*., 1998). CtrA recognizes and binds the 9-mer consensus sequence TTAA(N_7)TTAAC, where the length of the linker N_7 was shown to be important for the optimal binding of CtrA (Quon *et al*., 1998). The *Cori* is located between *hemE* and the RP001 genes and it contains five CtrA binding boxes. Studies of these boxes revealed that CtrA binding to these boxes is cooperative, CtrA monomers binding each of the TTAA sites contained in a CtrA box, and the phosphorylated state of CtrA enhancing this cooperation (Siam *et al*., 2000). Seven DnaA-binding boxes are present in the *Cori*, among them one overlaps with a CtrA boxe. This overlap was suggested to be involved in the CtrA-dependent inhibition of replication by creating a competition between CtrA and DnaA for binding to *Cori* (Quon *et al*., 1998).

The origin of replication also contains five GANTC sites which are methylated by CcrM in *C. crescentus*. However, unlike what is observed in *E. coli* with the GATC sites (Waldminghaus and Skarstad, 2009), these methylation sites do not seem to be involved in replication regulation since normal chromosome content is maintained in mutant lacking CcrM (Gonzalez *et al*., 2014).

Note that the alarmone (p)ppGpp (guanosine tetra- penta-phosphate) was also shown to play a role in the regulation of replication in *E. coli* as in *C. crescentus*. This regulation will be discussed in details in the next part of the Introduction (Chapter III: The stringent response).

II.5. The CtrA pathway in *B. abortus*

The actors involved in the CtrA regulatory pathway in *C. crescentus*, *i.e.* PleC/DivJ/DivK and CckA/ChpT/CtrA are conserved in *B.* abortus (Hallez *et al*., 2004; Brilli *et al*., 2010). It was shown that homologs of CckA, ChpT and CpdR interact similarly in *B. abortus*, and both *B. abortus* PleC and DivK are able to heterocomplement the absence of the corresponding factors in *C. crescentus,* suggesting a conservation of the protein functions (Hallez *et al*., 2007; Willett *et al*., 2015). This could indicate, to some extent, that the whole DivK-CtrA regulation network initially described in *C. crescentus* is conserved in *B. abortus*.

Interestingly, a third histidine kinase homologous to PleC and DivJ, named PdhS (PleC DivJ Homologous Sensor), is found in *Brucella* species, but is absent in *C. crescentus* (Hallez *et al*., 2004). The *pdhS* gene was shown to be essential (Hallez *et al*., 2007), a thermosensitive mutant cannot grow at restrictive temperature and expression of non-functional alleles of *pdhS* led to abnormal morphologies typically observed during division defects (Van der Henst *et al*., 2012). As expected, DivK from *B. abortus*, which is also essential (Van der Henst *et al*.,

2012), has been shown to interact with DivJ, PleC, DivL and PdhS in a yeast two-hybrid assay (Hallez *et al*., 2007). Moreover, PdhS is localized exclusively at the old pole of the bacterium where it co-localizes with DivK (Hallez *et al*., 2007). It was also observed that DivK is delocalized in a *pdhS* thermosensitive strain at restrictive temperature (Van der Henst *et al*., 2012). Altogether, these results support the hypothesis of a functional interaction between PdhS and DivK in *B. abortus*.

Some targets of CtrA are conserved between *C. crescentus* and *B. abortus* such as genes involved in division (*ftsQ*) and DNA methylation (*ccrM*), suggesting that CtrA is also involved in cell cycle regulation in *B. abortus* (Bellefontaine *et al*., 2002). However, $CtrA_{abortus}$ was not found to bind to the origin of replication, and there are no CtrA boxes in the *oriI* region, suggesting that CtrA could not generate DNA replication inhibition as it is the case for $CtrA_{crescentus}$. However, $CtrA_{abortus}$ could act indirectly to control replication initiation for example through the regulation of the *dnaA* gene expression (Francis *et al*., 2017).

The identification of different CtrA targets in *B. abortus*, for example controlling outer membrane composition (Francis *et al*., 2017) or DNA repair (Poncin *et al*., 2019), compared to *C. crescentus,* supports the relative plasticity of the CtrA network among these species, as previously suggested (Bellefontaine *et al*., 2002; Hallez *et al*., 2004).

III. Chapter 3: (p)ppGpp and the stringent response

The heterogeneous environments encountered by a bacterium can constitute a diverse source of stresses that can compromise the survival of this bacterium. In order to cope with these stresses, survive, and remain competitive, bacteria have evolved different strategies to quickly adapt their physiology to the new environment. One of those processes involves the accumulation of the small alarmone guanosine tetra- and penta- phosphate, abbreviated as (p)ppGpp, in response to nutrient stresses. In 1969, Cashel and Gallant identified this nucleotide second messenger in *E. coli* and introduced for the first time the notion of stringent response to indicate a drastic decrease of rRNA synthesis upon amino acid starvation (Cashel and Gallant, 1969). By extension, the term of “stringent response” is now used to refer to an increase of intracellular (p)ppGpp level in bacteria following the exposure to any stress. The production of the alarmone leads to physiological changes, and especially, transcriptional reprogramming in the cells that allows them to deal with the stress.

III.1. Homeostasis of (p)ppGpp

The proteins responsible for the (p)ppGpp homeostasis are conserved in almost all bacterial species and can be divided into two types, the "small" and the "long" RSH (RelA SpoT Homolog). The small enzymes consist in the presence of a unique hydrolytic domain (SAHs, Small Alarmone Hydrolases) or a unique synthetic domain (SASs, Small Alarmone Synthetase), whereas the long enzymes present both hydrolysis and synthesis domains. These two types of enzymes can be found in a single species as exemplified with *Bacillus subtilis* and *Listeria monocytogenes* (Nanamiya *et al*., 2008; Wolz *et al*., 2010), or some species can present only one enzyme, such as *C. crescentus* or *B. abortus* which have one long RSH enzyme. pppGpp and ppGpp are produced from the addition of a pyrophosphate moiety, coming from an ATP, to the 3' position of GTP and GDP respectively (Figure 12). Conversely, the hydrolysis of the alarmone leads to the formation of GDP/GTP and a pyrophosphate.

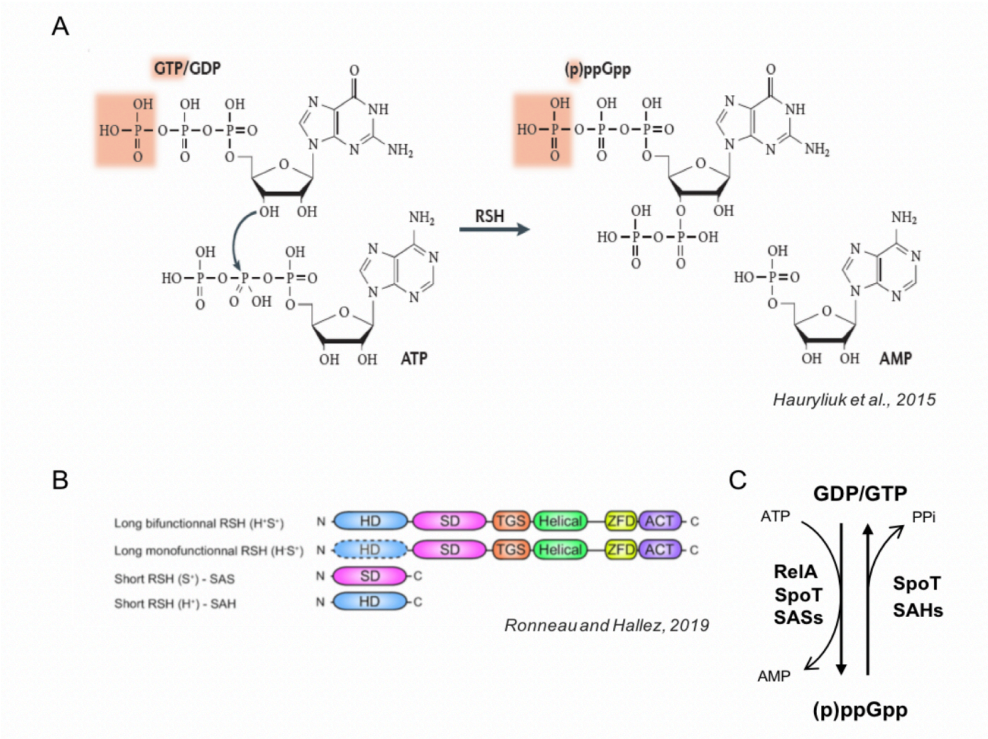

Figure 12: Homeostasis of (p)ppGpp. (p)ppGpp (guanosine 3'-diphosphate 5'-triphosphate) is produced from GDP/GTP by the addition of a pyrophosphate group in 3' position. Modified from Hauryliuk *et al*., 2015 (A). Representation of the different enzymes involved in (p)ppGpp homeostasis. RSH (RelA SpoT Homolog), SAS (Small Alarmone Synthetase), SAH (Small Alarmone Hydrolase), HD (Hydrolase Domain), SD (Synthetase Domain), TGS (ThrRS, GTPase and SpoT), ZFD (Zing-Finger Domain), ACT (Aspartate kinase, Chorismate mutase and TyrA). The $^{+}$ and $^{-}$ indicate if the HD or SD are functional or not. Modified from Ronneau and Hallez., 2019 (B). Recapitulative scheme showing the activity of enzymes involved in (p)ppGpp homeostasis (C).

III.1.1. Structure and function of long RSH proteins

The long RSH enzymes are bifunctional or monofunctional so they can synthetize and/or hydrolyse (p)ppGpp. These proteins show several domains in which we found two catalytic and two regulatory domains (Figure 12). The hydrolase domain (HD) and the synthetase domain (SD) are located at the N-Terminal part (NTD) of the protein. The C-Terminal part (CTD) contains the two regulatory domains named TGS (ThrRS, GTPase and SpoT) domain, and ACT (Aspartate kinase, Chorismate mutase and TyrA) domain and includes also two structural elements, a helical domain and a putative zinc finger domain (Brown *et al*., 2016) (Figure 12).

As mentioned before, bacteria can have several RSH proteins, and this is especially observed in β- and γ-proteobacteria. In *E. coli* there are two RSH named SpoT and RelA which seem to originate from a duplication event during evolution. Both proteins present a HD and a SD, however, due to the absence of catalytic residues, the hydrolytic activity of RelA is not functional (Aravind and Koonin, 1998). While RelA exclusively constitutes a (p)ppGpp synthetase, SpoT can both hydrolyse and synthesize the alarmone although this enzyme presents a weak synthetase activity compared to RelA (Mechold *et al*., 2002).

III.1.2. Regulation of long RSH proteins

While RelA and SpoT are considered as homolog, both proteins seem to be regulated by different signals in *E. coli*.

The synthetase activity of RelA is stimulated during amino acid starvation and heat shock (Gallant *et al*., 1977). During growth in nutrients rich conditions, aminoacylated tRNAs can deliver amino acids to A-sites of ribosomes in order to be added to the polypeptides that are currently in synthesis. However, during amino acid starvation, the level of deacylated tRNAs increases leading to A-sites that are empty and the stalled ribosome conformation leads to stimulation of synthetase activity of RelA, and thus, the production of (p)ppGpp. RelA can interact with ribosomes via its CTD regulatory domains, and more precisely, it has been shown that the deacylated state of the tRNA present in the ribosome is involved in the link with RelA and its synthetase activity stimulation (Richter *et al*., 1973; Agirrezabala *et al*. 2013). This is consistent with the fact that deletion of the *relA* CTD part leads to dissociation of RelA from ribosomes and production of (p)ppGpp (Figure 13) (Gropp *et al*., 2001; Agirrezabala *et al*. 2013; Gonzalez and Collier, 2014).

In addition to being activated by amino acid starvation, the RelA protein undergoes a positive allosteric feedback regulation by (p)ppGpp itself. This mechanism of regulation allows an amplification and a rapid response even with a weak input signal (Figure 13) (Shyp *et al.*, 2012).

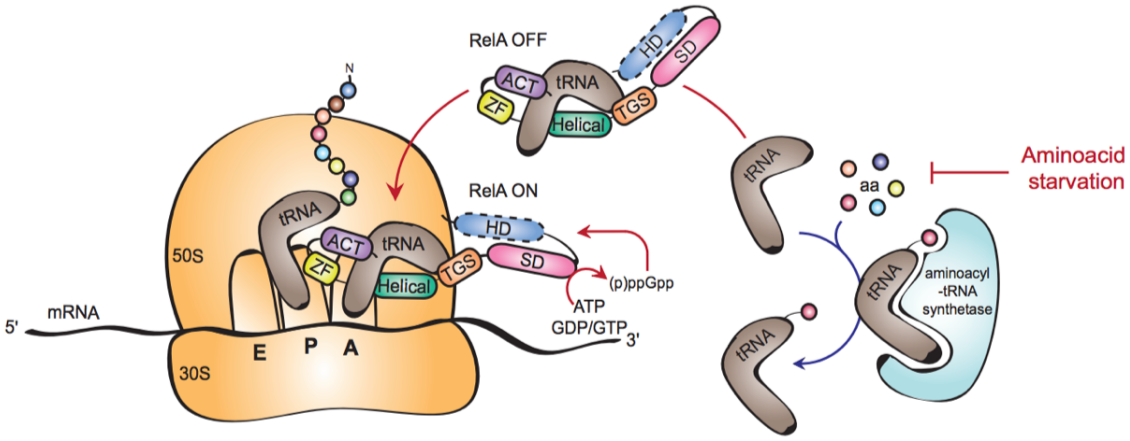

Modified from Ronneau and Hallez, 2019

Figure 13: RelA regulation upon amino acid starvation. When bacteria undergo amino acid starvation, deacylated tRNA interact with the RelA enzyme which is OFF at this time (unable to induce synthetic activity), but becomes ON at the A site of the stalled ribosome. This results in the activation of the synthetase activity of RelA and the production of (p)ppGpp. Positive allosteric regulation also occurs through the activation of RelA by (p)ppGpp. From Ronneau and Hallez, 2019.

The bifunctional enzyme $SpoT_{coli}$ was less characterized than RelA but was shown to be involved in response to different stresses compared to RelA. Compared to RelA, $SpoT_{coli}$ presents a weak synthetase activity and a strong hydrolase activity, and subsequently, the deletion of *spoT* alone in *E. coli* is lethal since the balance between synthesis and hydrolysis of (p)ppGpp is disrupted (Xiao *et al.*, 1991, Mechold *et al.*, 2002). $SpoT_{coli}$ has been shown to produce (p)ppGpp following several signals including carbon, iron and fatty acid (FA) starvation (Xiao *et al.*, 1991; Seyfzadeh *et al.*, 1993; Vinella *et al.*, 2005).

SpoT has been linked to fatty acid metabolism through the interaction of its TGS domain with ACP (Acyl Carrier Protein), which constitutes a sensor of intracellular FA and a cofactor involved in FA biosynthesis. During fatty acid starvation, $SpoT_{coli}$ undergoes a switch of function, from hydrolase activity to synthetase activity, that leads to (p)ppGpp production (Figure 14A) (Battesti and Bouveret, 2006).

The interaction of SpoT$_{coli}$ with the GTPase CgtA, also named Obg, which is notably involved in ribosome assembly, has also been reported in *E. coli* and *V. cholerae*. Since *cgtA* mutants presented an increase of (p)ppGpp level during exponential growth in rich medium, it was suggested that this protein regulates positively the SpoT$_{coli}$ hydrolysis activity in order to keep low (p)ppGpp concentration during normal growth conditions, *i.e.* in rich nutrient medium (Figure 14B) (Raskin *et al*., 2007; Jiang *et al*., 2007).

SpoT$_{coli}$ regulation has also been linked to the carbohydrate phosphotransferase system (PTS) through its interaction with Rsd (Regulator of Sigma D). Rsd physically interacts with non-phosphorylated HPr, a component of the sugar PTS (Park *et al*., 2013). During carbon starvation, HPr become phosphorylated and, as a consequence, free Rsd is released and can activate the hydrolysis activity of SpoT$_{coli}$ through its interaction with the TGS domain (Figure 14B). The Rsd-dependent stimulation of the SpoT$_{coli}$ hydrolase domain has been proposed to balance the level of the alarmone during stringent response, in order to avoid the deleterious effects caused by too much intracellular (p)ppGpp (Park *et al*., 2013; Lee *et al*., 2018).

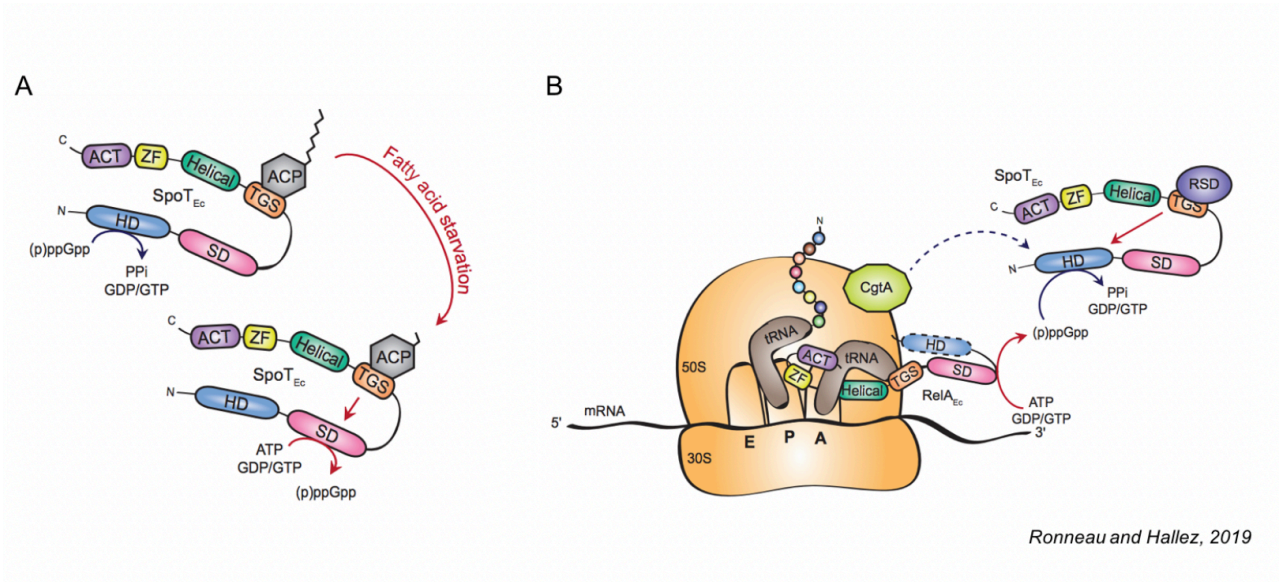

Figure 14: Regulations of SpoT enzymes. Upon fatty acid (FA) starvation, the synthetase activity of SpoT is activated through ACP which constitutes a FA sensor and interacts with the regulatory TGS domain of SpoT (A). CgtA and Rsd can interact with SpoT and stimulate its hydrolytic activity in order to balance strong (p)ppGpp production by RelA (B). From Ronneau and Hallez, 2019.

In the alphaproteobacterium *C. crescentus*, the unique RSH enzyme named SpoT$_{Cc}$ is also associated with ribosomes as it was reported in *E. coli*. However, amino acid starvation alone is not sufficient to trigger the accumulation of (p)ppGpp and *C. crescentus* needs in

addition carbon and nitrogen starvation to induce the stringent response (Chiaverotti *et al*., 1981; Lesley and Shapiro, 2008; Boutte and Crosson, 2011). It has been reported that the nitrogen phosphotransferase system (PTS^{Ntr}) is involved in response to nitrogen starvation, especially through HPr∼P and $EIIA^{Ntr}$ ∼P proteins which mediate (p)ppGpp production by $SpoT_{Cc}$ (Ronneau *et al*., 2016). These differences in regulation of (p)ppGpp production among bacteria highlighted the diversity of the control of the stringent response and exemplified how organisms adapt this control according to their various lifestyles.

III.1.3. SASs and SAHs proteins

SASs and SAHs are proteins containing only one catalytic domain which is respectively involved in (p)ppGpp synthesis and hydrolysis. These small alarmone synthetases and hydrolases are mainly found in Gram-positive bacteria, especially in species already containing an RSH enzyme (Atkinson *et al*., 2011).

SASs were first discovered in *Streptococcus mutans*, where the deletion of *relA* coding for the bifunctional enzyme did not suppress the intracellular level of (p)ppGpp (Lemos *et al*., 2004; Nascimento *et al*., 2008). By examining in the *S. mutans* genome, the authors found two paralogs of *relA,* named *relP* and *relQ,* but they presented limited sequence homology to RelA regarding the peptide sequences. Indeed, both RelP and RelQ lacked the RelA C-terminal and the hydrolase domains (Nascimento *et al*., 2008). Since it was reported that the RelQ and RelP subclasses of protein family, also renowned SAS1 and SAS2 respectively, showed different regulation mechanisms and are associated with distinct stress signaling, the presence of these specific enzymes could constitute an additional control level in order to fine tune the (p)ppGpp homeostasis in response to various stresses.

As observed for the SASs proteins, SAHs proteins are constituted of only one functional domain. Surprisingly, SAHs have been identified in metazoan despite the fact that (p)ppGpp was not detectable and that RSH synthetase enzymes are absent in these organisms. Still, a SAHs of *Drosophila melanogaster,* named Mesh1, has been shown to hydrolyze (p)ppGpp both *in vitro* and *in vivo* in *E. coli*, and to suppress the lethal phenotype of a Δ*spoT* mutant (Sun *et al*., 2010). The exact function of Mesh1 in metazoan is not clear, but recently a study reported that human Mesh1 was associated with an NADPH phosphatase activity (Ding *et al*., 2018).

III.2. Downstream of the (p)ppGpp

III.2.1. Targets of (p)ppGpp and the DksA mediator

One consequence of the intracellular elevation of (p)ppGpp is a global change in gene expression, either positively or negatively, in order to direct the response and face the stress. This modification of the transcription profile is especially mediated through the direct binding of (p)ppGpp to the RNA polymerase II (RNAP). Two sites of the *E. coli* RNAP were reported to be bound by (p)ppGpp (Figure 15) (Ross *et al*., 2013; Mechold *et al*., 2013; Ross *et al*., 2016).

The first one, referred as site 1, is located at the interface between the β' and ω subunits and is bound by both pppGpp and ppGpp *in vitro*. This interaction was demonstrated to have functional consequences *in vivo* since strains harboring mutations in the site 1, suppressing the binding of (p)ppGpp, presented phenotypes related to what is observed in bacteria lacking (p)ppGpp, *i.e.* a growth delay following a nutrient downshift. However, these mutants did not behave exactly as a (p)ppGpp null mutant, suggesting that (p)ppGpp had other targets in addition to the site 1 of the RNAP. (Ross *et al*., 2013; Mechold *et al*., 2013).

A second RNAP site bound by (p)ppGpp, named site 2, was discovered at the interface between the β' subunit and the DksA protein (Ross *et al*., 2016). DksA is a transcription factor (TF) which binds the secondary channel of the RNAP and was shown to be required for rRNA promoters inhibition during amino acid starvation *in vivo* and to amplify the (p)ppGpp effects on transcription *in vitro*. Indeed, the *in vitro* transcription of rRNA promoters was inhibited 2- to 3-fold in the presence of (p)ppGpp, while in presence of DksA this inhibition reached 20-fold. (Barker *et al*., 2001; Paul *et al*., 2004). It was shown that DksA affects the transcription by decreasing the time of the open complex conformation of the RNAP (Paul *et al*., 2004). The upregulation or the downregulation of promoters by (p)ppGpp/DksA synergy seems to be dictated by enrichment of AT or GC respectively, between the -10 box and the +1 transcription site. Indeed, the exchange of the AT-rich discriminator found in the *uspA* promoter, which is positively regulated by (p)ppGpp/DksA, by the GC-rich discriminator found in the P*rrnBP1*, which is known to be negatively regulated by (p)ppGpp/DksA, induced the inhibition of the *PuspA in vitro* and *in vivo* by (p)ppGpp/DksA. Futhermore, the RNAP-promoter complex was destabilized when the AT-rich discriminator was replaced by the GC-rich sequence, suggesting that one of the regulations mediated by (p)ppGpp/DksA acts on the transcription initiation (Gummesson *et al*., 2013).

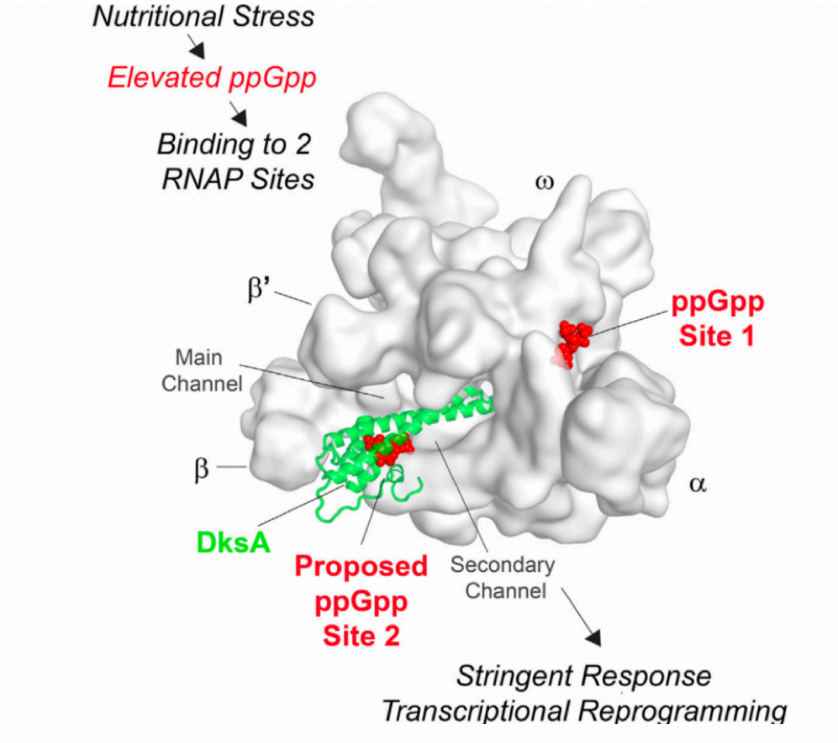

Figure 15: Two sites of the RNA polymerase are bound by (p)ppGpp. The site 1 is directly linked by (p)ppGpp and the site 2 in linked by (p)ppGpp and DksA. The two sites linked by (p)ppGpp are highlighted in red. The DksA mediator is in green. From Ross *et al*., 2016.

An indirect transcriptional control mediated by (p)ppGpp/DksA is based on σ factor competition (Figure 16). In bacteria, the promoter selection by RNAP is especially mediated by σ factors which allow the RNAP-promoter complex formation and are therefore involved in transcription initiation. In *E. coli*, the σ^{70}, also known as RpoD, is a housekeeping sigma factor which allows the transcription of most of the genes during normal growth. Other alternative σ factors, involved in response to environmental changes, are present in bacteria but they show less affinity for RNAP and are less abundant than the σ^{70} factor. During the stringent response, the σ^{70}-dependent promoters are inhibited by (p)ppGpp/DksA and RNAP are subsequently free for transcription via alternative σ factors (Bernardo *et al*., 2006; Costanzo *et al*., 2008).

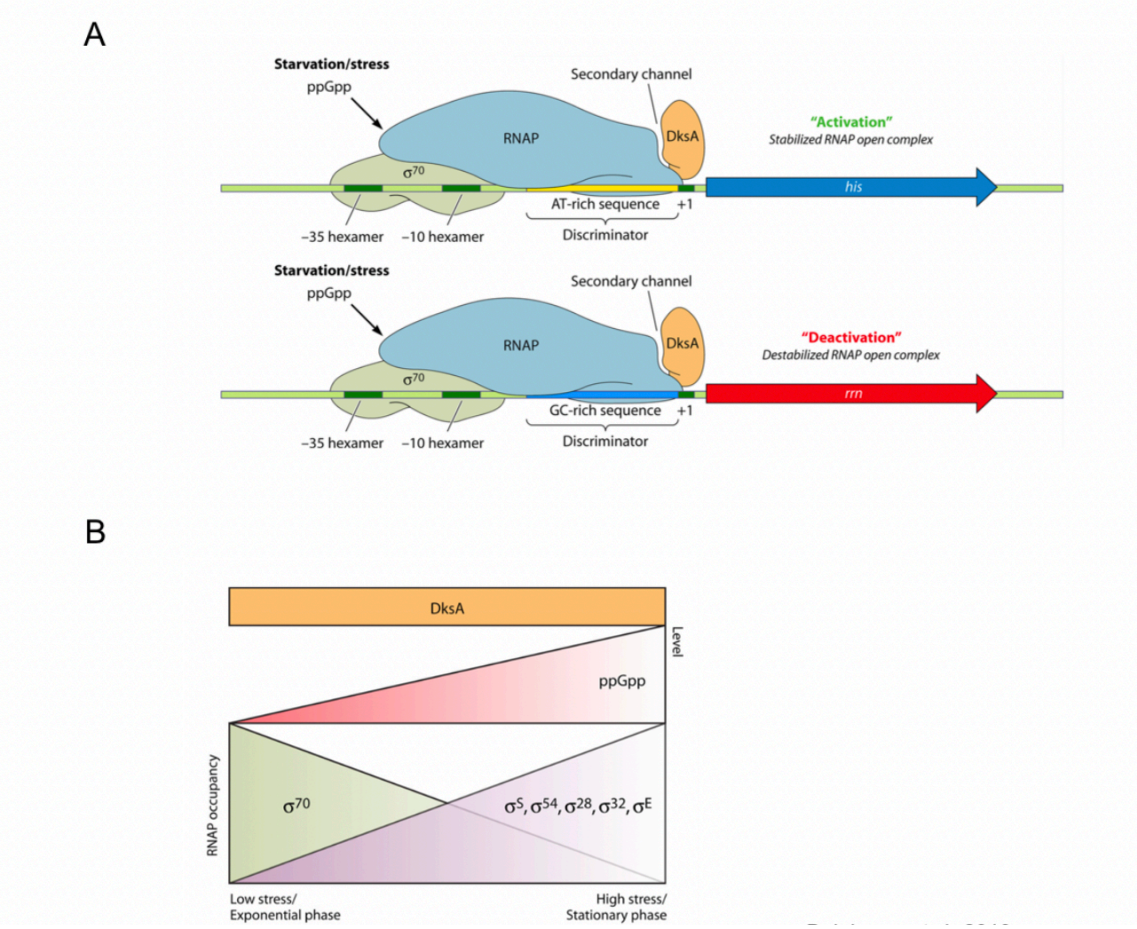

Figure 16: Transcriptional regulation mediated by (p)ppGpp and DksA in *E. coli*. Promoters that typically present AT-rich discriminator between the -10 box and the +1 site of transcription are activated by (p)ppGpp/DksA. On the contrary, promoters presenting an GC-rich sequence at the same place are negatively regulated by (p)ppGpp/DksA (A). The regulation of transcription by (p)ppGpp/DksA is also mediated through sigma factors competition. During exponential phase of growth, when nutrients are available, the σ^{70} is present in high concentration and allows the transcription of housekeeping genes such as rRNA operons. During stress, (p)ppGpp increases and, with the cooperation of DksA, inhibits the transcription from rRNA promoters, leading the RNAP free to be bound by alternative σ factors involved in stress response (B). Modified from Dalebroux *et al*., 2010

In addition to its role in transcriptional regulation, DksA was shown to be involved in double strands breaks repair since a Δ*dksA* mutant is more sensitive to DNA damaging agents like UVs or ionizing radiations. The exact mechanism involved in this process is still unknown, but the authors proposed that DksA could help DNA repair process by destabilizing the RNAP-DNA complex, therefore leaving the way open for recombination proteins (Myka *et al*., 2019).

III.2.2. Effect on DNA replication

Since bacterial growth involves three main processes which are the increase in cellular mass, the DNA replication and the cell division, it was not surprising that (p)ppGpp exerts also an inhibition on DNA replication. This regulation was investigated in different bacterial models and the studies revealed a particular plasticity regarding the (p)ppGpp-mediated control of chromosome replication.

(p)ppGpp has been shown to inhibit the DnaG primase directly, which is part of the DNA polymerase III holoenzyme, in both *E. coli* and *B. subtilis*. However, studies reported first that the replication steps targeted were different between both species, and secondly that pppGpp was more efficient than ppGpp in *B. subtilis*, while it was the opposite in *E. coli*, *i.e.* ppGpp showed a stronger effect than pppGpp (Zyskind and Smith, 1992; Schreiber *et al*., 1995; Wang *et al*., 2007). In *E. coli*, the overexpression of a truncated version of *relA* (without the C-terminal domain), that induced an increase of intracellular (p)ppGpp, led to a partial inhibition of DNA replication but did not prevent septum formation and division. This led to smaller cells as it is generally observed during stationary phase condition. (p)ppGpp mainly affects replication at the initiation step and does not impact the elongation phase, since replication forks were shown to progress until termination during (p)ppGpp overproduction condition and that bacteria can therefore finish an ongoing replication round (Schreiber *et al*., 1995; Ferullo and Lovett, 2008).

In addition to impact the DnaG primase, (p)ppGpp was shown to affect the intracellular levels of DnaA in *E. coli*, which could explain why the initiation step was principally affected in this species (Zyskind and Smith, 1992; Chiaramello and Zysking, 1990). However, a recent study highlighted that replication was still inhibited by (p)ppGpp even when DnaA was produced ectopically, indicating that other regulation mechanisms should be targeted by (p)ppGpp (Kraemer *et al*., 2019). Indeed, mutations in *seqA* and *dam* genes prevented the replication inhibition observed during stringent response, suggesting that these factors could also been involved in (p)ppGpp-mediated replication arrest in *E. coli* (Ferullo and Lovett, 2008).

Another model for replication regulation the during stringent response is based on the presence of an active transcription. It was already reported that transcription by RNAP was needed to induce new rounds of chromosome replication (Lark, 1972). During transcription, the RNAP induces supercoils in DNA which promote the origin melting and thus, replication initiation (Asai *et al*., 1990). In their study, Kraemer *et al*. showed that (p)ppGpp can act on

replication through the modulation of the supercoiling in *oriC*. By maintaining transcription at the origin, they showed that initiation still occurs in the presence of high (p)ppGpp concentration, by using a mutant of the RNAP which is unresponsive to (p)ppGpp or by inserting a promoter which is not regulated by (p)ppGpp near *oriC* (Kraemer *et al*., 2019).

As observed in *E. coli*, (p)ppGpp was shown to modulate cell cycle progression and especially the DNA replication process in *C. crescentus* (Lesley and Shapiro, 2008; Boutte *et al*., 2012; Gonzalez and Collier, 2014). In *C. crescentus*, carbon starvation, which triggers the stringent response and (p)ppGpp production, induced a decrease in DnaA concentration. It was reported that swarmer cells lacking *spoT* initiated DNA replication even upon carbon starvation (Lesley and Shapiro 2008). Moreover, the proteolysis of CtrA, known to block initiation of replication, was induced in the *spoT* mutant (Boutte *et al*., 2012). The modulation of both DnaA and CtrA proteins during the stringent response was demonstrated to be mediated through (p)ppGpp since the levels of DnaA and CtrA respectively decreased and increased in a mutant able to overproduce (p)ppGpp in the absence of starvation. The overproduction of (p)ppGpp induced an extension of the G1 phase before the S phase starts rather than a complete arrest of the cell cycle, correlating with the hypothesis that in addition to mediate response to stresses, (p)ppGpp could be involved in controlling the length of the G1 phase (Gonzalez and Collier, 2014).

III.3. (p)ppGpp and virulence

The acquisition of virulence factors constitutes an adaptation for pathogenic bacteria, in order to reach, invade, and colonize new host environments, and (p)ppGpp has been reported to regulate such pathogenic features.

In *Legionella pneumophila*, (p)ppGpp has been linked to the differentiation event that occurs during its infection cycle. *L. pneumophila* presents two distinct forms which determines its life cycle (Rowbotham *et al*., 1986; reviewed in Dalebroux *et al*., 2010; Oliva *et al*., 2018). Upon nutrient limitations, which is typically the environment encountered when bacteria enter in its host cells, *L. pneumophila* presents a transmissive form characterized by motility, lysosomes resistance, and cytotoxicity towards host cells. This state is characterized by an increase in intracellular (p)ppGpp and, when the environment become more favorable, in the ER-derived vacuole, bacteria convert into the replicative form and proliferate exponentially (Rowbotham *et al*., 1986). This transition between both forms has been linked to the degradation of (p)ppGpp by the HD of SpoT. When conditions start to deteriorate with the

acidification of the vacuole and that nutrients decline, the SD domain of SpoT produces (p)ppGpp and bacteria enter in their transmissive form (Dalebroux *et al*., 2009). It has been reported that the artificial synthesis of (p)ppGpp is sufficient to induce the transition between the replicative form to the transmissive form. This later is especially competent to resist to lysosomal degradation and to migrate to new host cells in order to establish a new infection (Abu-Zant *et al*., 2006). (p)ppGpp has been demonstrated to be essential for the transmission to new hosts, since a double mutant for *relA* and *spoT* can replicate in macrophages but is rapidly degraded with acidification of the vacuole and therefore is not able to spread (Abu-Zant *et al*., 2006).

Brucella spp. encode an RSH homolog of $SpoT_{coli}$ showing 36% identity (for RSH of *B. melitensis,* RSH_{Bm}). Several studies have highlighted the role of *Brucella* RSH in the survival in minimal poor medium and during pathogenesis (Köhler *et al*., 2002; Kim *et al*., 2003; Dozot *et al*., 2006). A screen for *B. suis* mutants that are unable to replicate inside human macrophages revealed that transposon insertions in *rsh* gene led to an attenuation in infection (Köhler *et al*., 2002). In addition, this study highlighted the essentiality of amino acid synthesis pathways during infection, suggesting that this nutrient is not available, or is too low in host cells and therefore reinforces the hypothesis that bacteria encounter starvation during the infection process. This was consistent with the *rsh* mutant attenuation observed during infection, since (p)ppGpp was shown to be involved in the response to amino acid starvation in other bacteria. Further studies indicated that RSH from *B. melitensis*, *B. suis* and *B. abortus* was also required for the establishment of a successful infection process *in vitro* and in mice, suggesting that the importance of *rsh* in pathogenesis could constitute a common characteristic among *Brucella spp*. (Kim *et al*., 2005; Dozot *et al*., 2006). However, investigations of the survival of *rsh* mutants in acidic environment highlighted different phenotypes according to the species tested. *B. abortus rsh* mutants were more sensitive to acidic conditions than the WT, whereas in *B. melitensis* and *B. suis* RSH was not important for acid resistance (Kim *et al*., 2005; Dozot *et al*., 2006). This suggested the existence of a plasticity among *Brucella* species regarding the RSH-mediated response according to stresses encountered.

The phenotype observed during infection for mutants lacking *rsh* was suggested to be linked to the Type 4 Secretion System (T4SS) encoded by the *virB* operon. The T4SS is a virulence factor which is essential for bacteria to reach the replicative niche inside the host. Indeed, bacteria lacking the *virB* operon cannot reach the ER and are stalled in the Lamp1-positive compartment. The deletion of *rsh* in *B. suis* and *B. melitensis* was shown to inhibit the expression of the *virB* operon in cultures. On the opposite, the overexpression of *rsh* led to

expression of *virB* during mid-exponential phase of growth whereas the WT strain did not show expression during this phase (Dozot *et al*., 2006). These data suggest a link between *rsh* expression and *virB* expression, but the molecular mechanism is unkown.

The pleiotropic effect induced by the lack of RSH has been illustrated by a cDNA microarray experiment which reported the differential transcription profiles of *B. suis* WT and Δ*rsh* strains in poor minimal medium. Among the 379 genes differentially expressed between both strains, which represents 11.6% of the genome, genes coding for proteins related to metabolism (amino acids, fatty acids and proteins), transcription regulation, cell envelope, and transport were shown to be particularly impacted by the lack of RSH (Hanna *et al*., 2013).

Objectives

Objectives

The cell cycle of *Brucella abortus* was demonstrated to be intimately linked to its virulence. First, bacteria that are in G1 phase were shown to be more infectious in a context of *in vitro* infection. Secondly, the infection process presented two distinct phases, with a first non-proliferative step where bacteria are blocked in G1 phase and do not grow, and a second step characterized by the active proliferation of the pathogen inside its intracellular niche. The fact that bacteria remain blocked in G1 phase during the first hours of the infection suggests that their cell cycle is differentially regulated in this condition compared to in rich culture medium (Deghelt *et al*., 2014).

The aim of this project is the investigation of the replication regulation in *B. abortus*, in order to get insight on mechanisms potentially involved in the replication arrest observed during the infection. In this context, we want to develop our investigation based on what is already known in *C. crescentus* regarding the regulation of replication. We focused our study on factors that are involved in the control of the replication initiator DnaA in *C. crescentus*, which are conserved in *B. abortus.* In that purpose, we first want to create mutants depleted for (p)ppGpp and mutants in which the alarmone is overproduced. Using these strains, we first plan to study the impact of (p)ppGpp on the cell cycle of *B. abortus* with emphasis on DNA replication regulation. Secondly, the characterization of these strains during *in vitro* infection of host cells will allow us to learn more about the involvement of (p)ppGpp in the *B. abortus* virulence. Secondly, the ClpSA protease, which is in part responsible for the proteolysis of DnaA in *C. crescentus*, is conserved in *B. abortus*. In order to study the potential involvement of this protease in the regulation of replication we plan to create a deletion strain for *clpSA* and monitor the level of DnaA as well as the ability of this strain to infect host cells. Finally, we would like to investigate the role of HdaA in *B. abortus* and more particularly its subcellular localization since HdaA from *C. crescentus* colocalized with the replisome. In that purpose, we plan to create a *B. abortus* strain producing a HdaA-YFP fusion protein. With this work, we will attempt to decipher mechanisms used by *B. abortus* to control its DNA replication and which are potentially involved in cell cycle control during infection.

A second part of the project will be based on *in silico* analyses of genomic regions which should be involved in DNA replication, *i.e* the replication origins *oriI* and *oriII*, as well as the *dnaA* locus and how this later could be transcriptionally regulated. We especially plan to focus these analyses on the prediction of DnaA-binding boxes, GANTC motifs and GcrA-binding sites. These analyses could be of great interest for further investigations on replication control and on the synchronization of chromosome I and chromosome II replication in *B. abortus*.

Results

Results

The results presented here is a modified part of a scientific article which is currently in preparation, and include additional data that are not planned to be published.

I. Investigation of the role of (p)ppGpp in *Brucella abortus*.

I.2. The *rsh* deletion impacts the growth in minimal medium and the infection process

The Δ*rsh* mutant presented aberrant morphologies, such as branched or swolled bacteria, during exponential growth in 2YT rich medium (Figure 17). We assayed the growth of Δ*rsh* in 2YT rich culture medium as well as in Plommet minimal medium supplemented by erythritol as carbon source. The growth of Δ*rsh* in 2YT was similar to the WT strain during exponential phase but the shift into stationary phase occurred later and at a higher OD compared to the WT (Figure 18A). However, in Plommet minimal medium supplemented by erythritol as carbon source, Δ*rsh* showed a clear growth defect compared to the WT as the OD rapidly decreased during mid-exponential phase. This indicated that Δ*rsh* mutant was impaired for growth (and maybe survival) in this medium, as expected for a $ppGpp^0$ mutant (Figure 18B). As the eBCV is known to be an acidic environment during the infection process we repeated this growth experiment in Plommet erythritol at pH 5.0 (Figure 18C). The growth of both WT and Δ*rsh* was impaired in this medium, with a more pronounced defect for the Δ*rsh* strain even with the presence of a high variability between the three independent experiments.

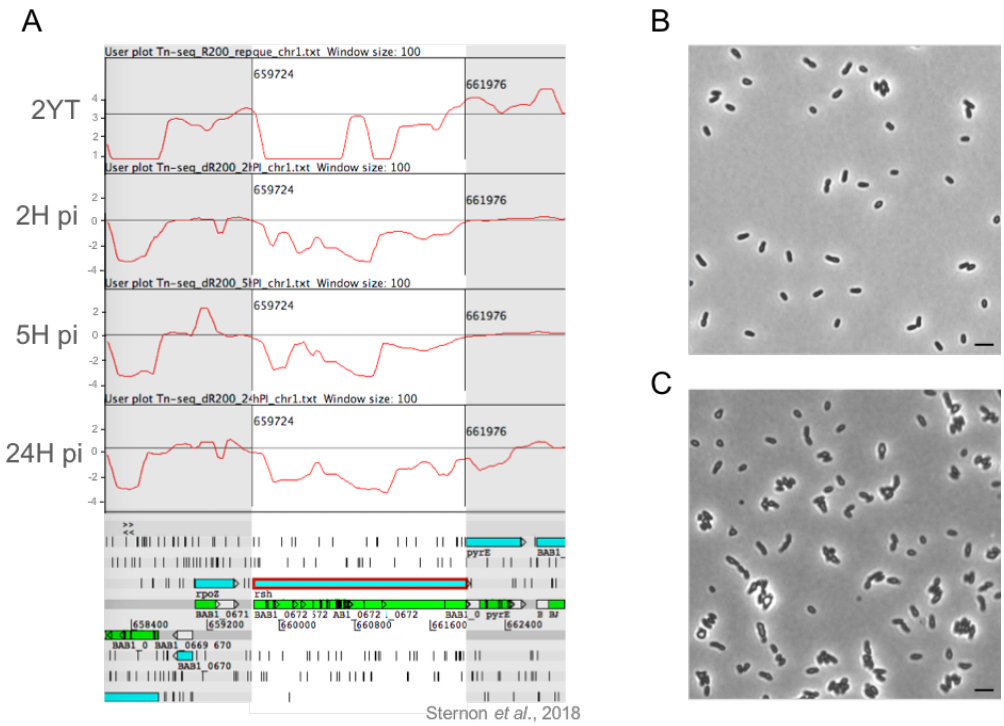

Figure 17: Tn-seq profile of the *rsh* gene and morphology of the Δ*rsh* mutant. (A) The Tn-seq profiles in the control 2YT rich medium, 2 hours (2H pi), 5 hours (5H pi) and 24 hours (24H pi) post-infection, are shown with the red lines which represent the global insertion of transposons in the genome (R200 representing the log10 of the number of mini-Tn5 insertion(s)+1 computed in a sliding window of 200 bp). The thin gray line represents the mean of transposons insertion (R200) per chromosome. The corresponding genomic map (position of the coding sequences) is indicated below. Morphology of WT **(B)** and Δ*rsh* mutant **(C)** was observed by phase contrast microscopy using bacteria in exponential phase of growth in 2YT rich culture medium. Scale bar represents 2 µm.

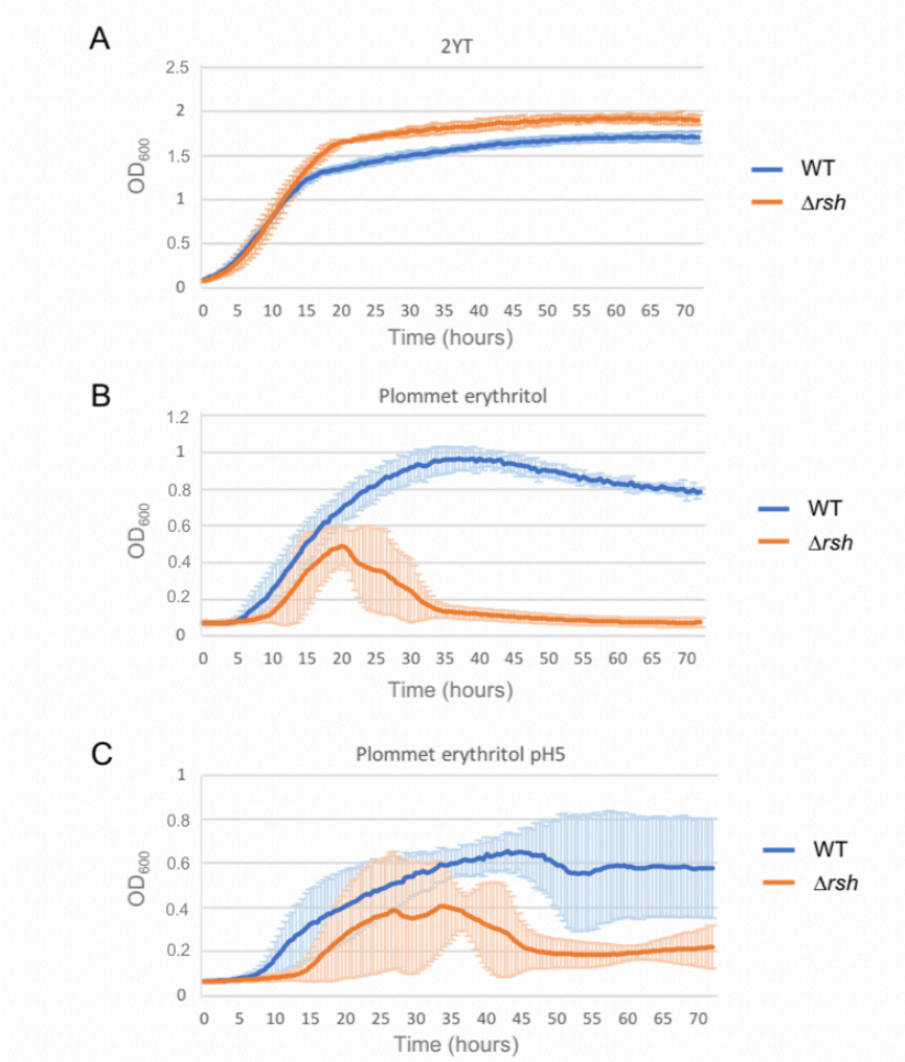

Figure 18: Growth curves using *B. abortus* WT and Δ*rsh* strains in different culture media. Bacteria in exponential phase of growth in 2YT medium were used and the OD_{600} was normalized at 0.1 before starting the experiments. Bacteria were incubated at 37°C with shaking and the OD_{600} was measured every 30 minutes. The graph represents biological triplicates of three independent experiments and the error bars represent the standard deviation from the mean for each measured time point. The experiments were performed in 2YT rich medium (A), in Plommet minimal medium supplemented by erythritol (2g/L) (B), and in Plommet minimal medium supplemented by erythritol (2g/L) at pH 5.0 (C).

In the previous study of Kim *et al*., 2005 the authors indicated that a *B. abortus* Δ*rsh* mutant failed to replicate inside bone-marrow-derived macrophages. We tested the ability of Δ*rsh* to infect and multiply inside RAW 264.7 macrophages *in vitro* compared to the WT strain by performing CFUs experiments. The Δ*rsh* mutant showed a significant decrease in CFUs number at 4 hours and 24 hours post-infection compared to the WT strain (Figure 19) suggesting that *rsh* gene is required for the establishment of the infection process and probably the survival at short times post-infection in this cellular model.

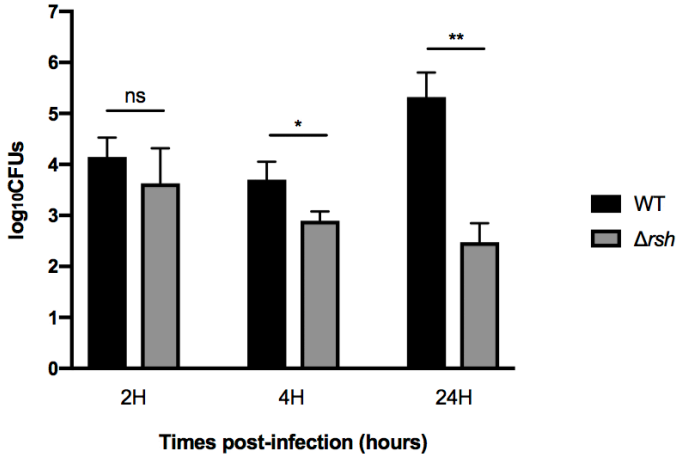

Figure 19: Infection of RAW 264.7 macrophages with *B. abortus* WT and Δ*rsh* strains. CFUs (Colony Forming Units) were counted after 2 hours, 4 hours and 24 hours post-infection. Bacteria used for the experiments were in exponential phase of growth and a MOI (Multiplicity of Infection) of 50 was used for the infection. Error bars represent the standard deviation from the means of three independent experiments (biological triplicates). A *t* test was used for the statistical analyses. The significant differences in CFUs number are indicated by * ($p < 0.05$) and ** ($p < 0.01$).

I.3. The artificial hydrolysis of (p)ppGpp leads to a Δ*rsh* phenotype during infection

Since RSH is responsible for (p)ppGpp homeostasis and that a Δ*rsh* mutant failed to proliferate inside host cells, we decided to test the involvement of (p)ppGpp in the infection process. To do so, we took advantage of the *mesh1* gene from *Drosophila melanogaster* that encodes a strong (p)ppGpp hydrolase as described in Sun *et al*., 2010. We adapted the *mesh1* coding sequence for codon bias usage of *B. abortus* and expressed the resulted gene from an IPTG inducible promoter on a replicative plasmid (*B. abortus* pBBRi-*mesh1b* strain). The resulting strain did not show abnormal morphologies as the Δ*rsh* mutant. The growth of this strain in 2YT rich medium with or without IPTG was assessed by bioscreen and was comparable to the WT. We tested the growth of this strain in Plommet minimal medium supplemented by erythritol, with or without IPTG (Figure 20). The pBBRi-*mesh1b* strain presented a slight growth defect compared to the WT. The addition of IPTG for the induction of *mesh1b* led to the same phenotype than when IPTG is absent probably because our IPTG-inducible system is slightly leaky. Indeed, since Mesh1 possesses a strong hydrolase activity, even in *E. coli* (Sun *et al*., 2010), the weak expression of *mesh1b* that occurs without IPTG could be sufficient to lead to the same phenotype than the one observed for pBBRi-*mesh1b* strain during the

induction. Alternatively, IPTG induction may be inefficient in this strain, or excess of Mesh1 due to the induction could be cleared from the bacteria.

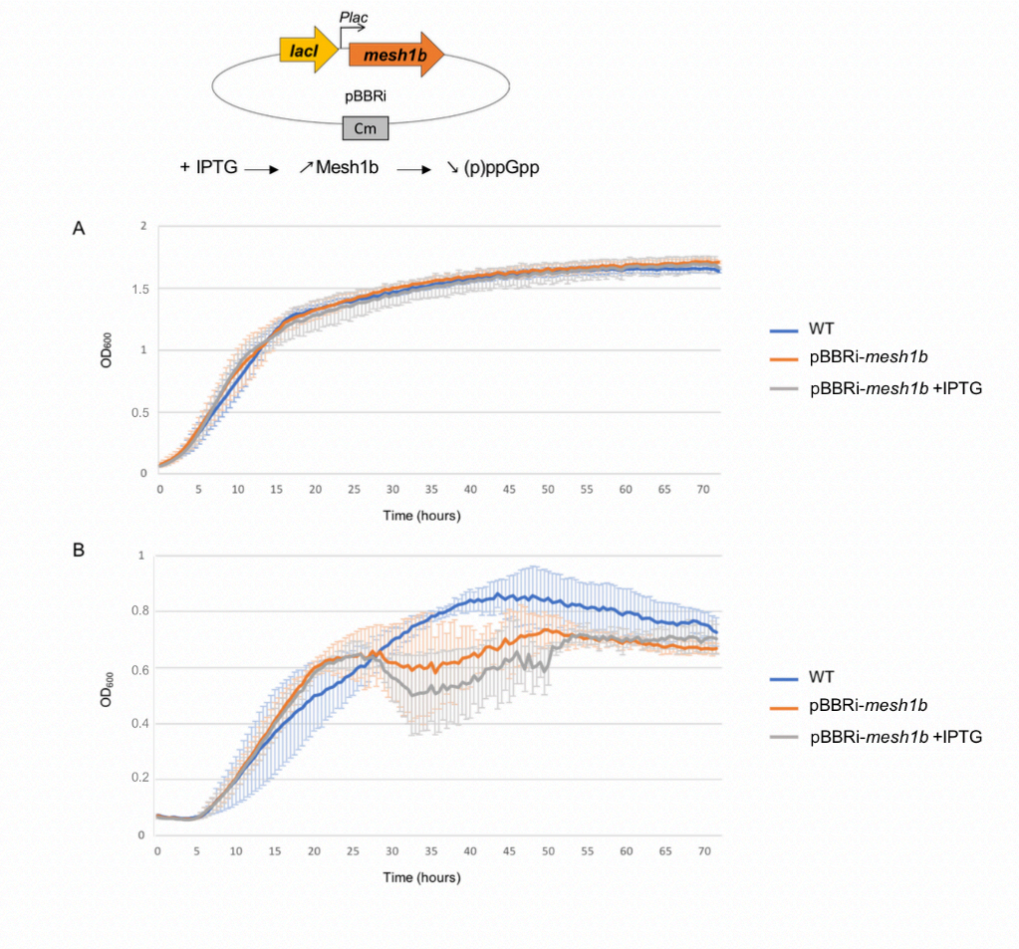

Figure 20: Growth of pBBRi-*mesh1b* strain. Growth curve of the *B. abortus* WT and pBBRi-*mesh1b* in 2YT rich culture medium (A) and in Plommet minimal medium supplemented with erythritol (B), with or without IPTG. Bacteria in exponential phase of growth were used and the OD_{600} was normalized at 0.1 before to start the experiments. Bacteria were incubated at 37°C with shaking and the OD_{600} was measured every 30 minutes. The graphs represent biological triplicates of three independent experiments and the error bars represent the standard deviation from the mean for each OD_{600} measure.

We assessed the ability of the pBBRi-*mesh1b* strain to infect and proliferate inside RAW 264.7 macrophages *in vitro*. Bacteria were induced in 2YT IPTG (1 mM) during 3 hours and then were used to infect host cells. The induction was kept during the whole infection experiment by adding IPTG (10 mM) to the infection medium. Interestingly, the pBBRi-*mesh1b* strain showed an absence of increase in CFUs number at 24 hours post-infection compared to the WT (Figure 21). Again, as we observed with the growth experiment, the same phenotype was obtained for the pBBRi-*mesh1b* strain whether bacteria are induced or not with IPTG.

The phenotype observed for the pBBRi-*mesh1b* compared to the WT was less dramatic than the one observed for the Δ*rsh* mutant compared to the WT. This "intermediate" phenotype could be the reflect of an equilibrium between endogenous (p)ppGpp synthesis and its hydrolysis by Mesh1b. This result suggests that (p)ppGpp should play an important role in proliferation inside macrophages and in the establishment of a successful infection.

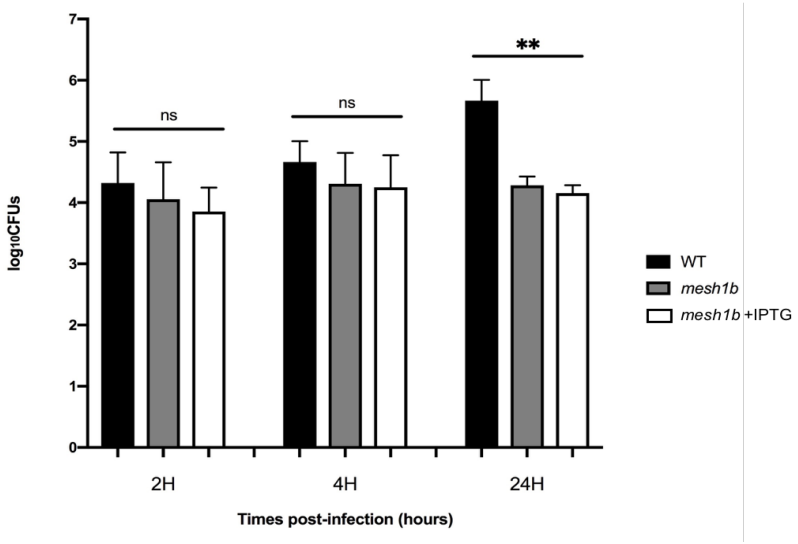

Figure 21: Infection of RAW 294.7 macrophages with the WT and the *pBBRi-mesh1b* strains. Bacteria used for the experiments were in exponential phase of growth and a MOI (Multiplicity of Infection) of 50 was used for the infection. CFUs were harvested and counted at 2, 4, and 24 hours post-infection. Error bars represent the standard deviation from the means of three independent experiments (biological triplicates). A *t* test was used for the statistical analyses. The significant difference in CFUs number is indicated by ** ($p < 0.01$).

I.4. Mutation in hydrolase domain of *rsh*

In order to get more insight on the role of (p)ppGpp in *B. abortus,* we wanted to create a strain presenting an increase in the concentration of the alarmone. In the study of Ronneau *et al*., 2016 the authors showed that the D81G mutation in the hydrolase domain of *C. crescentus* SpoT abolished the hydrolase activity of the protein that led to an intracellular increase in (p)ppGpp. The D81G mutant presented a growth delay in rich culture medium as well as an increase of G1 bacteria (Ronneau *et al*., 2016). An alignment of $SpoT_{crescentus}$ and $RSH_{abortus}$ sequences revealed that the aspartate D81 is conserved in *B. abortus* and corresponds to the residue D62 (Figure 22). We constructed the D62G mutant strain of *B. abortus* by allelic exchange and tested its growth in 2YT rich medium (Figure 23). The mutant

presented the same growth than the WT indicating that the D62G mutation does not lead to the same phenotype than the one observed in *C. crescentus* D81G.

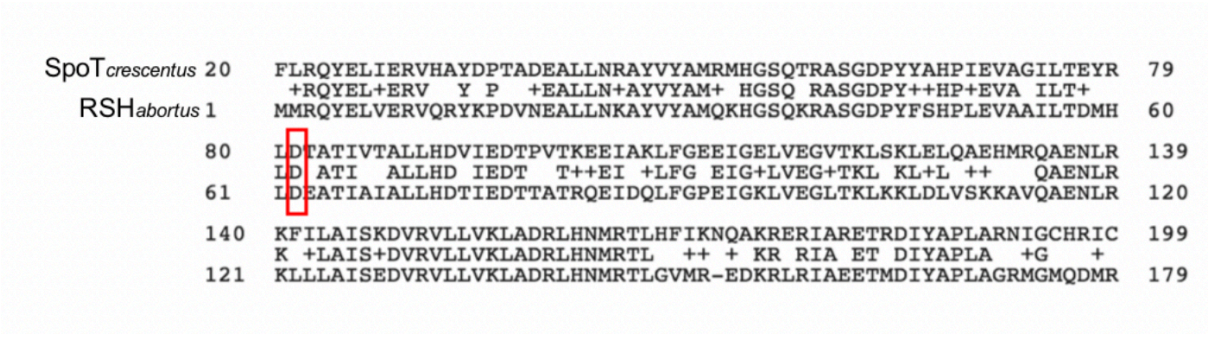

Figure 22: Alignment of SpoT*crescentus* and RSH*abortus*. The conserved aspartate residue (81D in *C. crescentus* and 62D in *B. abortus*) is framed in red.

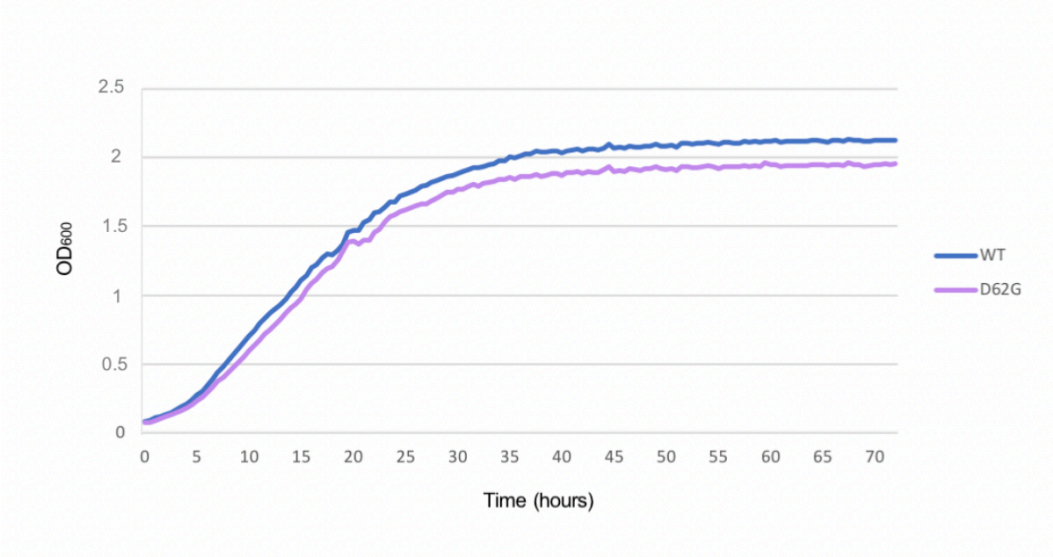

Figure 23: Growth curve of the *B. abortus* WT and the D62G mutant in 2YT rich culture medium. Bacteria in exponential phase of growth were used and the OD_{600} was normalized at 0.1 before starting the experiments. Bacteria were incubated at 37°C with shaking and the OD_{600} was measured every 30 minutes.

I.5. Artificial production of (p)ppGpp impacts bacterial growth and chromosome replication

In order to get more insight about the role of (p)ppGpp in *B. abortus* and since the D62G mutation has no impact on growth, we constructed a strain that artificially produces this alarmone. We used a version of the *relA* gene from *E. coli*, named *relA'-flag* (Gonzalez and Collier, 2014) that we inserted downstream an ITPG-inducible promoter on the pSRK replicative plasmid (Khan *et al*., 2008). The RelA'-flag version is truncated in order to remove regulatory domains at the C-Terminal part so that the protein can synthetize (p)ppGpp constitutively. The resulting plasmid named pSRK-*relA'* produces a non-regulated (p)ppGpp synthetase in *Brucella* when IPTG is added to the medium. As negative controls, we used strains containing the pSRK-∅ (empty vector) and the pSRK-*relA'** containing a point mutation leading to a non-functional version of RelA that cannot synthesize (p)ppGpp (Gonzalez and Collier, 2014). We assayed the growth of these strains in 2YT rich culture medium with or without IPTG induction. The pSRK-*relA'*, pSRK-∅, pSRK-*relA'** and the WT strains grew equally in 2YT, however, when IPTG was added to the medium a growth delay was only observed for the pSRK-*relA'* strain (Figure 24 and 25).

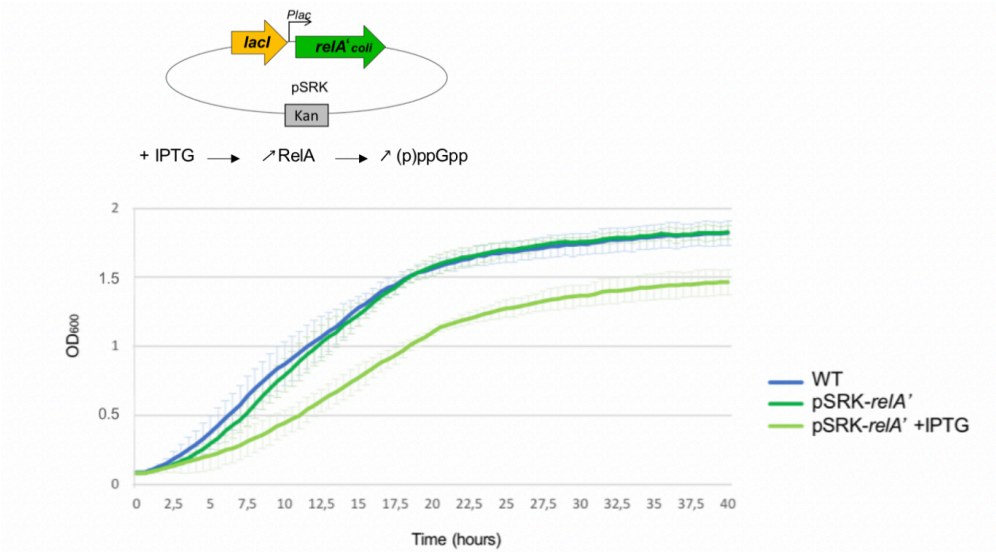

Figure 24: Structure of the pSRK-*relA'* plasmid and growth curve of *B. abortus* pSRK-*relA'*. The *relA'* gene was placed under the control of the *lacI-Plac* promoter system on the replicative plasmid pSRK. The addition of IPTG in the culture medium leads to the expression of *relA'*, and subsequently, the production and RelA' and (p)ppGpp. The growth of this strain was assessed in 2YT rich medium with or without IPTG at 37°C with shaking.

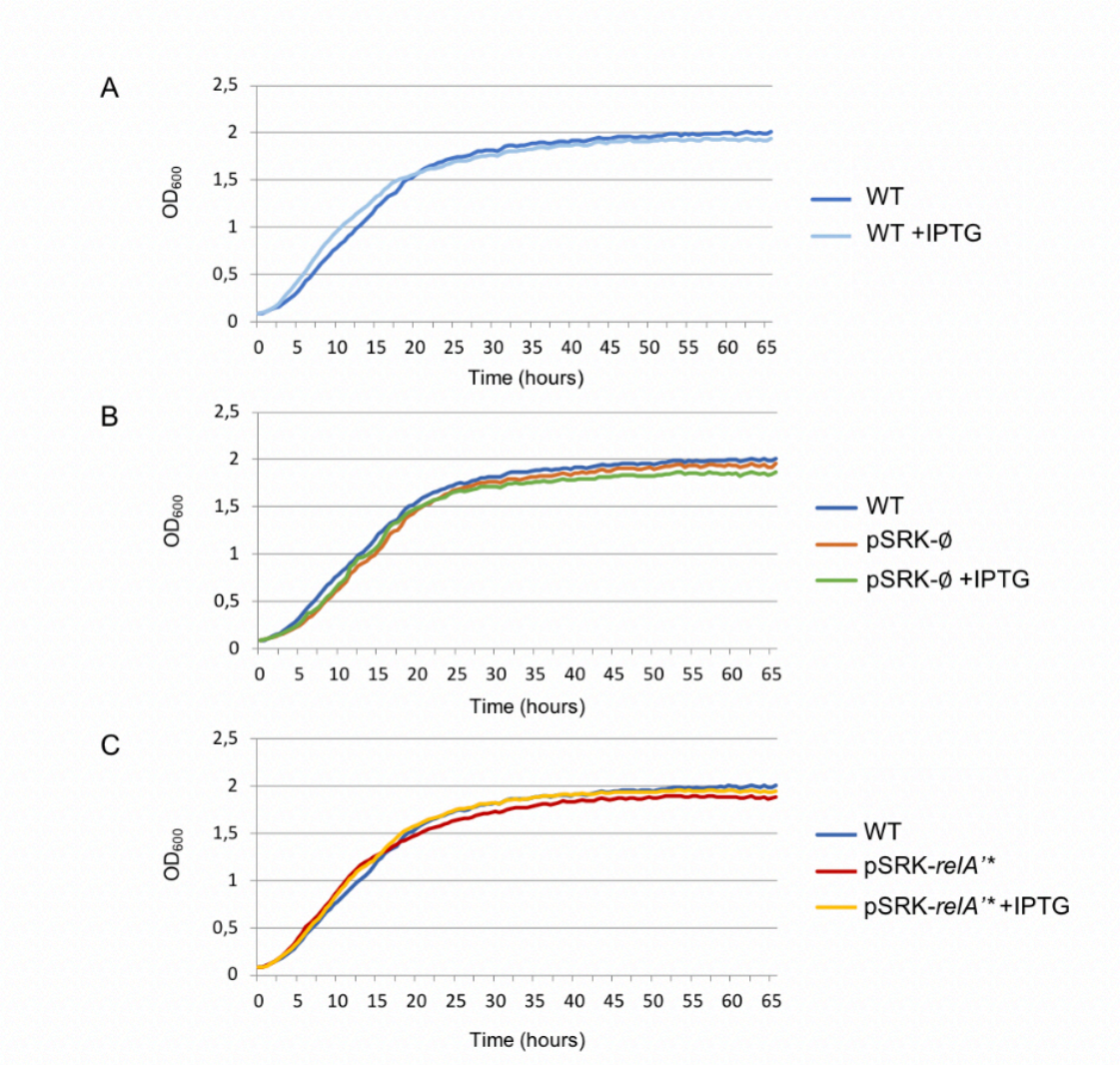

Figure 25: Negative controls for the pSRK-*relA'* growth experiments. We tested the effect of IPTG on the growth of WT strain (A), on the growth of *B. abortus* containing the pSRK empty vector (pSRK-∅) (B) and on the growth of *B. abortus* containing the pSRK-*relA'** (C). All these controls were performed in 2YT at 37°C with shaking and used exponential phase bacteria to start the experiments. A concentration of 1mM IPTG was used.

Since *rsh* is present in the pSRK-*relA'* containing strain, the (p)ppGpp molecules that are overproduced can still be degraded by the hydrolase domain of RSH. We constructed a pSRK-*relA'* strain where *rsh* was deleted in order to see the effect of a (p)ppGpp overproduction without RSH-dependent degradation. As expected, the delayed growth phenotype of this strain in 2YT with IPTG was accentuated compared to the strain where *rsh* is still present (Figure 26). The growth of the Δ*rsh* pSRK-*relA'** strain in presence or absence of IPTG was used as negative control (data not shown).

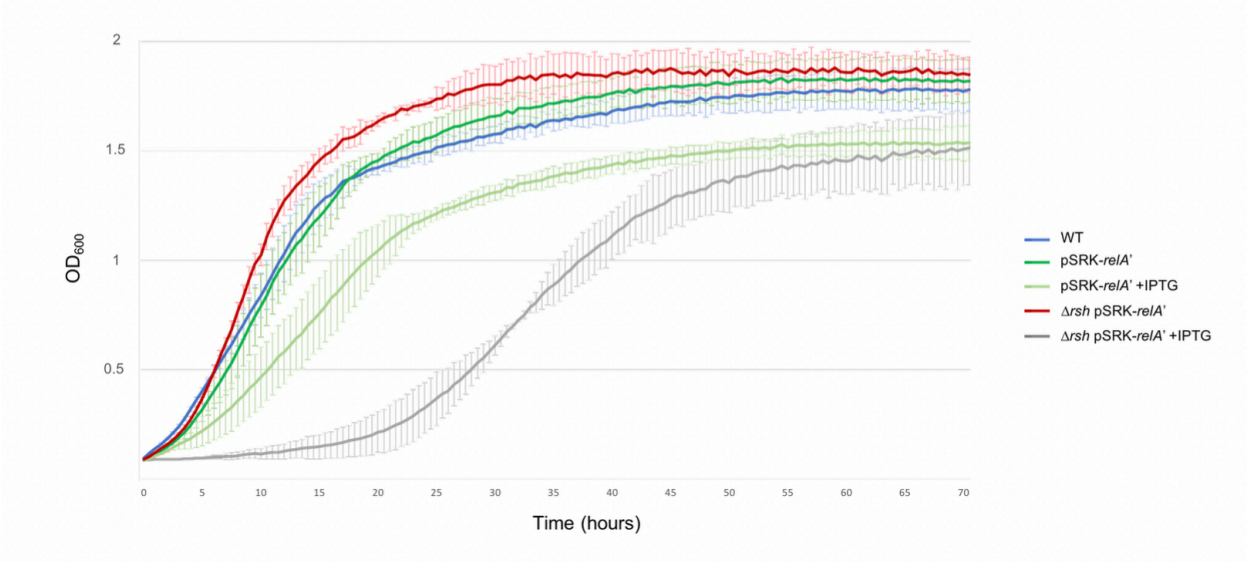

Figure 26: Growth curve of WT, pSRK-*relA'* and Δ*rsh* pSRK-*relA'*. Bacteria in exponential phase of growth were used at time 0H and the OD_{600} was normalized at 0.1 before starting the experiments. The growth of these strains was assessed in 2YT rich medium with or without IPTG (1mM) at 37°C with shaking.

We analysed the morphology of the pSRK-*relA'* strain induced for 6 hours by phase microscopy and noticed that bacterial cells were smaller than the non-induced cells, with a coccobacillus shape typically observed during the stationary phase (Figure 27). Since it was already reported that (p)ppGpp has an impact on DNA replication in other bacterial species (Schreiber *et al*., 1995; Gonzalez and Collier, 2014; Ronneau *et al*., 2016), we also analyzed the DNA content in pSRK-*relA'* induced and non-induced with IPTG by flow cytometry. We clearly saw an increase of bacteria presenting one copy of the genome, *i.e*. the peak corresponding to 1n (Figure28). To confirm this result and because we cannot distinguish chromosome I from chromosome II with flow cytometry, we took advantage of a *B. abortus* strain allowing us to monitor the chromosomal replication status at the single cell level in order to study the impact of (p)ppGpp overproduction on DNA replication of chromosome I. This strain expresses a *mcherry-parB* allele that allows to highlight replication origin(s) of chromosome I (*i.e* one mCherry focus means that replication/segregation has not yet started and the bacterium is in G1 phase, and two mCherry foci correspond to two segregated replication origins meaning that bacteria have already started replication and are subsequently in S or G2 phase) (see section I.6. of the Introduction part) (Deghelt *et al*., 2014). Because this strain was kanamycin resistant and that the pSRK plasmid confers the same resistance, we created two new strains expressing *mcherry-parB* but resistant to other antibiotics. The first strain was constructed

using the same strategy than the “old” one, i.e. contained a pSKoriTcat-*PgidA-mcherry-parB* inserted in the *parB* locus and was chloramphenicol resistant. The second strain was created using the Tn7 system which consist in transposition of mini-Tn7 expressing *mcherry-parB* under the control of its endogenous promoter *PgidA* and the resistance cassette to ampicillin/carbenicillin at the *glmS* locus (mini-Tn7-*PgidA-mcherry-parB*). Both strains were confirmed by fluorescence microscopy for the production of mCherry-ParB (Figure 29). We inserted the pSRK-*relA’* and pSRK-*relA’** in the *B. abortus* mini-Tn7-*PgidA-mCherry-parB* strain and counted the number of G1 bacteria every two hours until 6 hours after inoculation of bacteria in 2YT with or without IPTG. Interestingly, we observed an increase of G1 bacteria over the time of induction for the pSRK-*relA’* strain while the G1 number of the non-induced pSRK-*relA’* and both the induced and non-induced pSRK-*relA’** remained stable (Figure 30). These results strongly suggested that artificial induction of (p)ppGpp synthesis could delay the transition between the G1 phase to the S phase, and subsequently, could have an impact on initiation of chromosomal replication in *B. abortus*.

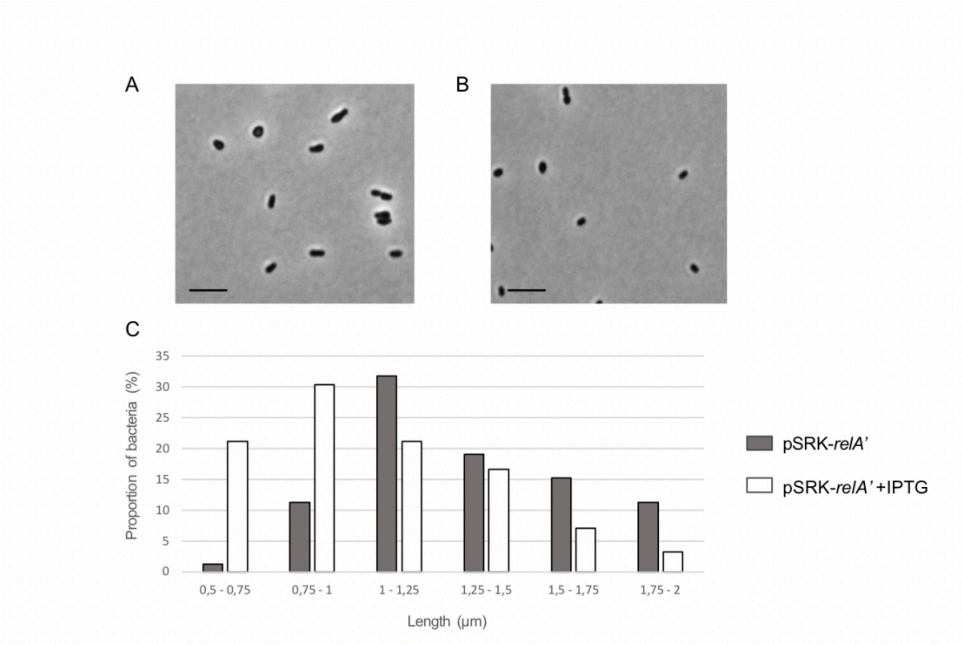

Figure 27: Morphology of the pSRK-*relA’* strain and classification of bacterial cells by length. Bacteria used for the experiment were in exponential phase of growth. They were diluted at OD 0.1 and incubated with shaking at 37°C for 6 hours in 2YT without (A) or with (B) IPTG (1mM). Bacteria were then put on PBS agarose pads and observed with optical phase microscopy. We measured bacterial length with the MicrobeJ software and classified them from 0.5 µm to 2 µm with an interval of 0.25 µm. (n=230 for pSRK-*relA’* +IPTG and n=391 for pSRK-*relA’*) (C). Scale bars represent 5 µm.

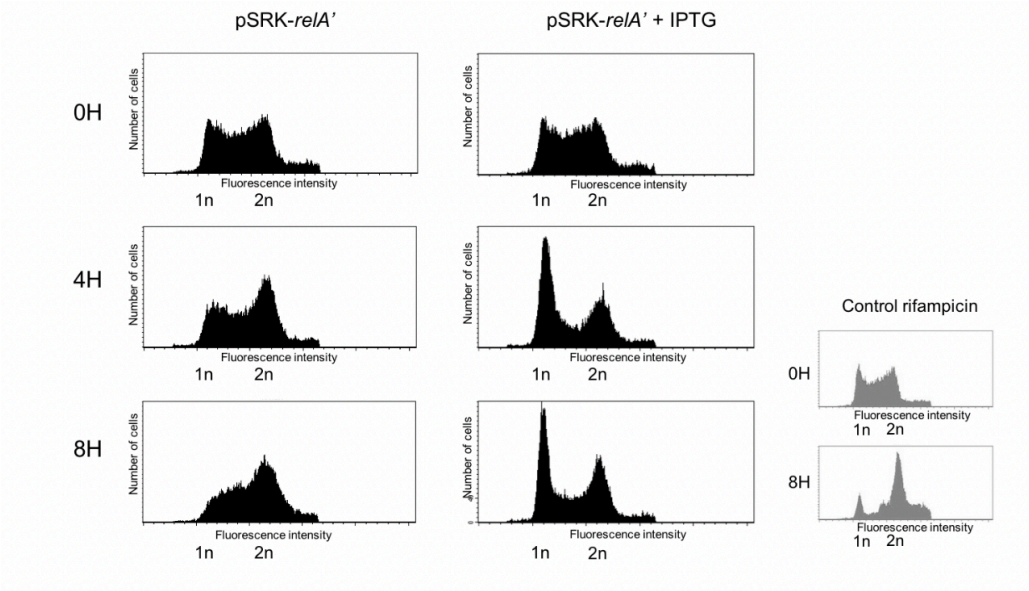

Figure 28: Analysis of DNA content for the pSRK-*relA'* strain with flow cytometry. Bacteria used for the experiments were in exponential phase of growth. They were diluted at OD 0.1 and incubated with shaking at 37°C in 2YT with or without IPTG (1mM). Bacteria were harvested at time 0H, 4H, and 8H and were fixed with ethanol. Samples were labelled with Sytox green prior to be analysed by flow cytometry. A control with rifampicin added to the 2YT was performed as rifampicin blocks initiation of replication.

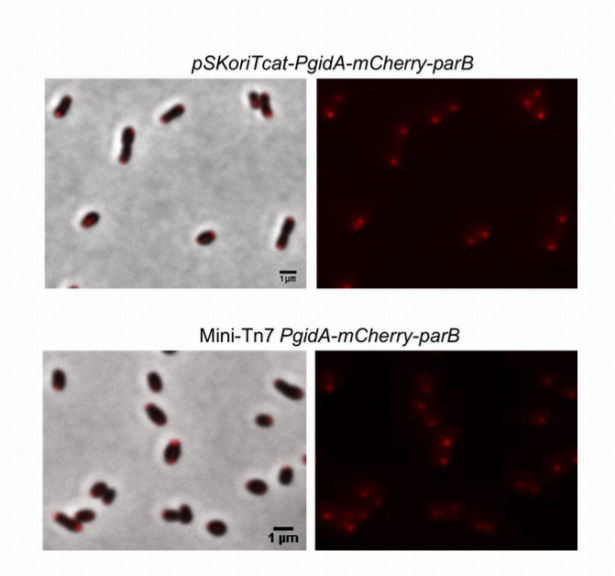

Figure 29: Creation of strains expressing *mcherry-parB* and presenting chloramphenicol and ampicillin resistances. Bacteria used for the experiment were in exponential phase of growth. Bacteria were washed, then put on PBS agarose pad and observed with fluorescence microscope. Scale bars represent 1um.

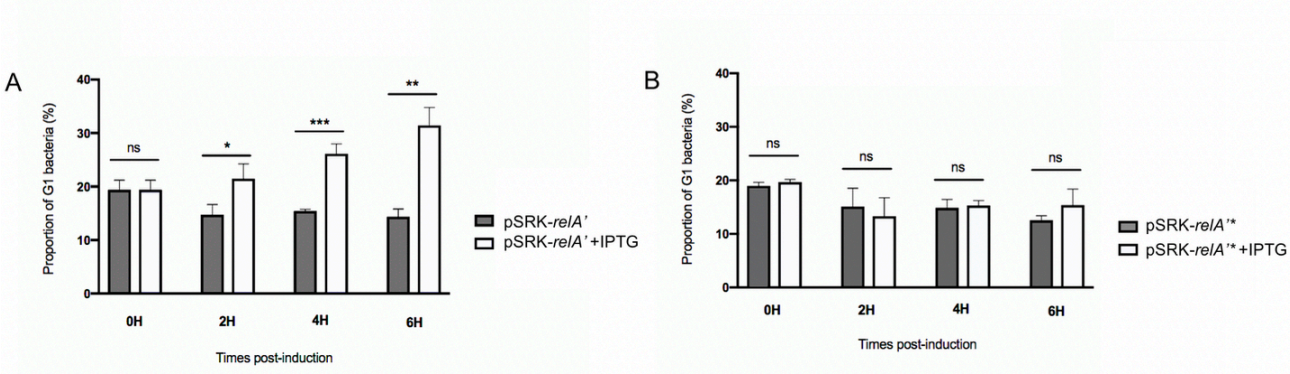

Figure 30: Proportion of G1 bacteria for the *pSRK-relA'* and *pSRK-relA' strains.** Bacteria used for the experiment were in exponential phase of growth, pSRK-*relA'* strain (A), and pSRK-*relA'** (B). They were diluted at DO 0.1 and incubated with shaking at 37°C in 2YT with or without IPTG. Samples were taken every 2 hours and put on PBS agarose pad and were observed with a fluorescence microscope. Bacteria in G1 phase (presenting only one focus of mCherry-ParB) were counted for each time post-induction. Error bars represent the standard deviation from the means of three independent experiments (biological triplicates). The significant differences are indicated by * ($p < 0.05$), ** ($p < 0.01$) and *** ($p < 0.001$).

I.6. (p)ppGpp impacts the level of DnaA

Since an increase of (p)ppGpp induced an increase of G1 bacteria, which probably reflects a blockage of initiation of replication, we compared the abundance of DnaA in WT, Δ*rsh*, pSRK-*relA'* and Δ*rsh* pSRK-*relA'* strains induced or non-induced with IPTG for six hours (Figure 31). Interestingly, we observed a clear decrease of DnaA for both strains pSRK-*relA'* and Δ*rsh* pSRK-*relA'* when they were induced for (p)ppGpp production. The decrease of DnaA was more pronounced for the pSRK-*relA'* strain which lacks *rsh,* and so where (p)ppGpp concentration should be the highest because of the lack of (p)ppGpp hydrolase activity.

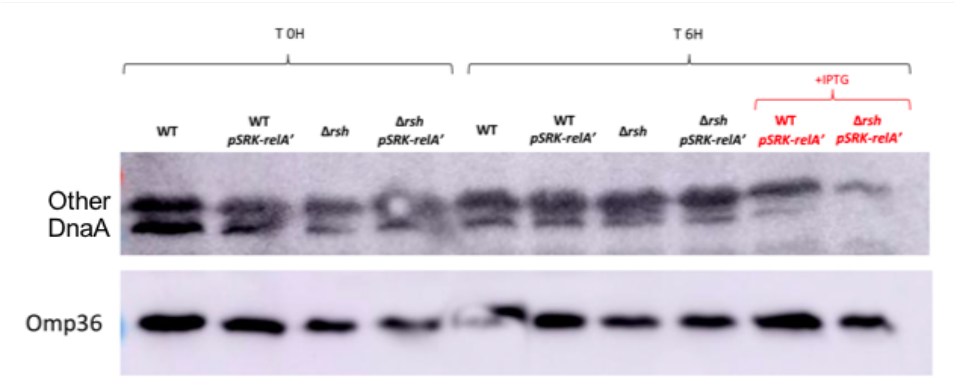

Figure 31: Western blot analysis of WT, pSRK-*relA'*, Δ*rsh and* Δ*rsh* pSRK-*relA'* strains using antibody against DnaA$_{abortus}$. Bacteria in exponential phase of growth were diluted at 0.2 OD at time 0H (T 0H) and were induced (in red) or not with IPTG during 6 hours. Samples were harvested at T 0H and T 6H and were normalized to obtain an OD of 10. The "Other" bands correspond to contamination bands. The Omp36 was used as loading control.

I.7. Overproduction of (p)ppGpp during infection leads to no proliferation in infection

Since (p)ppGpp overproduction seemed to have an impact on replication, *i.e.* an increase of G1 cells in bacterial population, and that the G1 bacteria are more infectious, we decided to investigate the effect of overproduction of (p)ppGpp on the infection process. We infected HeLa epithelial cells and RAW 264.7 macrophages with the pSRK-*relA'* strain induced or not induced with IPTG (Figure 32). To be sure that *relA'* is expressed during infection, we incubated bacteria three hours before the infection in 2YT with or without IPTG (1 mM). We then infected host cells and kept the IPTG during the infection for the induced condition. We observed no proliferation for the induced condition compared to the pSRK-*relA'* non-induced and WT conditions. This result indicated that overproduction of (p)ppGpp during the infection prevents the establishment of a correct infection process.

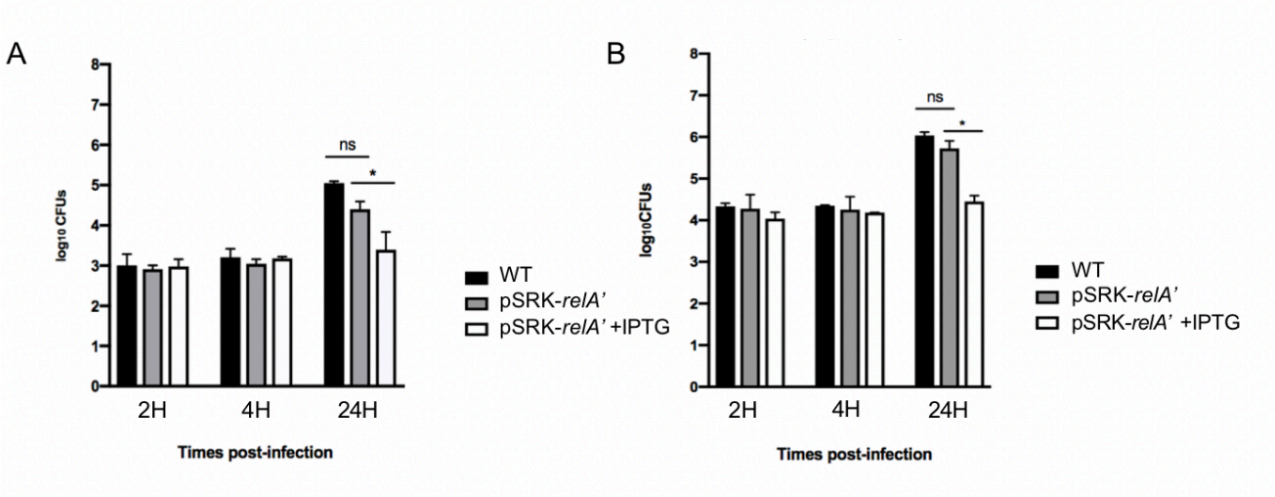

Figure 32: Infection of HeLa epithelial cells (A) and RAW 264.7 macrophages (B) with *B. abortus pSRK-relA'*. Bacteria used for the experiments were in exponential phase of growth. For the IPTG-induced condition, bacteria were incubated in 2YT with IPTG (1 mM) three hours before the infection, and IPTG (10 mM) was kept during the infection. A MOI (Multiplicity of Infection) of 300 was used to infect HeLa cells and a MOI of 50 was used for the infection of RAW 264.7 cells. Bacteria were harvested and CFU were counted at 2, 4, and 24 hours post-infection. Error bars represent the standard deviation from the means of three independent experiments (biological triplicates). A *t* test was used for the statistical analyses. The significant differences in CFUs number are indicated by * ($p < 0.05$).

I.8. Investigation of the link between (p)ppGpp and DksA

Since the DksA protein mediates (p)ppGpp transcriptional response in certain bacteria, we investigated its role in the growth delay observed for the *pSRK-relA'* strain during (p)ppGpp artificial synthesis. A *dksA* deletion strain was constructed in both WT and pSRK-*relA'* backgrounds (Δ*dksA* and Δ*dksA pSRK-relA'* respectively). Since Δ*rsh* mutants showed morphological defects, we analyzed the morphology of Δ*dksA* by phase contrast microscopy and observed that bacteria presented also abnormal morphologies (Figure 33). We assessed the growth of the Δ*dksA* mutant in 2YT rich culture medium and in Plommet minimal medium supplemented by erythritol as carbon source (Figure 34). The Δ*dksA* strain grew as the WT in 2YT rich medium (Figure 34). However, the OD of the mutant decreased during stationary phase in Plommet medium compared to the WT, probably reflecting bacterial lysis. We complemented the Δ*dksA* strain by inserting the endogenous promoter of *dksA* followed by *dksA* coding sequence at the *glmS* locus located on the ChrII and the growth was restored during stationary phase in Plommet medium (data not shown).

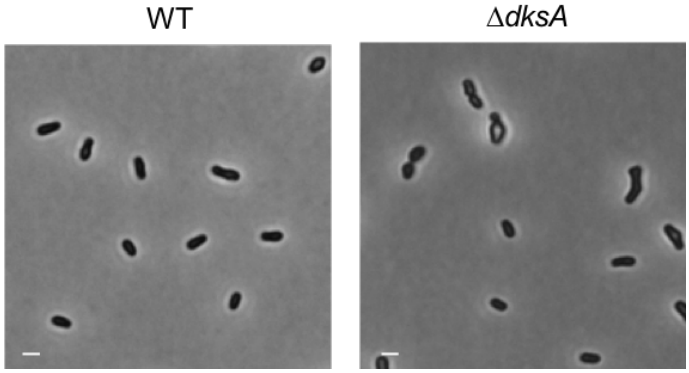

Figure 33: Morphology of the mutant Δ*dksA*. Bacteria in exponential phase of growth in 2YT medium were loaded on PBS agarose pad and observed by phase contrast microscopy. Scale bar represents 1 μm.

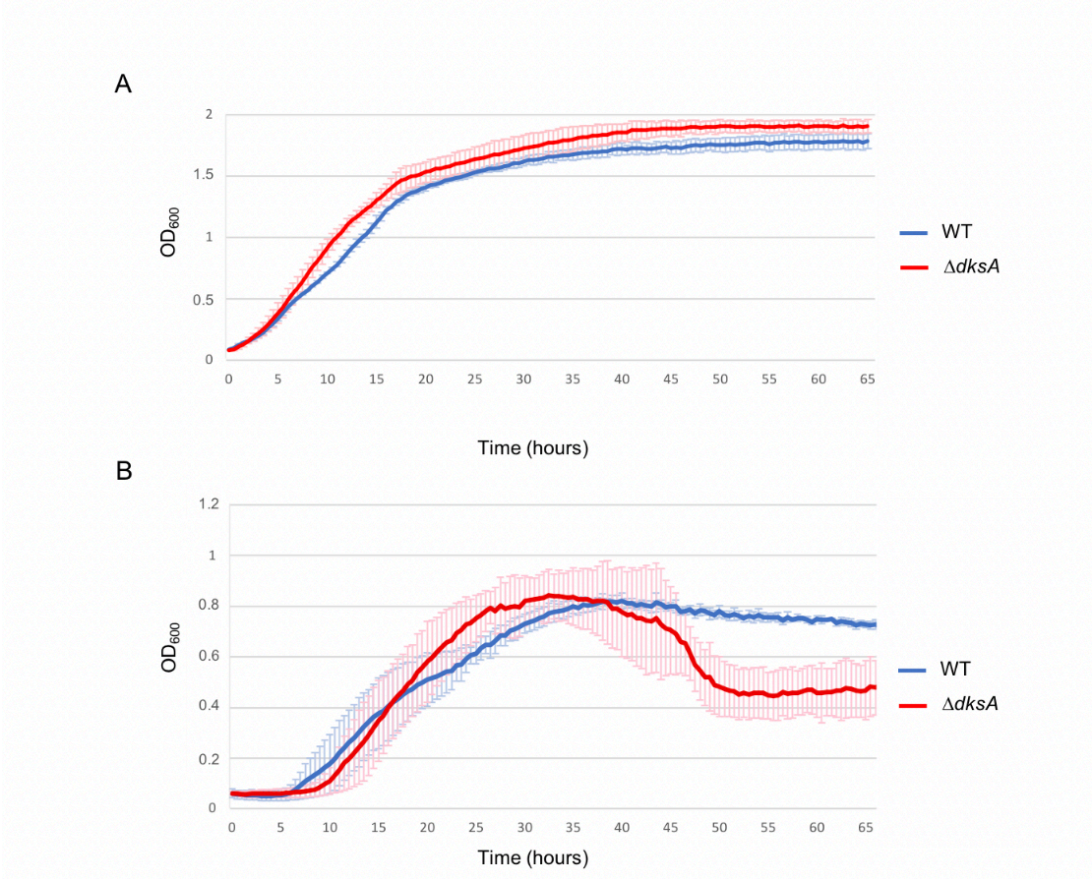

Figure 34: Growth of Δ*dksA* in 2YT rich medium (A) and in Plommet minimal medium (B). The growth of both strains was assessed in 2YT (A) and in Plommet supplemented with erythritol (2g/L) (B) at 37°C with shaking. Bacteria in exponential phase of growth were used and the OD_{600} was normalized at 0.1 before starting the experiment.

Interestingly, in 2YT medium, the induction of *pSRK-relA'* still induced a growth delay in strain deleted for *dksA* (Figure 35). This probably indicated that in the tested conditions, the delayed growth due to (p)ppGpp overproduction did not crucially involve DksA.

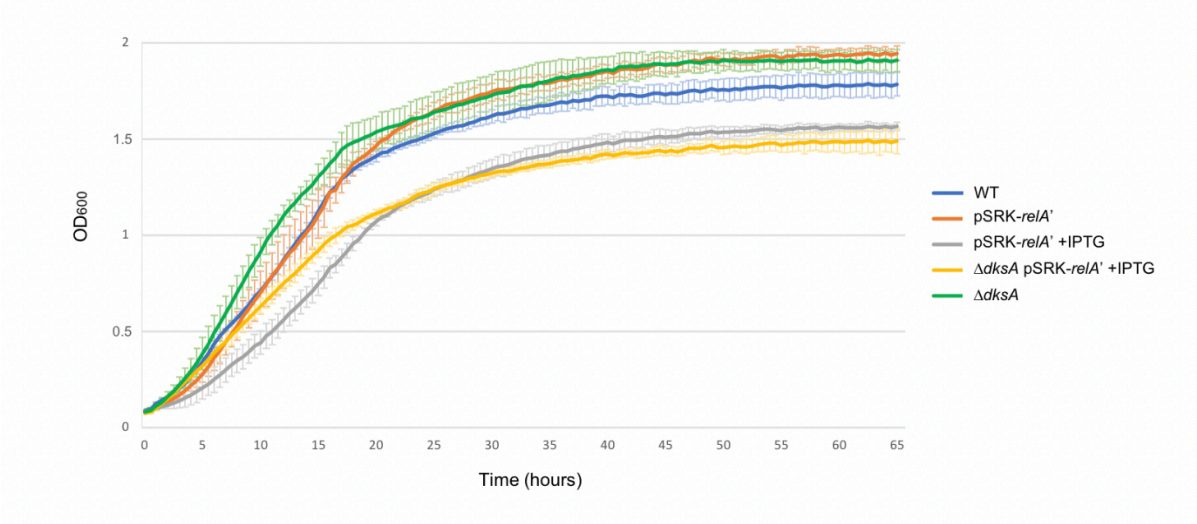

Figure 35: Growth of Δ*dksA* pSRK-*relA'* strain in 2YT with or without IPTG. Bacteria in exponential phase of growth were used and the OD_{600} was normalized at 0.1 before to start the experiment. The growth of these strains was assessed in 2YT rich medium with or without IPTG at 37°C with shaking.

I.9. DksA is not required during the infection process

Because (p)ppGpp seemed important during the host infection and that DksA is involved in (p)ppGpp transcriptional response in other species, we tested the ability of the Δ*dksA* strain to infect and proliferate inside RAW 264.7 macrophages. No difference in CFUs number was observed between WT and Δ*dksA* strains (Figure 36) meaning that DksA is not crucially involved in the infection process and that the phenotype observed for (p)ppGpp-deprived mutants (Δ*rsh* and *pBBRi-mesh1b*) is probably not mediated through DksA.

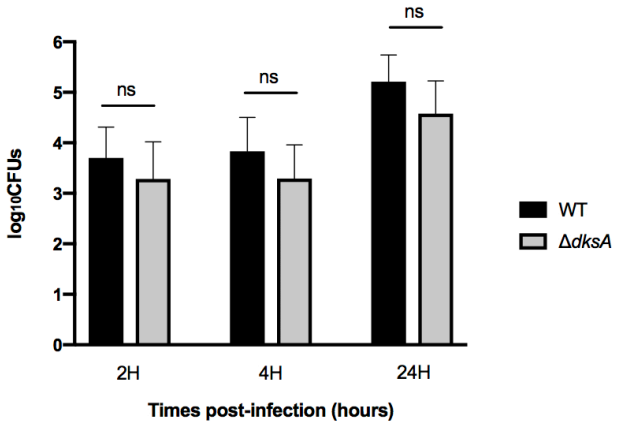

Figure 36: Infection of RAW 264.7 macrophages with the WT and the Δ*dksA* strains. Bacteria used for the experiments were in exponential phase of growth and a MOI (Multiplicity of Infection) of 50 was used for the infection. CFUs were harvested and counted at 2, 4, and 24 hours post-infection. The graph represents the mean of two biological replicates. Error bars represent the standard deviation from the means of three independent experiments (biological triplicates). A *t* test was used for the statistical analyses.

II. Investigation of potential mechanisms regulating DnaA and the replication

II.1. Prediction of DnaA boxes in the B. abortus genome

We used the Regulatory Sequence Analysis Tools (RSAT) Prokaryotes available online (http://embnet.ccg.unam.mx/rsat/) to predict DnaA boxes in the genome of *Brucella abortus*. We searched for the pattern TTATCCACA (the conserved DnaA-box in *E. coli*), allowing one substitution, in the *B. abortus* genome and found 322 matches in the chromosome I and 158 matches in the chromosome II.

Three of these boxes were located in the origin of chromosome I (*oriI*), just downstream an AT-rich region (Figure 37A) which was consistent with what is observed in other bacterial species (see part II.1 of the Introduction). Among these three boxes, one was fully conserved compared to the DnaA-boxes consensus sequence found in *E. coli* and the two other represented 8/9 conserved nucleotides. The Tn-seq profile of the *ori* region revealed an essential region upstream the three DnaA-boxes. Interestingly, when looking at this essential region, we found five GANTC sites which are located close to each other, the whole *oriI* region containing seven GANTC sites in total (Figure 37C). The ChIP-seq profile highlighting GcrA binding on the genome (Poncin *et al*., 2019), indeed indicated that GcrA binds this region *in vivo* (Figure 37B).

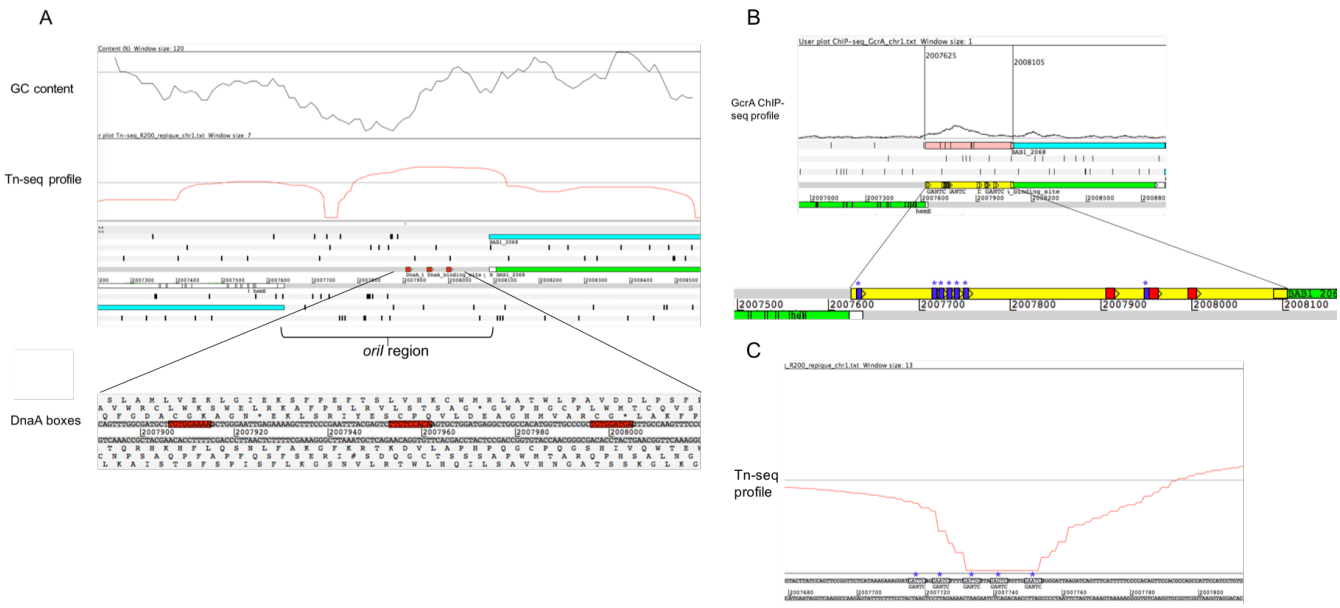

Figure 37: Genomic features of the *oril* region in *B. abortus*. Tn-seq profile is shown with the red line, the GC content is highlighted with the black line and the three DnaA binding-boxes are in red (A). The GcrA ChIP-seq profile is highlighted with the black line, the *oril* region is highlighted in yellow, the seven GANTC sites are highlighted in purple and DnaA-binding boxes are in red (B). The Tn-seq profile of the region containing GANTC sites is represented by the red line (C).

We found two DnaA-binding boxes, separated by one nucleotide, located 783 bp upstream the ATG of *dnaA* gene, and 145 and 259 bp from +1 transcription sites according to an RNA-seq experiment (M. Roop, personal communication) (Figure 38). It has to be noted that the RNA-seq experiment highlighted two +1 sites indicating that *dnaA*$_{abortus}$ gene is probably under the control of two promoters, and that the second promoter seems to be stronger than the first one, as it was the case in *E. coli.* This analysis also reveals that the 5' untranslated region of the major *dnaA* mRNA could be very long (about 450 bases). Six GANTC sites were also found in the promoter region of *dnaA*.

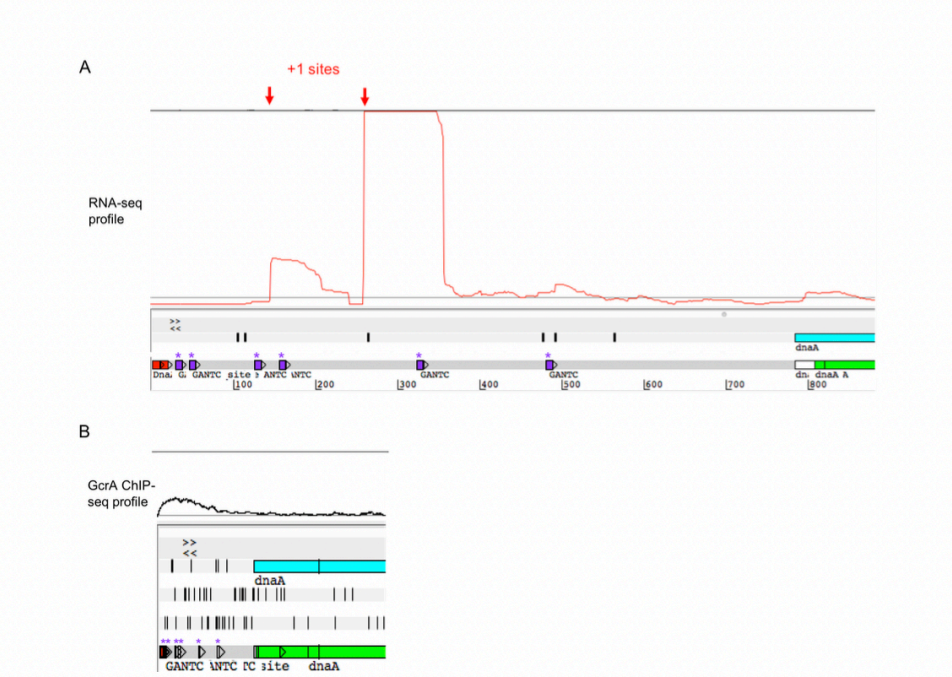

Figure 38: Prediction of DnaA-binding boxes and GANTC sites at the *dnaA* gene locus. Two DnaA-boxes in red are located upstream the *dnaA* gene. The RNA-seq profile is shown in the red line and the +1 sites, corresponding to the transcription start, are highlighted by red arrows. The six GANTC sites are shown in purple (A). The ChIP-seq profile of GcrA is represented by the dark line (B).

Interestingly, we found two DnaA boxes between the *repB* and *repC* genes and one inside *repC* (Figure 39), RepC constituting the replication initiator of chromosome II, and the *oriII* is located inside the *repC* ORF.

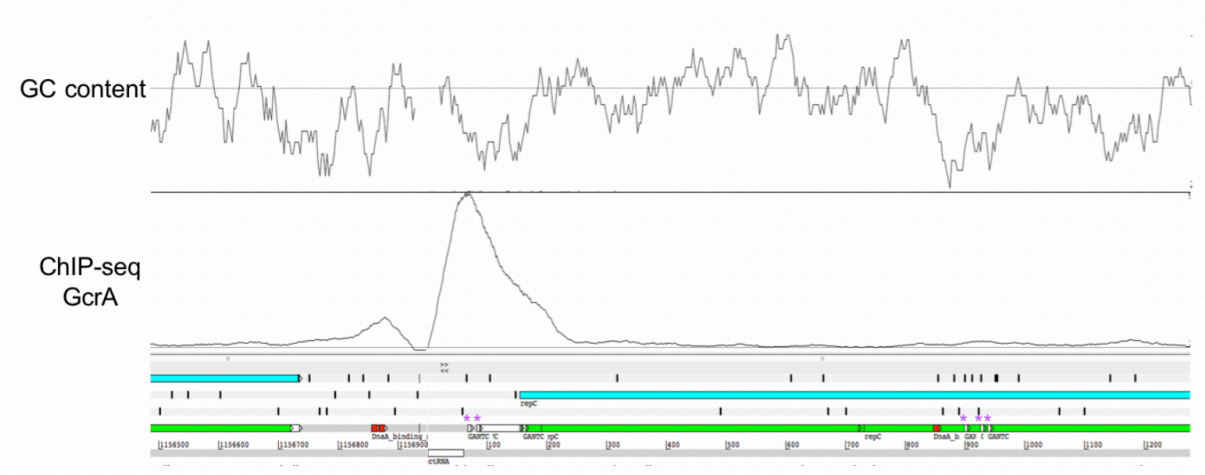

Figure 39: Prediction of DnaA-binding boxes near the origin of chromosome II. Two DnaA-boxes, highlighted in red, were located upstream the *repC* gene and one inside *repC.* GANTC sites are highlighted with purple asterisks. GC content is represented in the higher part and the GcrA ChIP-seq profile on the lower part of the graph.

II.2. Production of antibodies against DnaA$_{abortus}$ for ChIP-seq experiment

Since the prediction of DnaA-binding boxes is based on *in silico* analysis we wanted to to get more insights about the *in vivo* genomic targets of DnaA. In particular, we were interested to see if DnaA is able to bind *oriII*, unlike the replication origin of megaplasmids in the Rhizobiales, and also if DnaA is able to bind promoter regions, like those predicted for the *dnaA* gene itself. For that purpose, we decided to performed a ChIP-seq experiments to highlight DNA regions of the genome that are physically bound by DnaA *in vivo*. We attempted to add a flag tag do DnaA in order to performed the ChIP-seq experiment using anti-FLAG antibodies, but we were not able to obtain viable clones. So, we decided to generate antibodies against DnaA. We never obtained *E. coli* clones expressing the full length DnaA$_{abortus}$, probably because of the toxicity of the protein. We therefore used a truncated version of DnaA$_{abortus}$ without the C-Terminal domain IV, which mediates the binding to DNA. We purified the truncated protein and immunized a rabbit for antibody production and took three different bleedings, named S1, S2 and S3. We assessed DnaA$_{abortus}$ recognition by these antibodies by Western-blot experiment (Figure 40). The S1, S2 and S3 antibodies seemed to present aspecificity since we observed other bands corresponding to proteins with lower

molecular weight, but the S2 and S3 aspecificity appeared lower than the S1. We thus selected the anti-DnaA$_{abortus}$ S3 to perform the ChIP-seq experiment. We used bacteria grown until exponential phase and stationary phase in order to compare both conditions since stationary phase bacteria are characterized by a proliferation (and replication) arrest. The sequencings of the ChIP-seq samples are currently in progress.

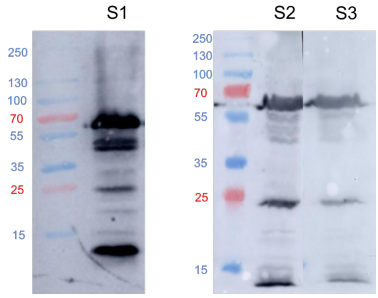

Figure 40: Test of antibodies against DnaA$_{abortus}$ by Western blot. The expected size for DnaA$_{abortus}$ is 55.1 kDa. S1, S2 and S3 respectively refer to the first, the second and the third bleeding.

II.3. Characterization of the ClpAP protease

We decided to investigate the potential role of the protease ClpAP in the control of replication, especially in the control of the DnaA proteolysis, since it was previously reported in *C. crescentus* that this protease was involved in DnaA degradation during stationary phase. In *C. crescentus* and *B. abortus*, the *clpA* gene is in operon with *clpS*. This later codes for the adaptor protein ClpS, which inhibits the degradation of DnaA by ClpAP when it is present. The Tn-seq profile of *clpA* showed no essentiality of the gene for the growth in 2YT condition but an attenuation for the 2YT control replating and 24 hours post-infection conditions (Figure 41A). We created a deletion strain for the *clpSA* operon, since ClpS was shown to be also involved in the control of DnaA in *C. crescentus*. This strain presented morphological defects and a slightly slowed down growth in 2YT rich medium (Figure 41B and 41C). A CFUs experiment was performed in RAW 264.7 macrophages since the Tn-seq profile revealed that Tn insertion in *clpSA* induced attenuation at 24 hours post-infection, however, no clear difference in term of CFUs was observed between the mutant and the WT strains (Figure 42).

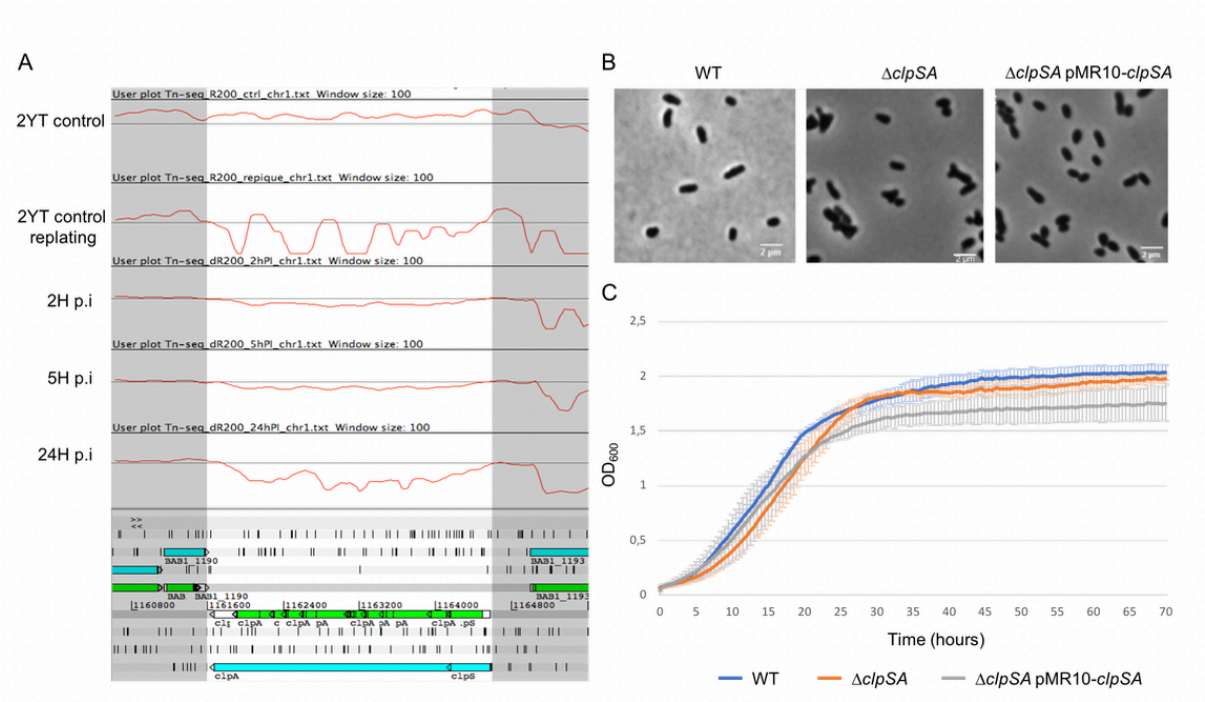

Figure 41: Tn-seq analysis of *clpSA* gene and characterization of Δ*clpSA* strain. The Tn-seq profiles are shown with red lines for the 2YT control (only one plating), 2YT control replating (two successive platings), 2 hours, 5 hours and 24 hours post-infection (A). Phase contrast microscopy (B) and growth analysis in 2YT rich medium (C) of the WT, Δ*clpSA* and Δ*clpSA* pMR10-*clpSA* complementation strains.

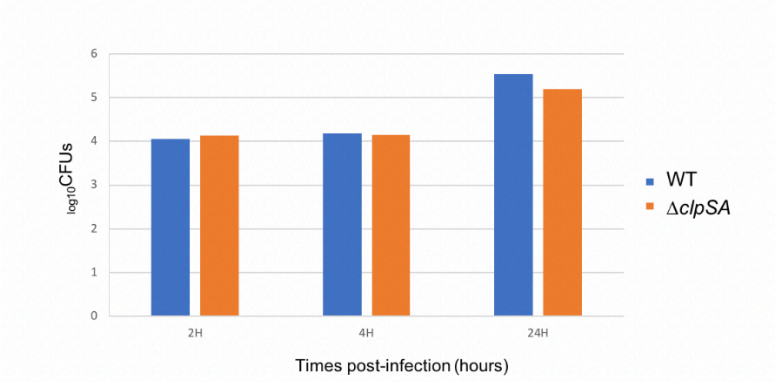

Figure 42: Infection of RAW 264.7 macrophages with Δ*clpSA* strain. CFUs were counted after 2 hours, 4 hours, 24 hours post-infection. Bacteria used for the experiments were in exponential phase of growth and a MOI (Multiplicity of Infection) of 50 was used for the infection. The graph represents the mean of two biological replicate.

We performed a western blot experiment to investigate the DnaA abundance in Δ*clpSA* compared to the WT strain in exponential and in stationary phase of growth (Figure 43). No difference in the DnaA level was observed between the WT and the Δ*clpSA* strain during exponential phase. Surprisingly, a decrease of DnaA was observed during stationary phase for the Δ*clpSA* mutant compared to the WT.

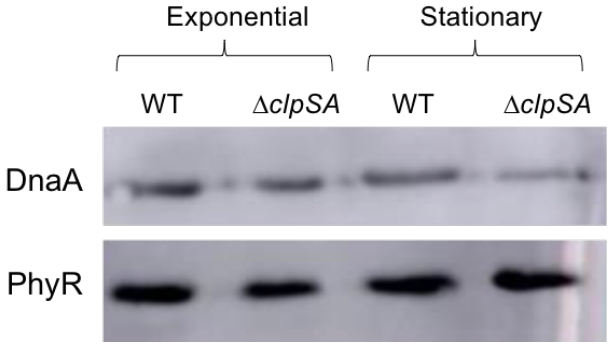

Figure 43: Western blot against DnaA for WT and Δ*clpSA* strains. Samples were harvested during both exponential (OD 0.4) and stationary (OD 2.1) phases of growth, and were normalized to have an OD of 1. PhyR was used as loading control.

II.4. HdaA in *B. abortus*

By looking for the $HdaA_{crescentus}$ homolog of *B. abortus* we found the BAB1_0733 gene coding for a protein homologous to HdaA but, surprisingly, with a large additional domain located at the N-Terminal part, that is absent in HdaA homologs (Figure 44). A domain prediction analysis revealed that this additional domain was composed of seven transmembrane segments (Figure 44C). The Tn-seq analysis of the BAB1_0733 region showed that the C-Terminal region corresponding to $hdaA_{crescentus}$ was clearly essential for growth on 2YT rich medium but not the N-Terminal part corresponding to transmembrane domain (Figure 44A). Alignment of both $HdaA_{abortus}$ and $HdaA_{crescentus}$ revealed that the three amino acids (**Q**FK**L**P**L**) important for the link with DnaN in *C. crescentus* are conserved in *B. abortus.*

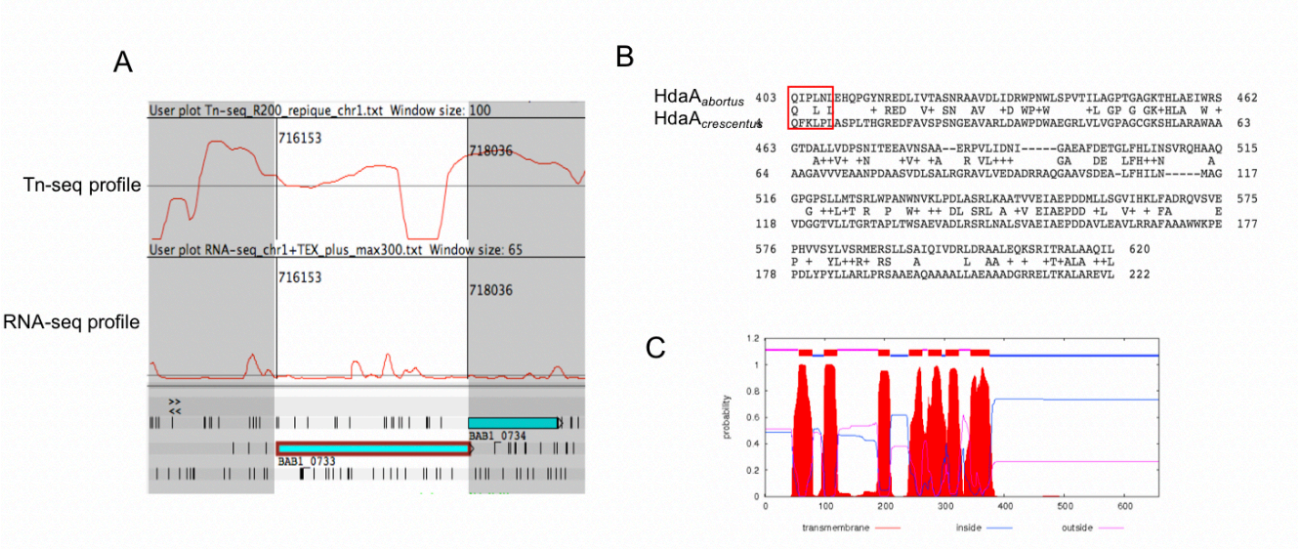

Figure 44: HdaA homolog in *B. abortus*. Tn-seq and RNA-seq profiles for the *hdaA* (BAB1_0733) gene region (A). Alignment of HdaA$_{abortus}$ and HdaA$_{crescentus}$. The motif involved in HdaA$_{crescentus}$ association with the replisome is highlighted by a red frame (B). Sequence analysis of the entire HdaA$_{abortus}$ using www.cbs.dtu.dk indicated the presence of seven transmembrane segments highlighted in red on the graph (C).

Since HdaA was shown to be localized at the replisome in *C. crescentus* we created a *B. abortus* strain where HdaA was fused to a YFP fluorescent protein at the C-terminal domain. The resulting strain named *hdaA-yfp* grew as the WT in 2YT rich medium (data not show). This strain presented one or more YFP foci per bacterium indicating that HdaA is sublocalized in *B. abortus* (Figure 45). It has to be noted that *B. abortus hdaA-yfp* grown until stationary phase showed almost zero foci corresponding to HdaA-YFP (Figure 45). Since the *oriI* is fixed at the old pole of the G1 bacteria, in *B. abortus* (Deghelt *et al*.,2014), we wanted to investigate if the HdaA-YFP tended to be localized close to one pole or another. We created a *hdaA-yfp* strain producing the old pole marker PdhS-mCherry in order to distinguish the old pole from the new one. We performed a demograph analysis by organizing bacteria from the smallest one to the largest one, and by using PdhS-mCherry focus we oriented them according to their poles (the old pole on the left and the new pole on the right) (Figure 46A). However, the distribution of HdaA-YFP did not show a strict subcellular localization according to the demograph (Figure 46B).

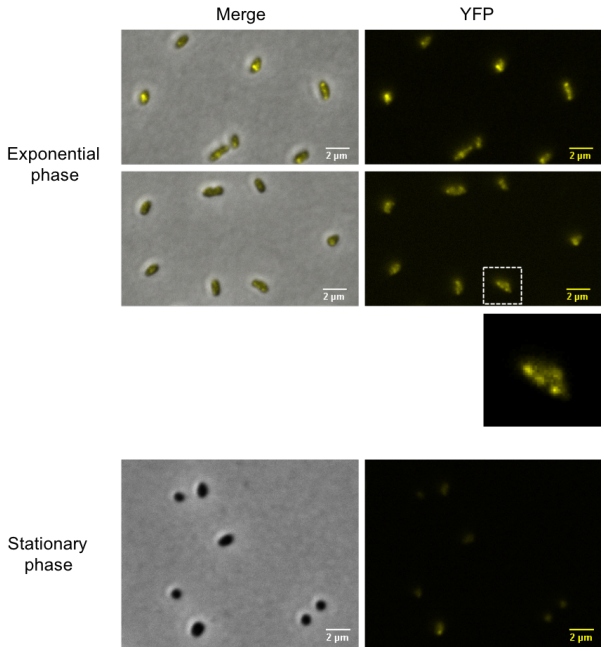

Figure 45: Localization of HdaA in *B. abortus*. A YFP was fused to the C-Terminal part of HdaA$_{abortus}$. Bacteria used for the observation were in exponential or in stationary phase of growth. They were washed twice with PBS and then loaded on PBS agarose pad before their observation by fluorescence microscopy.

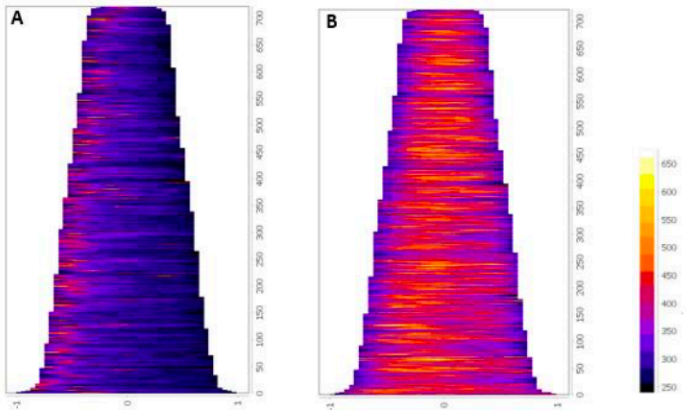

Figure 46: Demograph of subcellular distribution of HdaA-YFP in *B. abortus*. Bacteria expressing *pdhS-mCherry* (A) and *hdaA-yfp* (B) were organized according to their sizes from the smallest one to the larger one, respectively from the highest to the lowest part of the graph and to have the signal corresponding to PdhS-mCherry (to the old pole) on the left.

In order to get more insight about the function of the large additional transmembrane domain (TM) located in the N-terminal part of HdaA$_{abortus}$, we deleted this part of the gene in a WT and *hdaA-yfp* backgrounds and the resulting strains were respectively named Δ*TM-hdaA* and Δ*TM-hdaA-yfp*. As expected with the Tn-seq profile, the Δ*TM-hdaA* and Δ*TM-hdaA-yfp* strains were not impaired for growth in 2YT rich medium compared to the WT (data not show). Interestingly, the sublocalization of HdaA-yfp was lost when the TM was deleted (Figure 47).

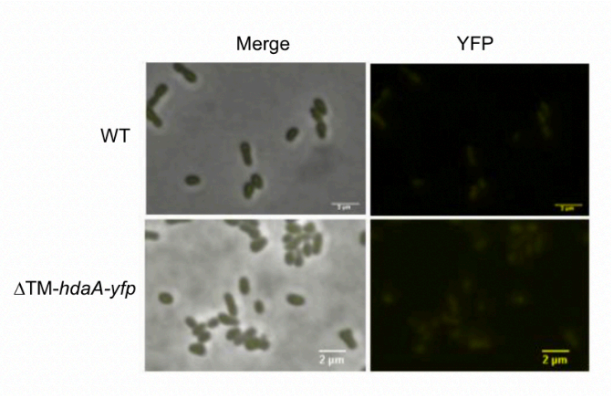

Figure 47: Localization of ΔTM-HdaA-YFP. Bacteria used for the experiment were in exponential phase of growth. They were washed twice with PBS and then loaded on PBS agarose pad before their observation by fluorescence microscopy.

We performed western blot analysis on *hdaA-yfp* and Δ*TM-hdaA-yfp* using antibodies recognizing the YFP in order to confirm that HdaA$_{abortus}$ protein is produced *in vivo* with this additional TM domain. The expected weight of HdaA-YFP with and without the TM domain are respectively of 98.7 kDa and 55.2 kDa considering that the YFP alone is 26 kDa. *hdaA-yfp* 2 and 4, corresponding to two different clones, were analyzed as well as the Δ*TM-hdaA-yfp* and WT strains grew until exponential phase or stationary phase (Figure 48). Both *hdaA-yfp* clones presented bands with a size of approximately 55 kDa, which corresponds to the predicted size of HdaA-YFP without the TM domain, suggesting that HdaA is produced without this domain *in vivo.* The western blot analysis also revealed that Δ*TM-hdaA-yfp* strain presented a band of approximately 25 kDa (probably corresponding to the YFP alone), a band of approximately 55 kDa (corresponding to HdaA-YFP) and a third band of approximately 70 kDa. The presence of this later band was probably due to the way we constructed the Δ*TM-hdaA-yfp.* Indeed, for the deletion of the TM region, we added a START codon in the construction in order to ensure that the downstream region of the TM domain (corresponding

to the “conserved” *hdaA* region) was translated. So, the resulting strain probably contained two ATG start codons, leading to the production of two different proteins with different sizes.

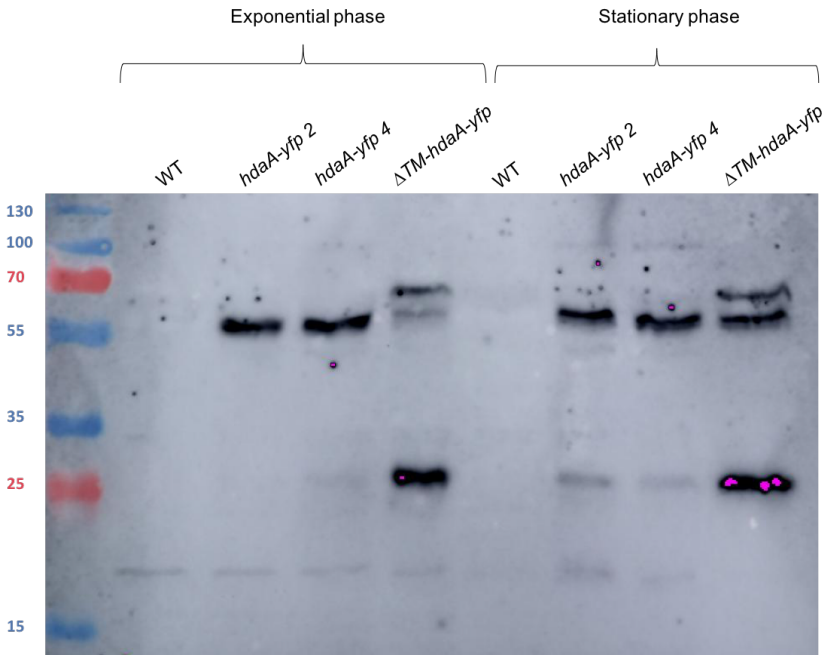

Figure 48: Western blot highlighting HdaA-YFP. WT, *hdaA-yfp 2*, *hdaA-yfp 4* (corresponding to two different clones) and *ΔTM-hdaA-yfp* strains were grown until exponential phase or stationary phase. Samples were normalized to have a final OD of 10 and YFP antibody was used for the western blot experiment.

Discussion and perspectives

Discussion and perspectives

Bacteria use distinct mechanisms to tightly control their cell cycle and more particularly the initiation of their DNA replication. This regulation is especially important when bacteria encounter conditions which are non-optimal for growth, such as nutrient-poor environments, temperature stresses, or adverse conditions met by intracellular bacteria inside their host cells for example. Such cell cycle control has been proposed during the intracellular trafficking of *B. abortus,* characterized by a first non-proliferative step where bacteria are blocked in the G1 phase and a second step where bacteria actively proliferate. Moreover, the link between the cell cycle of this pathogen and its virulence was strengthened with the fact that G1 bacteria are more infectious than the other cell types (Deghelt *et al*., 2014). However, nothing is known on mechanism(s) used by *B. abortus* to control its cell cycle and DNA replication, and, more specifically, how this pathogen is able to block its DNA replication during the first hours of the infection process.

In this project, we attempted to get more insight on the control of chromosomal replication in *B. abortus* by investigating factors that have been shown to be involved in regulation of DNA initiation replication and DnaA in other bacterial species. Among these factors, we decided to study the role of the alarmone (p)ppGpp, the protein HdaA and the protease ClpSA.

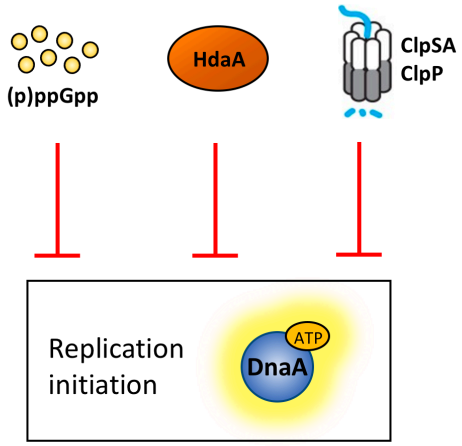

Investigation of the role of (p)ppGpp in *B. abortus*

(p)ppGpp impacts the cell cycle of *B. abortus*

In order to better understand the role of (p)ppGpp in *B. abortus,* we generated the pSRK-*relA'* strain which overproduces (p)ppGpp in presence of the IPTG inducer. The RelA' protein does not contain regulatory domains, meaning that (p)ppGpp is synthesized constitutively when RelA' is produced (Gonzalez and Collier, 2014). This strain is especially interesting to study the effects of an increase of (p)ppGpp during a given time without inducing a global stringent response, by starvation for example, which could lead to phenotypes independently from the (p)ppGpp action.

The fact that the induced *pSRK-relA'* strain showed a growth delay in rich culture medium compared to the WT, the *pSRK-Ø* and the *pSRK-relA'** strains suggested that an increase in (p)ppGpp could lead to a general slowdown of the *B. abortus* cell cycle (Figure 24 and 25). Indeed, the doubling time of the WT and non-induced *pSRK-relA'* strains, during exponential phase, were approximately 3 hours and 3.5 hours respectively, whereas the induced *pSRK-relA'* strain showed a doubling time of approximately 6.7 hours. The induction of *relA'* in a Δ*rsh* background, which cannot hydrolyze (p)ppGpp, and thus, where the concentration of the alarmone should be the highest, impacted drastically the *B. abortus* growth. Indeed, starting from an OD_{600} of 0.1, the non-induced pSRK-*relA'* took approximately 3 hours to reach an OD_{600} of 0.2, compared to 4.5 hours upon IPTG induction, and the Δ*rsh* pSRK-*relA'* strain took approximately 19.5 hours to reach 0.2 of OD_{600} upon IPTG induction (Figure 26). However, since this strain presented almost no growth for approximately 10 hours, we cannot exclude that the growth restart was due to a loss of the pSRK-*relA'* plasmid (since no antibiotic is added during experiment) or was due to the appearance of suppressors. The first hypothesis could be tested either by plating bacteria on kanamycin after the growth experiment or by repeating the experiment in presence of kanamycin.

In addition to impact the growth, (p)ppGpp overproduction also had an effect on DNA replication since an increase of G1 bacteria was observed by flow cytometry analysis of DNA content and by using the mCherry-ParB fluorescent reporter system (Figure 28 and 30). This was consistent with the growth defect observed in rich medium and probably indicated a delay in cell cycle progression when the alarmone concentration increases. Since DnaA

constitutes the replication initiator of chromosome I and that an increase in (p)ppGpp led to a decrease in DnaA levels in *C. crescentus* (Gonzalez and Collier, 2014), we investigated the intracellular levels of this protein by western blot when *B. abortus* overproduced (p)ppGpp (Figure 31). As expected, the amount of DnaA decreased as *relA'* was induced and this drop was more important for the Δ*rsh pSRK-relA'* strain. Altogether these results suggest that (p)ppGpp negatively impacts the DnaA pool of bacteria, which could be at the origin of the replication defects observed during *relA'* induction.

However, we do not know how (p)ppGpp regulates replication, and mediates the decrease in DnaA levels, and if this decrease is sufficient to explain the replication delay observed. Indeed, in *E. coli*, (p)ppGpp has been shown to affect *dnaA* expression but this inhibition alone was not necessary to arrest replication upon (p)ppGpp production (Zyskind and Smith, 1992; Chiaramello and Zysking, 2010; Kraemer *et al*., 2019). In order to investigate a potential *dnaA* transcriptional regulation in *B. abortus*, qRT-PCR experiments could be performed during (p)ppGpp overproduction condition.

In *C. crescentus*, it has been suggested that (p)ppGpp can act on replication regulation by decreasing DnaA (notably during carbon starvation) and by increasing the level of CtrA (Lesley and Shapiro, 2008; Gonzalez and Collier, 2014). However, it is not known if the replication inhibition function of CtrA observed in *C. crescentus* is conserved in *B. abortus.* As remind, CtrA can inhibit initiation of DNA replication by binding the replication origin in *C. crescentus* (Quon *et al*., 1998). In *B. abortus*, a ChIP-seq experiment revealed that CtrA does not bind the origin of replication (Francis *et al*., 2017), suggesting that CtrA is not involved in the regulation of DNA replication, or that it can regulate this process by a different way than in *C. crescentus*.

The DnaA proteolysis has been shown to be mediated through Lon and ClpAP proteases in *C. crescentus*. It would be interesting to assess the intracellular DnaA levels in *B. abortus* overproducing (p)ppGpp (in the *pSKR-relA'* and Δ*rsh pSKR-relA'* strains) where *lon* or *clpAP* have been deleted or depleted, in order to study the involvement of these proteases in the (p)ppGpp-mediated DnaA decrease.

(p)ppGpp plays a role during growth in minimal medium and during infection

The Tn-seq profile for growth on rich 2YT culture medium indicated that transposon insertion in the *rsh* gene led to growth impairment on plate containing 2YT rich culture medium (Sternon *et al*., 2018). Indeed, the Δ*rsh* strain showed smaller colonies than the WT on 2YT agar plates, however, the growth rate of this mutant during exponential phase was similar to the WT strain in 2YT liquid medium. Interestingly, the Δ*rsh* strain showed an extended exponential phase and enters in stationary phase later than the WT (Figure 18). Since RSH mediates stringent response in other species, this would suggest that *B. abortus* may encounter stress, at some extent, when cultivated on 2YT agar. One hypothesis which could explain this growth delay is the limited nutrient availability in 2YT agar medium compared to in 2YT liquid medium.

As expected for a (p)ppGpp null mutant, the Δ*rsh* strain presented growth defects in Plommet minimal medium (deprived of amino acid) compared to the WT strain (Figure 18). First, the lag phase of the Δ*rsh* mutant was extended compared to the WT. The mutant was then able to grow until an OD_{600} of 0.5 but rapidly dropped, probably indicating bacterial lysis. Since bacteria were washed two times in PBS before starting the experiments, thus, the slight growth observed for the Δ*rsh* strain was likely not due to residual 2YT in the Plommet medium. One hypothesis could be that *B. abortus* disposes of intracellular nutritional reserves allowing bacteria to grow, but that those reserves rapidly deplete after a few hours. Another hypothesis which could explain this growth is that DksA could compensate for the loss of (p)ppGpp. Indeed, it was already shown that overproduction of DksA can compensate, or partially compensate, some phenotypes induced by the loss of (p)ppGpp. This compensation was shown to be species-specific. For example, overproduction of DksA rescued the *E. coli* MG1655 (p)ppGpp null mutant from amino acid auxotrophy but it was not the case in the MC4100 (p)ppGpp null strain (Brown *et al*., 2002; Magnusson *et al*., 2007). The generation of a double deletion mutant for *dksA* and *rsh* in *B. abortus* could be interesting to perform in order to verify this hypothesis.

We repeated the experiment in Plommet medium at pH 5.0 to mimic the environment that bacteria encounter inside host cells, at early stages of the infection. Both he Δ*rsh* and the WT strains presented growth defects, but the phenotype was more pronounced for the Δ*rsh* mutant, which probably showed bacterial lysis, compared to the WT (Figure 18). The growth

defect observed for the WT indicated that *B. abortus* already had problems to grow in acidic minimal medium which is consistent with a first non-proliferative phase observed during infection.

Previous studies highlighted the importance of *rsh* in the infection process of *B. melitensis, B. suis and B. abortus* (Köhler *et al*., 2002; Kim *et al*., 2003; Dozot *et al*., 2006). Here, we confirmed that the *rsh* deletion in *B. abortus* led to a strong attenuation during the infection of RAW 264.7 macrophages (Figure 19). In addition to presenting no increase in CFUs at 24 hours, as it is observed for the WT, the Δ*rsh* mutant showed a CFUs decrease already at 4 hours p.i., indicating a survival defect inside cells. However, CFUs in rich culture medium should be performed in order to test the viability of the mutant and to confirm that the phenotype observed during infection is directly linked to the infection condition rather than a compromised fitness of the mutant already present in culture condition. Since we showed that (p)ppGpp has an impact on DNA replication, one interesting perspective would be the study of the cell cycle of Δ*rsh* mutant in rich and minimal medium conditions as well as during infection.

Altogether, these results suggested that RSH is important for the growth and survival in minimal medium as well as inside macrophages. In order to confirm that the lack of (p)ppGpp is responsible for these attenuated phenotypes, we generated a *B. abortus* strain producing the strong (p)ppGpp hydrolase Mesh1 originally found in *D. melanogaster*. This strain should normally present the same phenotypes as a Δ*rsh* mutant since the (p)ppGpp produced is hydrolyzed by Mesh1. As the Δ*rsh* mutant, the strain carrying pBBRi-*mesh1b* did not show any growth defect when cultivated in 2YT rich medium (Figure 20). After inoculation in Plommet minimal medium this strain grew during approximately 20 hours but the OD_{600} started to decline probably reflecting growth defect/cell lysis (Figure 20). Interestingly, this strain was also attenuated in infection of RAW 264.7 macrophages but the phenotype was less marked than the one observed for the Δ*rsh* strain (Figure 21). These intermediate phenotypes during growth and infection experiments could be explained by the existence of a balance between the production of (p)ppGpp and its degradation, leading to the presence of some residual alarmone, which is not the case in the Δ*rsh* mutant since the synthetase is not present.

Surprisingly, we obtained the same phenotypes whether we added IPTG or not to induce the expression of *mesh1b*, for the growth experiment as well as for the infection experiment. Since Mesh1 was previously shown to be a strong (p)ppGpp hydrolase (Sun *et al*., 2010), one explanation could be that the inducible system is leaky and that the slight gene expression is enough to hydrolyze (p)ppGpp and leads to the same phenotype than in induced condition. It is also possible that induction of *mesh1b* expression by IPTG is not occurring.

Nevertheless, the fact that both the pBBRi-*mesh1b* and Δ*rsh* strains presented growth defects in minimal medium and was attenuated in infection strongly suggest that (p)ppGpp plays a central role in adaptation to poor environments and in establishing the infection process.

The concentration of (p)ppGpp is important during the infection

Since (p)ppGpp was important for the infection process, and since this alarmone was shown to be tightly regulated in other bacteria species, we tested the ability of *B. abortus* to infect and proliferate inside host cells when (p)ppGpp is overproduced using the pSRK-*relA'* strain. Because an increase of G1 bacteria was one consequence of the (p)ppGpp overproduction, and that G1 bacteria were shown to be more infectious, we expected to see a CFUs increase at early times post-infection. However, the entry inside host cells was not impacted whether pSRK-*relA'* was induced or not prior the infection experiment, compared to the WT suggesting that the overproduction of (p)ppGpp did not improve the internalization process. We can thus hypothesize that the preferential internalization of G1 bacteria is not due the fact that bacteria are in G1 phase but it is rather due to the fact these G1 bacteria are newborn cells and are probably in another physiological state.

Interestingly, the induction of *relA'* seemed to lead to no proliferation inside host cells as the induced pSRK-*relA'* did not show increase of CFUs between 4 hours and 24 hours post-infection. However, since the *relA'* expression already showed growth delay in rich medium we cannot conclude that this constant CFUs number is not due to delayed bacterial growth. Another hypothesis is the existence of a balance between bacterial proliferation and killing inside host cells leading to the constant CFUs number phenotype. Still, preliminary data suggest that this phenotype reflects the inability of induced pSRK-*relA'* to replicate. Indeed, by performing immunofluorescence experiments in HeLa cells we noticed that at 24 hours p.i,

approximately 88% of infected cells presented only one bacterium per cell for the induced pSRK-*relA'* condition compared to 48% and 36% for the non-induced pSRK-*relA'* and WT conditions respectively. This suggested that bacteria constitutively overproducing (p)ppGpp inside host cells failed to replicate during infection and that the production of (p)ppGpp at an appropriate concentration and/or at precise time during infection is important to establish a successful infection process. Nevertheless, this immunofluorescence experiment has been performed once and needs to be repeated in order to confirm this result.

Investigation of the DksA role in *B. abortus*

Since DksA was shown to mediate a part of the (p)ppGpp transcriptional response in *E. coli*, and that the Tn-seq profile indicated that transposon insertion in *dksA* led to attenuation in infection of macrophages, we generated a Δ*dksA* strain to investigate its potential role in growth and survival in minimal medium and in infection.

In 2YT rich medium, the *B. abortus* Δ*dksA* mutant presented a slightly better growth than the WT. In *E. coli*, it was previously shown that *dksA* is required to grow in minimal medium deprived of amino acids (Brown *et al*., 2002). Here, we showed that *B. abortus* Δ*dksA* was able to grow in Plommet minimal medium deprived of amino acids, but still, the growth curve showed differences with the WT strain (Figure 34). First, the lag phase of the mutant was slightly extended compared to the WT, a phenotype already observed for the Δ*rsh* strain. Secondly, the mutant presented a higher growth rate than the WT during the exponential phase. And finally, the OD_{600} of the Δ*dksA* mutant decreased drastically during the stationary phase, reflecting bacterial lysis, while the WT did not show such decrease. This result suggested that DksA may play an important role in survival during the stationary phase, in minimal medium. In order to investigate this hypothesis, it would be interesting to perform CFUs experiment to test the survival of the mutant in (late) stationary phase.

To investigate if DksA potentiates (p)ppGpp in *B. abortus* as it is the case in *E. coli*, we generated a strain overproducing (p)ppGpp with the pSRK-*relA'* system, where we deleted *dksA* (Δ*dksA* pSRK-*relA'*). Upon induction with IPTG in 2YT rich medium, this strain presented a slower growth compared to the Δ*dksA* strain, indicating that (p)ppGpp still has an impact on growth even in the absence of DksA. This result suggests that the growth inhibition observed during (p)ppGpp overproduction would be not crucially DksA-dependent, in the tested

conditions, which does not indicate that DksA is not involved at all in the (p)ppGpp-mediated response. The *E. coli* RNA polymerase is bound by (p)ppGpp at two distinct sites, and DksA has been shown to stabilize the interaction between the site 2 and (p)ppGpp (Ross *et al*., 2016). The generation of RNA polymerase mutants that suppress this interaction would be interesting to performed in order to test the responsiveness of the RNA polymerase lacking site 2 to (p)ppGpp overproduction. In order to investigate more deeply the mechanisms targeted by (p)ppGpp and DksA, an RNA-seq experiment could be performed in *B. abortus* strains lacking *dksA* or overproducing (p)ppGpp in absence or presence of *dksA*. This without a priori study could be of great interest to highlight genes that are simultaneously targeted by both (p)ppGpp and DksA, or genes that are only regulated by (p)ppGpp or by DksA.

The CFUs experiments in RAW 264.7 macrophages (Figure 35) revealed that DksA is not crucially involved in the infection process as it was expected with the Tn-seq profile. Since the Tn-seq experiment was based on generation of transposon mutants, one should keep in mind that this mutation method can create some polar effects which could explain the attenuation seen with the Tn-seq experiment but not with the deletion mutant. Still, a recent Tn-seq experiment performed in mice with *B. melitensis* revealed *dksA* as essential at late times post infection (Georges Potemberg, unpublished data). It would be thus interesting to test the ability of Δ*dksA* to infect and proliferate in mice and investigate if this deletion strain presents the same phenotype than transposon insertion mutants.

The deletion of *rsh* or *dksA* impact morphology of *B. abortus*

Previous studies revealed morphological abnormalities in *spoT*/*rsh* deletion mutants of *E. coli*, *Campylobacter jejuni*, *B. suis* and *B. melitensis*, and in *rsh* transposon mutant of *B. abortus*, suggesting that this *rsh*-dependent phenotype is conserved among bacteria. In *E. coli* the lack of (p)ppGpp or *dksA* led to filamentation during exponential phase and the spherical cell shape usually obtained in stationary phase was not observed (Cashel *et al*., 1996; Magnusson *et al*., 2007). The predominant morphological defects observed in Δ*rsh* and Δ*dksA* *B. abortus* were branched and swollen bacteria. Interestingly, the branched phenotype was previously associated with cell division defects in *B. abortus* (Van der Henst *et al*., 2012), which brings additional clues about the involvement of (p)ppGpp in cell cycle progression.

Another interesting feature is that, during stationary phase, the Δ*dksA* and Δ*rsh* cells appeared larger than the WT cells, which normally appear smaller during this phase (Figure 50). This experiment was performed only one time and needs to be quantified and repeated in order to be confirmed. Nevertheless, this result is consistent with the phenotype observed during overproduction of (p)ppGpp with the pSRK-*relA'* strain, i.e. the generation of smaller cells and would suggest that (p)ppGpp and DksA are involved in the "small cells" phenotype observed for the WT strain during stationary phase.

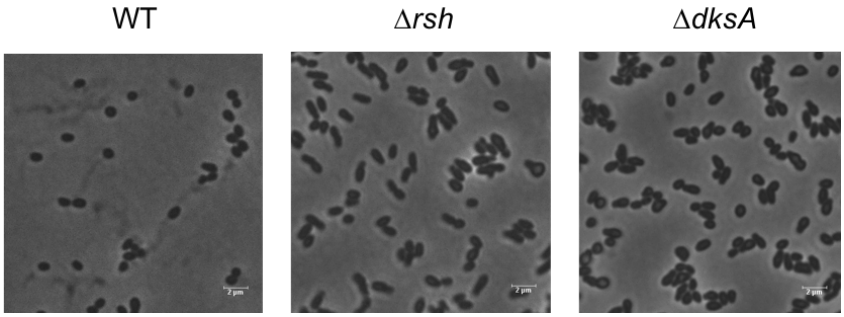

Figure 50: Morphology of the WT, the Δ*rsh* and the Δ*dksA* strains during stationary phase. Scale bar represents 2 µm.

The *B. abortus* pBBRi-*mesh1b,* induced or not with IPTG, did not show these morphological defects. Since this strain is not a (p)ppGpp null mutant, it is possible that the balance between (p)ppGpp production and degradation by Mesh1b leads to the presence of a small quantity of (p)ppGpp, and that this residual (p)ppGpp is enough to not induce morphological defects. It would be interesting to test if the expression of *mesh1b* in other bacterial species induce or not abnormal morphologies.

Construction of a reporter system for (p)ppGpp

One interesting perspective of this work is the generation of a reporter strain allowing the quantification of intracellular (p)ppGpp by fluorescence measurements. Recently, riboswitches for (p)ppGpp have been discovered in *Thermosediminibacter oceani* and *Desulfitobacterium hafniense* and were especially predicted to be involved in the regulation of branched-chain amino acids biosynthesis genes (Sherlock *et al*., 2018). The use of these riboswitches as (p)ppGpp reporter could be interesting to learn more about the conditions that induce (p)ppGpp production and degradation. This reporter could be confirmed by our (p)ppGpp overproduction system (pSRK-*relA'*), and (p)ppGpp degradation system (pBBRi-

mesh1b). Then, the characterization of this reporter strain during infection could be of great interest to investigate the (p)ppGpp homeostasis inside host cells, since (p)ppGpp is important for the infection process.

Study of potential DnaA regulatory factors

The HdaA protein

We studied the intracellular localization pattern of $HdaA_{abortus}$ by generating a *B. abortus hdaA-yfp* strain. The resulting strain presented one to four YFP foci per bacterium in exponential phase. Since HdaA is physically associated with the replisome during DNA replication in *C. crescentus*, the number of foci observed could be correlated with the number of replisomes formed during *B. abortus* replication, i.e two chromosomes with two replisomes by chromosome. Interestingly, we did not observe these foci during stationary phase, where it is expected that bacteria do not grow and replicate their DNA. If HdaA is well associated to the replisome in *B. abortus*, this would mean first that replisomes are absent during this phase and thus, that no DNA replication occurs, or that the replisome is released from the replication fork during this phase, or a third hypothesis is that HdaA is released from the replisome or is not produced at all. This later explanation is not likely since the western blot experiment highlighted HdaA-YFP during stationary phase, suggesting that HdaA is produced and present during this phase.

According to the genome of *B. abortus,* $HdaA_{abortus}$ would present a large transmembrane domain in the N-terminal part of the protein. Interestingly, the *ΔTM-hdaA-yfp* strain presented no fluorescent foci anymore, indicating a loss of localization when the TM domain is removed. To investigate if this protein is indeed produced with this additional domain, we performed a western blot experiment on the *hdaA-yfp* and the *ΔTM-hdaA-yfp* strains using anti-YFP antibodies to evaluate the size of the proteins (Figure 48). The size of HdaA-YFP (for two *hdaA-yfp* different clones) corresponded to the size predicted for HdaA-YFP without the additional domain, i.e approximately 55 kDa, meaning that $HdaA_{abortus}$ is produced *in vivo* without the TM domain. Importantly, the analysis of the size of ΔTM-hdaA-yfp by western blot showed that free YFP (without being fused to HdaA) is present in this strain, which could explain why we do not observe foci anymore in this strain.

Altogether these results indicated that HdaA is produced *in vivo* without this large additional domain. There would be several explanations for this. First, *hdaA* locus could be wrongly annotated in the genome, with the lack of a STOP codon between the TM region and the conserved *hdaA* region. The *hdaA* promoter would be thus localized in this TM region and the *hdaA* transcription would start in this region. Secondly, the whole protein could be produced and then cleaved between the TM domain and the conserved *hdaA* region.

Further investigations should be performed in order to get insight on the functional role of HdaA in *B. abortus*. The generation of a depletion strain for *hdaA* and the study of its chromosomes content could highlight its potential role on regulating DNA replication.

The ClpSA protease

As remind, the ClpA protein is involved in DnaA proteolysis during the stationary phase in *C. crescentus* and ClpS has been shown to inhibit this proteolysis. This results in the absence of DnaA protein during this phase of growth (Wargachuk *et al*., 2015; Liu *et al*., 2016). The deletion of *clpSA* slightly impacted the growth and led to branched morphology in 2YT rich medium, which could reflect cell cycle regulation defects. Since ClpAP mediates the proteolysis of different proteins in *C. crescentus*, this phenotype could reflect pleiotropic effects due to the loss of *clpSA*. The levels of DnaA did not change between the WT and the Δ*clpSA* during exponential growth, suggesting that ClpSA does not induce DnaA proteolysis during this phase. However, it is not excluded that other protases, such as Lon, could compensate for the loss of ClpSA. On the contrary to what is observed in *C. crescentus*, DnaA levels were maintained in the *B. abortus* WT strain during stationary phase probably indicating that DnaA is differentially regulated between both species. Indeed, even though *C. crescentus* constitutes a model to study the regulation of chromosomal replication in *B. abortus*, one should keep in mind that those species display different lifestyles and have evolved under different environmental pressures. The fact that *B. abortus* conserves its DnaA pool during stationary phase could, for example, constitute a strategy to rapidly restart DNA replication after nutrient repletion, rather than waiting for *de novo* DnaA synthesis.

Surprisingly, the Δ*clpSA* strain seemed to show a decrease in DnaA levels during stationary phase, which was not expected if ClpA induces DnaA proteolysis as it is the case in *C. crescentus*. One hypopthesis which could explain this decrease could be that the mutant

present survival defects during the stationary phase, leading to a global proteolysis mediated by other proteases. Another explanation could be that ClpA targets accumulate in the mutant during stationary phase and induce proteotoxic stress. Such stress has already been shown to activate the Lon protease which is also responsible for DnaA degradation in *C. crescentus* (Jonas *et al*., 2013). The assessment of DnaA levels in a *B. abortus lon* mutant could be of great interest to potentially get insight on post-translational DnaA regulatory mechanisms.

In silico analysis of the *oriI* region in *B. abortus*

Based on the DnaA box sequence found in *E. coli*, the *in silico* analysis of the *B. abortus oriI* revealed the presence of three conserved DnaA boxes (Figure 37). We also observed the presence of an AT-rich region upstream these boxes, which is consistent with what is observed in other bacterial species and probably consists in the DUE complex (Duplex Unwinding Element, see Chapter II.1 of the introduction).

Seven GANTC methylation sites among which five were relatively close to each other (separated from two to five nucleotides) were found in the *oriI* region. Some GANTC sites have been shown to be bound by the transcriptional regulator GcrA, which is involved in cell cycle regulation and is a part of the replication control process in *C. crescentus* (Fioravanti *et al*., 2013). The profile of the GcrA ChIP-seq revealed that this transcription factor bound *in vivo* the *oriI* region in *B. abortus*. By looking at the Tn-seq profile of the 2YT rich control, we observed that a region located in the *oriI* was essential for growth, and that this region corresponds to the DNA segment containing the GANTC sites. However, since the *oriI* is located between two ORFs corresponding to the *hemE* gene and the BAB1_2068 gene annotated as “coding for a PEP synthetase regulatory protein”, which were both essential according to the Tn-seq, we cannot exclude that insertion of transposon in the promoter region led to genes misregulation and lethality. In the same way, the binding of GcrA to this region could also involve transcriptional regulation of the surrounded genes instead of acting on replication. However, it is tempting to hypothesize that the binding of GcrA to the *oriI* region would be linked to regulation of DNA replication since GcrA constitutes a cell cycle regulator and was shown to drive genes expression required during the S phase in *C. crescentus*.

Since the complex GcrA-σ^{70} has been shown to promote transcription by inducing unwinding of dsDNA in *C. crescentus*, the binding of GcrA to the *oriI* region could, for example, help for the initiation of DNA replication. On the contrary, the binding of GcrA to the *oriI* could inhibit the DNA replication initiation by preventing the binding of factors involved in DNA replication such as DnaA. In addition, if GcrA is involved in DNA replication regulation, the fact that GcrA can distinguish fully methylated GANTC sites from hemi-methylated sites could constitute a mechanism of replication control since these sites present different methylation states during cell cycle progression. The involvement of methylation status of GANTC sites in DNA replication control could also be studied by creating a strain depleted for *ccrM* or overexpressing *ccrM.* Interestingly, Robertson *et al*. have been shown that *ccrM* overexpression in *B. abortus* led to different phenotypes such as branched morphology of the cells and an abnormal increase of chromosome number, indicating that CcrM would be involved in cell cycle regulation and more particularly in DNA replication (Robertson *et al*., 2000). However, the pleiotropic effects caused by an overexpression of *ccrM* do not allow to confirm that CcrM and GANTC methylation sites in oriI are directly involved in DNA replication. The generation of a strain lacking the GANTC sites present in the *oriI* and the study of the effects on GcrA binding and chromosomal replication could be interesting to perform in order to get insight on the potential role of GcrA and/or GANTC sites in DNA replication regulation.

In silico analysis of the *dnaA* locus

One way to regulate DNA replication in bacteria is the control of levels of DnaA initiator protein. According to an RNA-seq study, the upstream region of *dnaA* contains two promoters, as it was already described in *E. coli* (Figure 38) (Hansen *et al*., 1982). Interestingly, two DnaA binding boxes were present in the promoter region, suggesting that *dnaA* transcription could be controlled by its own product. In order to get insight about the DNA regions bound by DnaA *in vivo* in *B. abortus*, we generated polyclonal antibodies from immunized rabbit. The western blot experiments performed with this antibody revealed several bands in addition to the one presenting the size of DnaA, probably indicating contaminant proteins which are recognized by the antibody (Figure 40). The ChIP-seq experiment performed with this antibody and for which sequencing is in progress could confirm the binding of DnaA to its own promoter *in vivo*.

Six GANTC methylation sites were present in the promoter region of *dnaA* and the ChIP-seq profile of GcrA confirmed that this protein binds to this region *in vivo*. Since GcrA is

involved in cell cycle progression, and in control of components of the replisome in *C. crescentus*, this transcription factor could be also implicated in DNA replication in *B. abortus* by regulating the *dnaA* gene. The investigation of DnaA levels in a *gcrA* depletion strain could highlight potential involvement of GcrA in DnaA regulation. However, the pleiotropic effects induced by the loss of *gcrA* could lead to phenotypes that are not directly linked to GcrA. The mutation of the GANTC sites in the promoter of *dnaA* could be interesting to first confirm that GcrA binds this DNA region through the GANTC sites and secondly to study the effect of DNA methylation and /or GcrA binding on DnaA levels.

In silico analysis of the *oriII* region in *B. abortus*

As remind, the chromosome II is a *repABC*-type replicon, which are exclusively found in alphaproteobacteria. This replicon contains a *repABC* cassette, which encodes the segregation machinery (RepA and RepB) and the DNA replication initiator RepC, as well as the replication origin, usually located within the *repC* gene.

Interestingly, the prediction of DnaA boxes revealed that two of these boxes were located upstream the *repC* gene and one was located inside the gene (Figure 39), a feature which was not observed in *repABC* dependent chromosomes found in other rhizobiales. Both chromosomes of *B. abortus* showed coordinated initiation replication events, with the chromosome I being replicated before the chromosome II. This suggest a mechanism for communication between both chromosomes for replication initiation. Since *oriII* and promoter of *repC* contained DnaA boxes, it was tempting to hypothesize that DnaA could be involved in the control of chromosome II replication. This control could be mediated by different ways. Since DnaA has been shown to have a transcriptional activity, this protein could be implicated in transcriptional regulation of the *repC* gene for example. Or, the binding of DnaA to the *oriII* could prevent the chromosome II replication by preventing the binding of the RepC initiator. Nonetheless, the ChIP-seq experiment should give insight about the binding of DnaA to this region *in vivo*.

We also found six GANTC sites near the *repC* locus. Two were located between the ctRNA *repE* and the *repC* gene, one was located in *repC* coding sequence, 5 nucleotides downstream the ATG, and three were found in the *repC* ORF, in the AT-rich region, which was shown to consist in the replication origin in other species (Figure 39). The localization of these

GANTC sites was previously described in other *repABC*-type replicon such as the pTiR10 in *Agrobacterium tumefaciens*, and was shown to be a common feature of *repABC* operons (Brilli *et al*., 2010). *repE*, located upstream the *repC* gene in opposite direction, was previously shown to inhibit transcriptionally and post-transcriptionally *repC* in *A. tumefaciens* (Chai and Winans, 2005). The ChIP-seq profile of GcrA revealed, indeed, that GcrA bound the region between *repE* and *repC* and the supposed *oriII* region, although this later showed a lower pic than the one observed in the promoter. The methylation state of GANTC sites has been reported to affect the binding of GcrA to some GANTC sites, and to regulate transcription (Fioraventi *et al*., 2013). This may allow a regulation cell cycle dependent, since DNA presents either a fully methylated state or a hemimethylated state according to the phase of the cell cycle and according to the position of the GANTC motif on the chromosome. The transcriptional control of *repE* by methylated state of the GANTC sites located in its promoter could be a part of the *oriII* replication regulation observed during the cell cycle of *B. abortus*. To test this hypothesis, it could be interesting to generate depletion strain for *ccrM*, the essential GANTC-sites methylase in *B. abortus*, and to monitor the replication of the chromosome II during *ccrM* depletion condition. The mutation of these GANTC sites could be also interesting to perform in order to study their direct impacts on chromosome II replication.

The transcriptional regulator CtrA has also been shown to bind to the promoter of the *repABC* cassette in *B. abortus* (Francis *et al*., 2017), and this binding was already reported in *A. tumefaciens* (Brilli *et al*., 2010). Since CtrA does not bind *B. abortus oriI*, as it is the case in *C. crescentus*, it is possible that this regulator has evolved to control chromosome II replication in *B. abortus*.

Altogether, these analyses could underlie regulation mechanisms for the delay observed between replication/segregation of chromosome I and II origins in *B. abortus*, which could involve DnaA, GcrA and the methylation state of DNA, as well as the CtrA master cell cycle regulator.

General conclusion

Several years ago, the study of *B. abortus* DNA replication revealed that the cell cycle of this pathogen is linked to its ability to infect host cells. Indeed, the G1 bacteria represent the infectious form, and once they enter inside their host, bacteria remain in this G1 stage and do not grow for several hours. When they enter inside host cells, bacteria encounter stresses such as starvation or acidic pH conditions (Roop *et al*., 2009). Since (p)ppGpp is well known to mediate survival during stress conditions, such as starvation, in other bacterial species and that *Brucella rsh* mutants were previously reported to be attenuated during the infection, we decided to study the involvement of this alarmone in DNA replication control and in infection of *B. abortus*.

We confirmed that *rsh* is important for *Brucella abortus* survival in minimal medium and during the infection process, as a deletion mutant was impaired for growth in Plommet medium and in infection of RAW 264.7 macrophages. The fact that the pBBRi-*mesh1b* was also attenuated during infection strongly suggests that the cause of this defect was the absence of (p)ppGpp. Moreover, the precise concentration of the alarmone seemed to be important since the induced pSRK-*relA'* strain did not appear to proliferate in HeLa cells as well as in macrophages. This result suggested that (p)ppGpp might be produced at a precise concentration and/or time and had to be regulated during intracellular trafficking. The generation of a (p)ppGpp reporter strain and its characterization during infection could be of great interest to learn more about (p)ppGpp production/degradation during the trafficking.

The study of the pSRK-*relA'* strain showed that (p)ppGpp had an impact on growth and DNA replication in rich culture medium, and especially affected the intracellular DnaA levels, indicating that this alarmone could regulate cell cycle progression in *B. abortus*.

We showed that in the absence of DksA, mediating in part the (p)ppGpp response in other bacterial species, did not impact the infection of macrophages, suggesting that the phenotype observed for Δ*rsh* in infection was not strictly dependent on DksA.

However, the ClpSA, HdaA, and GcrA proteins in *B. abortus* need to be further investigated in order to learn more about their potential involvement in regulation of replication, and particularly in the coordination between replication of chromosome I and chromosome II. Nevertheless, the fact that GcrA is able to bind the origins of replication of both chromosomes and the promoter of *dnaA,* and that these three targets are directly linked to replication initiation, makes GcrA an interesting target for further studies on replication regulation in *B. abortus*.

Material and methods

Material and methods

Strains and growth conditions

The reference strain *B. abortus* 544 was used for all experiments and was grown on solid or in liquid 2YT medium (LB 32 g/L Invitrogen, Yeast Extract 5g/L, BD and Peptone 6 g/L, BD), or in the Plommet minimal medium (K_2HPO_4 7 g/L, KH_2PO_4 3 g/L, NaCl 5 g/L, $Na_2S_2O_3$ 0.1 g/L, $(NH_4)_2SO_4$ 0.5 g/L, $MgSO_4$ 10 mg/L, $MnSO_4$ 0.1 mg/L , $FeSO_4$ 0.1mg/L, Biotine 0.0001 mg/L, Nicotinate 0.2 mg/L, Thiamine 0.2 mg/L, Pantothenate 0.04 mg/L, Erythritol 2g/L, (Plommet, 1991) at 37°C.. *E. coli* strain DH10B was used for plasmid constructions and the conjugative strain *E. coli* S17-1 was used for mating with *B. abortus*. Both strains were cultivated in LB medium (Luria Bertani, Casein Hydrolysate 10g/L, NaCl 5g/L, Yeast Extract 5g/L) at 37°C. Depending on the plasmid used, different selection antibiotics were added into the culture medium: Ampicillin (100 µg/mL); Carbanecillin (100 µg/mL); Kanamycin (50 µg/mL for replicative plasmid, and 10 µg/mL for integrated plasmid); Nalidixic acid (25µL/mL); Chloramphenicol (20 µg/mL for replicative plasmid and 4 µg/mL for integrated plasmid).

Constructions of mutant strains

***rsh* deletion in *B. abortus*:**

We generated a Δ*rsh* strain by allelic replacement in *B. abortus* 544 as it was described in Dozot *et al*., 2006 in order to avoid polar effect on the downstream gene *pyrE*. We used the *rsh* deletion plasmid pMQ203 (M. Quebatte, unpublished), containing the upstream and downstream regions of *rsh* amplified with the following primers (hybridization sequences): 5'-ccggatgatctgaaggaa-3' 5'-gcgcatcatctgccgaaa-3' 5'-gtctgggacctcaagcat-3' 5'-cccgtggtgacgatatct-3'. The Tn-seq profile for *rsh* indicated that mutants of this gene are already impaired for growth in 2YT rich culture medium condition (Figure 17) (Sternon *et al*., 2018). Indeed, we never obtained the Δ*rsh* mutant with our classical methods of conjugation in *B. abortus*. To obtain this mutant, we added casamino acids (Bacto™ Casamino Acids from Thermo Fisher) in the conjugation medium, and we bypassed the step of overnight liquid culture without any antibiotic, which is supposed to allow the pop-out of the integrated deletion vector with less competition between the WT and the mutants.

G-block *mesh1b* sequence:

ccccccgggatggccacctatccgtcggccaagttcatggaatgcctgcagtatgccgccttcaagcatcgccagcagcgccgcaag
gatccgcaggaaaccccgtatgtgaatcatgtgatcaatgtgtcgaccatcctgtcggtggaagcctgcatcaccgatgaaggcgtg
ctgatggccgccctgctgcatgatgtggtggaagataccgatgcctcgttcgaagatgtggaaaagctgttcggcccggatgtgtgcg
gcctggtgcgcgaagtgaccgatgataagtcgctggaaaagcaggaacgcaagcgcctgcagatcgaaaatgccgccaagtcgtc
gtgccgcgccaagctgatcaagctggccgataagctggataatctgcgcgatctgcaggtgaataccccgaccggctggacccagg
aacgccgcgatcagtatttcgtgtgggccaagaaggtggtggataatctgcgcggcaccaatgccaatctggaactgaagctggatg
aaatcttccgccagcgcggcctgctgtgaaagcttggg

(p)ppGpp overproduction strains:

The construction of the pSRK-relA' plasmid was done by S. Ronneau, on the basis of Gonzalez and Collier, 2014. We constructed the pSRK-relA'* in the same way than it was described in Gonzalez and Collier, 2014.

Preparation of electrocompetent cells

Bacteria were inoculated in liquid 2YT medium and incubated overnight at 37°C with shaking. The culture was then diluted to obtain a final volume of 50 mL with an OD_{600} of 0.02. This culture was incubated at 37°C until it reaches an OD_{600} of 1 (approximately 15 hours), and was then incubated on ice during 10 minutes. Bacteria were centrifugated at 4200 *g*, for 10 minutes at 4°C. The pellet was then resuspended in 50 mL cold $_{dd}H_2O$. We repeated this washing step two times and with two different final volumes of cold $_{dd}H_2O$ used for the resuspension of bacteria, *i.e.* 25mL and 12.5mL. A final wash was performed using 500 µL of cold $_{dd}H_2O$ 10% glycerol and bacteria were aliquoted by 50µL and stored at -80°C.

Electroporation of *B. abortus*

50 µL of competent bacteria were mixed with 1 µg of plasmid DNA in an electroporation cuvette and incubated on ice for 1 minute. The electroporator was set as follow, 50 µF, 200 ohms and 500 ohms respectively, and 2.5 kV and one pulse was applied. Bacteria were directly added to 1 mL of 2YT liquid medium and incubated at 37°C for 6 hours. They were then plated on 2YT agar containing the antibiotic allowing the selection of resistant clones.

Conjugation

The conjugative strain *E. coli* S17 containing the plasmid of interest was used for mating with *B. abortus* 544. 50µL of an overnight culture of *E. coli* were added to 1 mL of *B. abortus* overnight culture and centrifuged at 7000 rpm during 2 minutes. The supernatant was removed and the pellet was resuspended in 1 mL of 2YT medium. This suspension was centrifuged again at 7000 rpm for 2 minutes, and the pellet was resuspended with 80µL of fresh 2YT. These two washes were performed to remove residual antibiotic of the precultures. The bacterial suspension was spotted on 2YT agar without being spread in order to improve the mating between *E. coli* and *B. abortus*. This plate was put at 37°C for 4 hours for replicative plasmids and at RT overnight for integrative plasmids. Then, a part of the drop was resuspended in 100µL of 2YT medium, spread on 2YT agar plate containing nalidixic acid and antibiotic corresponding to the resistance cassette carrying by the plasmid conjugated. The plate was placed at 37°C during approximately 4 days (time for colonies grow and appear). Colonies obtain were streaked on 2YT agar containing only the antibiotic for the resistance cassette of the conjugated plasmid and incubated at 37°C. For replicative plasmids, overnight bacterial cultures were performed from streaks in liquid 2YT medium with the corresponding antibiotic and stocks were performed at -80°C. For integrative plasmid, a bacterial culture was performed from a streak in liquid 2YT allowing the second crossing-over, and the pop-out of the plasmid which contains the counter-selection marker *sacB*. 100µL of this culture were spread on 2YT agar containing sucrose (5%) to select bacteria which had excised their plasmid and plates were incubated at 37°C. The colonies obtained were picked and spread on two plates containing respectively the antibiotic corresponding to the plasmid conjugated or sucrose. Only bacteria which had grown on sucrose but not on the antibiotic were selected to check for the deletion after being inactivated in sterile PBS at 80°C during 1 hour.

Growth assays

The bacterial growth curves were performed using a bioscreen (Epoch2 Microplate Photospectrometer from BioTek). Bacterial culture in exponential phase of growth were washed two times with PBS and were normalized at an OD 0.1 in a given medium. 200µL of the normalized culture were put in wells plates and each condition were performed in technical triplicate (3 times 200µL). Plates were placed at 37°C with shaking and the OD_{600} of each well was measured every 30 minutes. One biological replicate constitutes the mean of three technical replicates and experiments were repeated at least three times to obtained biological triplicates.

The doubling times of the WT and the *pSRK-relA'* strains induced and non-induced were calculated using the linear part of the growth curve with the following formula:

$$r = \frac{\ln(OD2/OD1)}{T2 - T1}$$

$$\text{Doubling time} = \frac{\ln(2)}{r}$$

Infections

RAW 264.7 cells

RAW macrophages were put in wells in DMEM medium (with decomplemented bovine serum, glucose, glutamine, and no pyruvate, Gibco®) to have 10^5 cells/mL. *B. abortus* 544 was grown in 2YT at 37°C until exponential phase and the OD of the bacterial culture was measured and dilutions were performed to have MOI equal to 50 (50 times more bacteria than macrophages). An input control was performed for each condition by plating bacteria on 2YT agar plate before to infect cells. Cells medium was removed to add the appropriate bacterial dilution. The mix was centrifuged 10 minutes at 1200 rpm (4°C) and incubated at 37°C, 5% CO_2 (this time point is set as time zero). After one hour of incubation, medium was removed and replaced by medium containing gentamycin (50 µg/ml) during 1 hour in order to kill extracellular bacteria, and then by medium containing gentamycin (10 µg/ml). Note that for the experiments using IPTG, the IPTG (10 mM) was kept during all the steps of the infection. At either 2 hours, 4 hours or 24 hours post infection, cells were first washed with sterile PBS and were then incubated in PBS + triton 0.1% at 37°C during 10 minutes in order to lyse the

cells while keeping bacteria alive. After that, cells were flushed and lysates were harvested. Serial dilutions were performed and each dilution was spotted on 2YT agar plates and put at 37°C.

HeLa cells

HeLa cells were put in wells in DMEM medium (with sodium pyruvate, non-essential amino acid, glucose, glutamine, and no pyruvate, Gibco®) to have $4x10^4$ cells/mL. *B. abortus* 544 was grown in 2YT at 37°C until exponential phase and the OD of the bacterial culture was measured and dilutions were performed to have MOI equal to 300. An input control was performed for each condition by plating bacteria on 2YT agar plate before to infect cells. Cells medium was removed to add the appropriate bacteria dilution. The mix was centrifuged 10 minutes at 1200 rpm (4°C) and incubated at 37°C, 5 % CO_2 (this time point is set as time zero). After one hour of incubation, medium was removed and replaced by medium containing gentamycin (50 μg/ml) in order to kill extracellular bacteria, and then gentamycin (10 μg/ml). Note that for the experiments using IPTG, the IPTG (10 mM) was kept during all the steps of the infection. At either 2 hours, 4 hours or 24 hours post infection, cells were first washed with sterile PBS and were then incubated in PBS + triton 0.1% at 37°C during 10 minutes in order to lyse the cells while keeping bacteria alive. After that, cells were flushed and lysates were harvested. Serial dilutions were performed and each dilution was spotted on 2YT agar plates and put at 37°C.

Construction for DnaA$_{abortus}$ antibody

For the overproduction of the protein fragment, we cloned the *dnaA*$_{abortus}$ ORF without the C-terminal DNA-binding domain (named *dnaA*-without-C-Ter) in the pET-28a(+) vector (Novagen) containing His-tag for protein purification. The sequences of the primers used for the *dnaA*-without-C-Ter were 5'-CCTAATTCCCATATGAAAATGGACAGTGCCGT-3' and 5'-CCGGAATTCTCACAGATGGCCGAGCAACTC-3' for forward and reverse primers respectively.

Western blots

Bacterial cultures were grown until exponential phase or stationary phase. For experiments requiring IPTG induction, cultures were normalized and induced or not with IPTG

1mM at time zero. Samples were taken and concentrated at an OD_{600} of 10 in PBS and were incubated at 80°C for 1 hour to lyse bacteria. Loading buffer was added at 1:4 final volume and samples were boiled for 10 minutes to denature proteins. Samples were loaded on 12% acrylamide gels and migrations were performed during 45 minutes, 200V, 40 mA (constant voltage). Proteins were then transferred to a nitrocellulose membrane (GE Healthcare) and the membrane was blocked overnight at 4°C in PBS Tween20 (0.05%) and milk (5%). The day after, the membrane was incubated in PBS Tween20 (0.05%) and milk (0,5%) containing the primary antibody (different concentrations used according to the antibody) for 1 hour, was washed three times in PBS Tween20 (0.05%), was incubated in PBS Tween20 (0.05%) and milk (0,5%) containing the secondary antibody (1:5000) and was incubated 1 hour. The membrane was then washed three times with PBS Tween20 (0.05%) and was revealed using the Clarity Western ECL Substrate (from Biorad) and Image Quant LAS 4000 (from General Electric).

ChIP-seq experiments

The ChIP-seq experiment was performed as previously described in Francis *et al.*, 2017. Bacterial cultures of 80 mL were harvested by centrifugation and proteins were cross-linked to DNA with 10 mM sodium phosphate buffer (pH 7.6) and 1% formaldehyde for 10 min at RT and 30 min on ice. In order to stop the crosslinking, glycine was added to the samples to have a final concentration of 125 mM. Bacteria were centrifuged and washed twice with cold PBS before to be resuspended in 450 µL of lysis buffer (10 mM Tris-HCl pH 7.5, 1 mM EDTA, 100 mM NaCl, 2.2 mg/ml lysozyme, and a half pill of complete protease inhibitor cocktail EDTA free from Roche). We lysed bacteria using Zirconia/Silica beads (Biospec Products) of 0.1 mm and 0.5 mm diameter in a cell disruptor (Scientific Industries) at maximal amplitude (2800) during 1 hour at 4°C in safelock tubes. We added then 550 µL of ChIP buffer (1.1% Triton X-100, 1.2 mM EDTA, 16.7 mM Tris-HCl pH 8.0, 167 mM NaCl, protease inhibitors) and incubated for 10 min. Samples were then sonicated with by applying 12 bursts of 30 seconds in order to obtain DNA fragments of approximately 300 bp. Bacterial debris were removed by centrifugation at 14,000 rpm for 5 min. We quantified proteins in the samples by measuring the absorbance at 280 nm and we normalized to have 7.5 mg of protein for each sample in 1 mL of ChIP buffer containing 0.01% SDS. 50 µL of magnetic protein A-agarose beads were prepared by incubation on rotator with 100 µg BSA at 4°C. The samples were pre-cleared with the prepared magnetic protein A-agarose beads (Roche) and 100 µg BSA. 10 µg of primary antibodies were added to samples and incubated overnight at 4°C on rotator. The samples

were then incubated with 50 µL of protein A-agarose beads pre-saturated with BSA for 2 hours at 4°C on rotator. Beads were then washed with the following buffers: low salt buffer (0.1% SDS, 1% Triton X-100, 2 mM EDTA, 20 mM Tris-HCl pH 8.1, 150 mM NaCl), high salt buffer (0.1% SDS, 1% Triton X-100, 2 mM EDTA, 20 mM Tris-HCl pH 8.1, 500 mM NaCl), LiCl buffer (0.25 M LiCl, 1% NP-40, 1% sodium deoxycholate, 1 mM EDTA, 10 mM Tris-HCl pH 8.1) and twice with TE buffer (10 mM Tris-HCl pH 8.1 and 1 mM EDTA). Sample were then eluted with 500 µL of elution buffer (1% SDS and 0.1 M $NaHCO_3$). The reverse- crosslinking was performed with 500 µL of 300 mM of NaCl overnight at 65°C. Samples were then treated with Proteinase K (in 40 mM EDTA and 40 mM Tris-HCl pH 6.5) for 2 h at 45°C and DNA was finally extracted with QIAGEN MinElute kit to be resuspended in 30 µL of water. DNA was sequenced with Illumina sequencing technology after creating a DNA library and the reads were aligned on the genome using the Bowtie2 program at the Galaxy platform (https://usegalaxy.org), and the resulting BAM file was converted to a tabular format.

Flow cytometry

Bacteria in exponential phase were induced or not with IPTG at time 0H and let grown. A control with only rifampicin 20 µg/mL added at time 0H was done for the experiments. Bacteria were washed twice in PBS, and were fixed with ice-cold PBS 70% ethanol and left overnight at -20°C. The day after the samples were washed twice in FACS staining buffer (10 mM Tris pH 7.2, 1 mM EDTA, 50 mM, Sodium Citrate, 0.01% Triton X-100) containing 0.1 mg/ml of RNaseA and were incubated at room temperature during 30 min. Cells were then centrifuged for 2 min at 8000g, resuspended in 1 ml of FACS staining buffer containing 0.5 µM of Sytox Green (Life Technologies), then incubated at room temperature in the dark for 5 min. Samples were analyzed by flow cytometry (FACS Calibur, BD Biosciences) at laser excitation of 488 nm.

Primers used for this study

Primer name	Sequence (5'→ 3')	Strain
ΔTM-hdaA-AMF	gggGTCGACcatcaatagcgatcttgagc	*ΔTM-hdaA-yfp*
ΔTM-hdaA-AMR	CATattgacatgaatgtcaccg	
ΔTM-hdaA-AVF	cggtgacattcatgtcaatATGcgttttgcattgaatagcta	
ΔTM-hdaA-AVR	gggGAATTCatctgtatcgccgatagaag	
ΔTM-hdaA-check-F	tgcacgaccagatcgttcac	
hdaA-yfp-AM-F	aaGTCGACcgggtgacaatacaggccg	*hdaA-yfp*
hdaA-yfp-AM-R	ttCTCGAGtccggcctgccccata	
yfp-for-hdaA-F	aaCTCGAGtcgaagggcgaag	
yfp-for-hdaA-R	ctCTGCAGtcacttatacagttcatc	
hdaA-yfp-AV-F	tttCTGCAGtgagggtggcggtcaca	
hdaA-yfp-AV-R	tttGAATTCggtcgtagagaccgcgctt	
ΔclpSA-AMF	cgcGGATCCcgtatccttgttgatgcg	*ΔclpSA*
ΔclpSA-AMR	gcgGAATTCggacgtcatatggggatt	
ΔclpSA-AVF	aaaGAATTCtaaacgcataaaaacggc	
ΔclpSA-AVR	aaaGCTAGCcgagataatgggcggaat	
clpSA-compl-F	aaaGGATCCgtgttcgcatcaacgacg	*ΔclpSA clpSA-compl*
clpSA-compl-R	aaaAAGCTTttatttcttgcgcggcac	
PgidAmChparBFnew	GGTACCtctgtggaatcctgtttgt	*pSKoriTcat-PgidA-mcherry-parB*
PgidAmChparBRnew	GAGCTCctagctttgaagac	
del-dksA-AM-F	ttGGATCCcaagcgccagatcttca	*ΔdksA*
del-dksA-AM-R	ttGAATTCttcactcattctgaatcacccc	
del-dksA-AV-F	ttGAATTCtgatatcgaataatggtttggaaa	
del-dksA-AV-R	ttAAGCTTcgcccagcttcaaattac	
dksA-compl-F2	aaaGGATCCtttcaacatctatgccaagc	*dksA-compl*
dksA-compl-R2	aaaAAGCTTtcagtcgtcgcgataaac	
ampR-F-SpeI	ttACTAGTttaccaatgcttaatcagtgagg	pUC18-*ampR*
ampR-R-BamHI	ttGGATCCttcaaatatgtatccgctcatga	

References

Abu-Zant, A., Asare, R., Graham, J. E., & Abu Kwaik, Y. (2006). Role for RpoS but not RelA of Legionella pneumophila in modulation of phagosome biogenesis and adaptation to the phagosomal microenvironment. *Infect Immun, 74*(5), 3021-3026. doi:10.1128/IAI.74.5.3021-3026.2006

Agirrezabala, X., Fernandez, I. S., Kelley, A. C., Carton, D. G., Ramakrishnan, V., & Valle, M. (2013). The ribosome triggers the stringent response by RelA via a highly distorted tRNA. *EMBO Rep, 14*(9), 811-816. doi:10.1038/embor.2013.106

Al Dahouk, S., Kohler, S., Occhialini, A., Jimenez de Bagues, M. P., Hammerl, J. A., Eisenberg, T., . . . Scholz, H. C. (2017). Brucella spp. of amphibians comprise genomically diverse motile strains competent for replication in macrophages and survival in mammalian hosts. *Sci Rep, 7*, 44420. doi:10.1038/srep44420

Aravind, L., & Koonin, E. V. (1998). The HD domain defines a new superfamily of metal-dependent phosphohydrolases. *Trends Biochem Sci, 23*(12), 469-472. doi:10.1016/s0968-0004(98)01293-6

Asai, T., Takanami, M., & Imai, M. (1990). The AT richness and gid transcription determine the left border of the replication origin of the E. coli chromosome. *EMBO J, 9*(12), 4065-4072.

Atkinson, G. C., Tenson, T., & Hauryliuk, V. (2011). The RelA/SpoT homolog (RSH) superfamily: distribution and functional evolution of ppGpp synthetases and hydrolases across the tree of life. *PLoS One, 6*(8), e23479. doi:10.1371/journal.pone.0023479

Atlung, T., Clausen, E., & Hansen, F. G. (1984). Autorepression of the dnaA gene of Escherichia coli. *Adv Exp Med Biol, 179*, 199-207. doi:10.1007/978-1-4684-8730-5_20

Atlung, T., Clausen, E. S., & Hansen, F. G. (1985). Autoregulation of the dnaA gene of Escherichia coli K12. *Mol Gen Genet, 200*(3), 442-450. doi:10.1007/bf00425729

Atluri, V. L., Xavier, M. N., de Jong, M. F., den Hartigh, A. B., & Tsolis, R. M. (2011). Interactions of the human pathogenic Brucella species with their hosts. *Annu Rev Microbiol, 65*, 523-541. doi:10.1146/annurev-micro-090110-102905

Barker, M. M., Gaal, T., & Gourse, R. L. (2001). Mechanism of regulation of transcription initiation by ppGpp. II. Models for positive control based on properties of RNAP mutants and competition for RNAP. *J Mol Biol, 305*(4), 689-702. doi:10.1006/jmbi.2000.4328

Battesti, A., & Bouveret, E. (2006). Acyl carrier protein/SpoT interaction, the switch linking SpoT-dependent stress response to fatty acid metabolism. *Mol Microbiol, 62*(4), 1048-1063. doi:10.1111/j.1365-2958.2006.05442.x

Bellefontaine, A. F., Pierreux, C. E., Mertens, P., Vandenhaute, J., Letesson, J. J., & De Bolle, X. (2002). Plasticity of a transcriptional regulation network among alpha-proteobacteria is supported by the identification of CtrA targets in Brucella abortus. *Mol Microbiol, 43*(4), 945-960. doi:10.1046/j.1365-2958.2002.02777.x

Bernardo, L. M., Johansson, L. U., Solera, D., Skarfstad, E., & Shingler, V. (2006). The guanosine tetraphosphate (ppGpp) alarmone, DksA and promoter affinity for RNA polymerase in regulation of sigma-dependent transcription. *Mol Microbiol, 60*(3), 749-764. doi:10.1111/j.1365-2958.2006.05129.x

Boschiroli, M. L., Ouahrani-Bettache, S., Foulongne, V., Michaux-Charachon, S., Bourg, G., Allardet-Servent, A., . . . O'Callaghan, D. (2002). The Brucella suis virB operon is induced

intracellularly in macrophages. *Proc Natl Acad Sci U S A, 99*(3), 1544-1549. doi:10.1073/pnas.032514299

Boutte, C. C., & Crosson, S. (2011). The complex logic of stringent response regulation in Caulobacter crescentus: starvation signalling in an oligotrophic environment. *Mol Microbiol, 80*(3), 695-714. doi:10.1111/j.1365-2958.2011.07602.x

Braun, R. E., O'Day, K., & Wright, A. (1985). Autoregulation of the DNA replication gene dnaA in E. coli K-12. *Cell, 40*(1), 159-169. doi:10.1016/0092-8674(85)90319-8

Braun, R. E., & Wright, A. (1986). DNA methylation differentially enhances the expression of one of the two E. coli dnaA promoters in vivo and in vitro. *Mol Gen Genet, 202*(2), 246-250. doi:10.1007/bf00331644

Brilli, M., Fondi, M., Fani, R., Mengoni, A., Ferri, L., Bazzicalupo, M., & Biondi, E. G. (2010). The diversity and evolution of cell cycle regulation in alpha-proteobacteria: a comparative genomic analysis. *BMC Syst Biol, 4*, 52. doi:10.1186/1752-0509-4-52

Brown, A., Fernandez, I. S., Gordiyenko, Y., & Ramakrishnan, V. (2016). Ribosome-dependent activation of stringent control. *Nature, 534*(7606), 277-280. doi:10.1038/nature17675

Brown, P. J., de Pedro, M. A., Kysela, D. T., Van der Henst, C., Kim, J., De Bolle, X., . . . Brun, Y. V. (2012). Polar growth in the Alphaproteobacterial order Rhizobiales. *Proc Natl Acad Sci U S A, 109*(5), 1697-1701. doi:10.1073/pnas.1114476109

Campbell, J. L., & Kleckner, N. (1990). E. coli oriC and the dnaA gene promoter are sequestered from dam methyltransferase following the passage of the chromosomal replication fork. *Cell, 62*(5), 967-979. doi:10.1016/0092-8674(90)90271-f

Cashel, M., & Gallant, J. (1969). Two compounds implicated in the function of the RC gene of Escherichia coli. *Nature, 221*(5183), 838-841. doi:10.1038/221838a0

Cashel, M., D. R. Gentry, V. J. Hernandez, and D. Vinella. 1996. The stringent response, p. 1458-1496. In F. C. Neidhardt, R. Curtiss III, J. L. Ingraham, E. C. C. Lin, K. B. Low, B. Magasanik, W. S. Reznikoff, M. Riley, M. Schaechter, and H. E. Umbarger (ed.), Escherichia coli and Salmonella: cellular and molecular biology, 2nd ed., vol. I. ASM Press, Washington, DC.

Celli, J., de Chastellier, C., Franchini, D. M., Pizarro-Cerda, J., Moreno, E., & Gorvel, J. P. (2003). Brucella evades macrophage killing via VirB-dependent sustained interactions with the endoplasmic reticulum. *J Exp Med, 198*(4), 545-556. doi:10.1084/jem.20030088

Cevallos, M. A., Cervantes-Rivera, R., & Gutierrez-Rios, R. M. (2008). The repABC plasmid family. *Plasmid, 60*(1), 19-37. doi:10.1016/j.plasmid.2008.03.001

Chai, Y., & Winans, S. C. (2005). A small antisense RNA downregulates expression of an essential replicase protein of an Agrobacterium tumefaciens Ti plasmid. *Mol Microbiol, 56*(6), 1574-1585. doi:10.1111/j.1365-2958.2005.04636.x

Chiaramello, A. E., & Zyskind, J. W. (1990). Coupling of DNA replication to growth rate in Escherichia coli: a possible role for guanosine tetraphosphate. *J Bacteriol, 172*(4), 2013-2019. doi:10.1128/jb.172.4.2013-2019.1990

Chiaverotti, T. A., Parker, G., Gallant, J., & Agabian, N. (1981). Conditions that trigger guanosine tetraphosphate accumulation in Caulobacter crescentus. *J Bacteriol, 145*(3), 1463-1465.

Ding Chien-Kuang Cornelia, Joshua Rose, Jianli Wu, Tianai Sun, Kai-Yuan Chen, po-Han Chen, Emily Xu, Sarah Tian, Jadesola Akinwuntan, Ziqiang Guan, Pei Zhou, Jen-Tsan Chi "Mammalian stringent-like response mediated by the cytosolic NADPH phosphatase MESH1" bioRxiv 325266; doi: https://doi.org/10.1101/325266

Collier, J., McAdams, H. H., & Shapiro, L. (2007). A DNA methylation ratchet governs progression through a bacterial cell cycle. *Proc Natl Acad Sci U S A, 104*(43), 17111-17116. doi:10.1073/pnas.0708112104

Collier, J., Murray, S. R., & Shapiro, L. (2006). DnaA couples DNA replication and the expression of two cell cycle master regulators. *EMBO J, 25*(2), 346-356. doi:10.1038/sj.emboj.7600927

Collier, J., & Shapiro, L. (2009). Feedback control of DnaA-mediated replication initiation by replisome-associated HdaA protein in Caulobacter. *J Bacteriol, 191*(18), 5706-5716. doi:10.1128/JB.00525-09

Costanzo, A., Nicoloff, H., Barchinger, S. E., Banta, A. B., Gourse, R. L., & Ades, S. E. (2008). ppGpp and DksA likely regulate the activity of the extracytoplasmic stress factor sigmaE in Escherichia coli by both direct and indirect mechanisms. *Mol Microbiol, 67*(3), 619-632. doi:10.1111/j.1365-2958.2007.06072.x

Crooke, E., Castuma, C. E., & Kornberg, A. (1992). The chromosome origin of Escherichia coli stabilizes DnaA protein during rejuvenation by phospholipids. *J Biol Chem, 267*(24), 16779-16782.

Curtis, P. D., & Brun, Y. V. (2010). Getting in the loop: regulation of development in Caulobacter crescentus. *Microbiol Mol Biol Rev, 74*(1), 13-41. doi:10.1128/MMBR.00040-09

Dalebroux, Z. D., Svensson, S. L., Gaynor, E. C., & Swanson, M. S. (2010). ppGpp conjures bacterial virulence. *Microbiol Mol Biol Rev, 74*(2), 171-199. doi:10.1128/MMBR.00046-09

Deghelt, M., Mullier, C., Sternon, J. F., Francis, N., Laloux, G., Dotreppe, D., . . . De Bolle, X. (2014). G1-arrested newborn cells are the predominant infectious form of the pathogen Brucella abortus. *Nat Commun, 5*, 4366. doi:10.1038/ncomms5366

Degnen, S. T., & Newton, A. (1972). Chromosome replication during development in Caulobacter crescentus. *J Mol Biol, 64*(3), 671-680. doi:10.1016/0022-2836(72)90090-3

Domian, I. J., Quon, K. C., & Shapiro, L. (1997). Cell type-specific phosphorylation and proteolysis of a transcriptional regulator controls the G1-to-S transition in a bacterial cell cycle. *Cell, 90*(3), 415-424. doi:10.1016/s0092-8674(00)80502-4

Dozot, M., Boigegrain, R. A., Delrue, R. M., Hallez, R., Ouahrani-Bettache, S., Danese, I., . . . Kohler, S. (2006). The stringent response mediator Rsh is required for Brucella melitensis and Brucella suis virulence, and for expression of the type IV secretion system virB. *Cell Microbiol, 8*(11), 1791-1802. doi:10.1111/j.1462-5822.2006.00749.x

Fernandez-Fernandez, C., Gonzalez, D., & Collier, J. (2011). Regulation of the activity of the dual-function DnaA protein in Caulobacter crescentus. *PLoS One, 6*(10), e26028. doi:10.1371/journal.pone.0026028

Ferullo, D. J., & Lovett, S. T. (2008). The stringent response and cell cycle arrest in Escherichia coli. *PLoS Genet, 4*(12), e1000300. doi:10.1371/journal.pgen.1000300

Fingland, N., Flatten, I., Downey, C. D., Fossum-Raunehaug, S., Skarstad, K., & Crooke, E. (2012). Depletion of acidic phospholipids influences chromosomal replication in Escherichia coli. *Microbiologyopen, 1*(4), 450-466. doi:10.1002/mbo3.46

Fioravanti, A., Fumeaux, C., Mohapatra, S. S., Bompard, C., Brilli, M., Frandi, A., . . . Biondi, E. G. (2013). DNA binding of the cell cycle transcriptional regulator GcrA depends on N6-adenosine methylation in Caulobacter crescentus and other Alphaproteobacteria. *PLoS Genet, 9*(5), e1003541. doi:10.1371/journal.pgen.1003541

Francis, N., Poncin, K., Fioravanti, A., Vassen, V., Willemart, K., Ong, T. A., . . . De Bolle, X. (2017). CtrA controls cell division and outer membrane composition of the pathogen Brucella abortus. *Mol Microbiol, 103*(5), 780-797. doi:10.1111/mmi.13589

Frandi, A., & Collier, J. (2019). Multilayered control of chromosome replication in Caulobacter crescentus. *Biochem Soc Trans, 47*(1), 187-196. doi:10.1042/BST20180460

Fujimitsu, K., & Katayama, T. (2004). Reactivation of DnaA by DNA sequence-specific nucleotide exchange in vitro. *Biochem Biophys Res Commun, 322*(2), 411-419. doi:10.1016/j.bbrc.2004.07.141

Fujimitsu, K., Senriuchi, T., & Katayama, T. (2009). Specific genomic sequences of E. coli promote replicational initiation by directly reactivating ADP-DnaA. *Genes Dev, 23*(10), 1221-1233. doi:10.1101/gad.1775809

Fuller, R. S., Funnell, B. E., & Kornberg, A. (1984). The dnaA protein complex with the E. coli chromosomal replication origin (oriC) and other DNA sites. *Cell, 38*(3), 889-900. doi:10.1016/0092-8674(84)90284-8

Gallant, J., Palmer, L., & Pao, C. C. (1977). Anomalous synthesis of ppGpp in growing cells. *Cell, 11*(1), 181-185. doi:10.1016/0092-8674(77)90329-4

Gonzalez, D., & Collier, J. (2014). Effects of (p)ppGpp on the progression of the cell cycle of Caulobacter crescentus. *J Bacteriol, 196*(14), 2514-2525. doi:10.1128/JB.01575-14

Gonzalez, D., Kozdon, J. B., McAdams, H. H., Shapiro, L., & Collier, J. (2014). The functions of DNA methylation by CcrM in Caulobacter crescentus: a global approach. *Nucleic Acids Res, 42*(6), 3720-3735. doi:10.1093/nar/gkt1352

Gropp, M., Strausz, Y., Gross, M., & Glaser, G. (2001). Regulation of Escherichia coli RelA requires oligomerization of the C-terminal domain. *J Bacteriol, 183*(2), 570-579. doi:10.1128/JB.183.2.570-579.2001

Gummesson, B., Lovmar, M., & Nystrom, T. (2013). A proximal promoter element required for positive transcriptional control by guanosine tetraphosphate and DksA protein during the stringent response. *J Biol Chem, 288*(29), 21055-21064. doi:10.1074/jbc.M113.479998

Haakonsen, D. L., Yuan, A. H., & Laub, M. T. (2015). The bacterial cell cycle regulator GcrA is a sigma70 cofactor that drives gene expression from a subset of methylated promoters. *Genes Dev, 29*(21), 2272-2286. doi:10.1101/gad.270660.115

Hallez, R., Bellefontaine, A. F., Letesson, J. J., & De Bolle, X. (2004). Morphological and functional asymmetry in alpha-proteobacteria. *Trends Microbiol, 12*(8), 361-365. doi:10.1016/j.tim.2004.06.002

Hallez, R., Mignolet, J., Van Mullem, V., Wery, M., Vandenhaute, J., Letesson, J. J., . . . De Bolle, X. (2007). The asymmetric distribution of the essential histidine kinase PdhS indicates a differentiation event in Brucella abortus. *EMBO J, 26*(5), 1444-1455. doi:10.1038/sj.emboj.7601577

Hanna, N., Ouahrani-Bettache, S., Drake, K. L., Adams, L. G., Kohler, S., & Occhialini, A. (2013). Global Rsh-dependent transcription profile of Brucella suis during stringent response unravels adaptation to nutrient starvation and cross-talk with other stress responses. *BMC Genomics, 14*, 459. doi:10.1186/1471-2164-14-459

Hansen, F. G., & Atlung, T. (2018). The DnaA Tale. *Front Microbiol, 9*, 319. doi:10.3389/fmicb.2018.00319

Hansen, F. G., Hansen, E. B., & Atlung, T. (1982). The nucleotide sequence of the dnaA gene promoter and of the adjacent rpmH gene, coding for the ribosomal protein L34, of Escherichia coli. *EMBO J, 1*(9), 1043-1048.

Hauryliuk, V., Atkinson, G. C., Murakami, K. S., Tenson, T., & Gerdes, K. (2015). Recent functional insights into the role of (p)ppGpp in bacterial physiology. *Nat Rev Microbiol, 13*(5), 298-309. doi:10.1038/nrmicro3448

Hecht, G. B., & Newton, A. (1995). Identification of a novel response regulator required for the swarmer-to-stalked-cell transition in Caulobacter crescentus. *J Bacteriol, 177*(21), 6223-6229. doi:10.1128/jb.177.21.6223-6229.1995

Hirota, Y., Mordoh, J., & Jacob, F. (1970). On the process of cellular division in Escherichia coli. 3. Thermosensitive mutants of Escherichia coli altered in the process of DNA initiation. *J Mol Biol, 53*(3), 369-387. doi:10.1016/0022-2836(70)90072-0

Hwang, D. S., & Kornberg, A. (1992). Opening of the replication origin of Escherichia coli by DnaA protein with protein HU or IHF. *J Biol Chem, 267*(32), 23083-23086.

Iniesta, A. A., Hillson, N. J., & Shapiro, L. (2010). Polar remodeling and histidine kinase activation, which is essential for Caulobacter cell cycle progression, are dependent on DNA replication initiation. *J Bacteriol, 192*(15), 3893-3902. doi:10.1128/JB.00468-10

Iniesta, A. A., McGrath, P. T., Reisenauer, A., McAdams, H. H., & Shapiro, L. (2006). A phospho-signaling pathway controls the localization and activity of a protease complex critical for bacterial cell cycle progression. *Proc Natl Acad Sci U S A, 103*(29), 10935-10940. doi:10.1073/pnas.0604554103

Jiang, M., Sullivan, S. M., Wout, P. K., & Maddock, J. R. (2007). G-protein control of the ribosome-associated stress response protein SpoT. *J Bacteriol, 189*(17), 6140-6147. doi:10.1128/JB.00315-07

Jonas, K., Liu, J., Chien, P., & Laub, M. T. (2013). Proteotoxic stress induces a cell-cycle arrest by stimulating Lon to degrade the replication initiator DnaA. *Cell, 154*(3), 623-636. doi:10.1016/j.cell.2013.06.034

Jumas-Bilak, E., Michaux-Charachon, S., Bourg, G., O'Callaghan, D., & Ramuz, M. (1998). Differences in chromosome number and genome rearrangements in the genus Brucella. *Mol Microbiol, 27*(1), 99-106. doi:10.1046/j.1365-2958.1998.00661.x

Kang, S., Han, J. S., Kim, K. P., Yang, H. Y., Lee, K. Y., Hong, C. B., & Hwang, D. S. (2005). Dimeric configuration of SeqA protein bound to a pair of hemi-methylated GATC sequences. *Nucleic Acids Res, 33*(5), 1524-1531. doi:10.1093/nar/gki289

Kato, J., & Katayama, T. (2001). Hda, a novel DnaA-related protein, regulates the replication cycle in Escherichia coli. *EMBO J, 20*(15), 4253-4262. doi:10.1093/emboj/20.15.4253

Khan, S. R., Gaines, J., Roop, R. M., 2nd, & Farrand, S. K. (2008). Broad-host-range expression vectors with tightly regulated promoters and their use to examine the influence of TraR and TraM expression on Ti plasmid quorum sensing. *Appl Environ Microbiol, 74*(16), 5053-5062. doi:10.1128/AEM.01098-08

Kim, S., Watanabe, K., Suzuki, H., & Watarai, M. (2005). Roles of Brucella abortus SpoT in morphological differentiation and intramacrophagic replication. *Microbiology, 151*(Pt 5), 1607-1617. doi:10.1099/mic.0.27782-0

Kim, S., Watarai, M., Kondo, Y., Erdenebaatar, J., Makino, S., & Shirahata, T. (2003). Isolation and characterization of mini-Tn5Km2 insertion mutants of Brucella abortus deficient in internalization and intracellular growth in HeLa cells. *Infect Immun, 71*(6), 3020-3027. doi:10.1128/iai.71.6.3020-3027.2003

Kitagawa, R., Mitsuki, H., Okazaki, T., & Ogawa, T. (1996). A novel DnaA protein-binding site at 94.7 min on the Escherichia coli chromosome. *Mol Microbiol, 19*(5), 1137-1147. doi:10.1046/j.1365-2958.1996.453983.x

Kitagawa, R., Ozaki, T., Moriya, S., & Ogawa, T. (1998). Negative control of replication initiation by a novel chromosomal locus exhibiting exceptional affinity for Escherichia coli DnaA protein. *Genes Dev, 12*(19), 3032-3043. doi:10.1101/gad.12.19.3032

Kohler, S., Foulongne, V., Ouahrani-Bettache, S., Bourg, G., Teyssier, J., Ramuz, M., & Liautard, J. P. (2002). The analysis of the intramacrophagic virulome of Brucella suis deciphers the environment encountered by the pathogen inside the macrophage host cell. *Proc Natl Acad Sci U S A, 99*(24), 15711-15716. doi:10.1073/pnas.232454299

Kraemer, J. A., Sanderlin, A. G., & Laub, M. T. (2019). The Stringent Response Inhibits DNA Replication Initiation in E. coli by Modulating Supercoiling of oriC. *MBio, 10*(4). doi:10.1128/mBio.01330-19

Lark, K. G. (1972). Evidence for the direct involvement of RNA in the initiation of DNA replication in Escherichia coli 15T. *J Mol Biol, 64*(1), 47-60. doi:10.1016/0022-2836(72)90320-8

Lee, J. W., Park, Y. H., & Seok, Y. J. (2018). Rsd balances (p)ppGpp level by stimulating the hydrolase activity of SpoT during carbon source downshift in Escherichia coli. *Proc Natl Acad Sci U S A, 115*(29), E6845-E6854. doi:10.1073/pnas.1722514115

Lemos, J. A., Brown, T. A., Jr., & Burne, R. A. (2004). Effects of RelA on key virulence properties of planktonic and biofilm populations of Streptococcus mutans. *Infect Immun, 72*(3), 1431-1440. doi:10.1128/iai.72.3.1431-1440.2004

Lesley, J. A., & Shapiro, L. (2008). SpoT regulates DnaA stability and initiation of DNA replication in carbon-starved Caulobacter crescentus. *J Bacteriol, 190*(20), 6867-6880. doi:10.1128/JB.00700-08

Liang, L., Leng, D., Burk, C., Nakajima-Sasaki, R., Kayala, M. A., Atluri, V. L., . . . Felgner, P. L. (2010). Large scale immune profiling of infected humans and goats reveals differential recognition of Brucella melitensis antigens. *PLoS Negl Trop Dis, 4*(5), e673. doi:10.1371/journal.pntd.0000673

Liu, J., Francis, L. I., Jonas, K., Laub, M. T., & Chien, P. (2016). ClpAP is an auxiliary protease for DnaA degradation in Caulobacter crescentus. *Mol Microbiol, 102*(6), 1075-1085. doi:10.1111/mmi.13537

Lu, M., Campbell, J. L., Boye, E., & Kleckner, N. (1994). SeqA: a negative modulator of replication initiation in E. coli. *Cell, 77*(3), 413-426. doi:10.1016/0092-8674(94)90156-2

Magnusson, L. U., Gummesson, B., Joksimovic, P., Farewell, A., & Nystrom, T. (2007). Identical, independent, and opposing roles of ppGpp and DksA in Escherichia coli. *J Bacteriol, 189*(14), 5193-5202. doi:10.1128/JB.00330-07

Margulies, C., & Kaguni, J. M. (1996). Ordered and sequential binding of DnaA protein to oriC, the chromosomal origin of Escherichia coli. *J Biol Chem, 271*(29), 17035-17040. doi:10.1074/jbc.271.29.17035

Masai, H., Nomura, N., & Arai, K. (1990). The ABC-primosome. A novel priming system employing dnaA, dnaB, dnaC, and primase on a hairpin containing a dnaA box sequence. *J Biol Chem, 265*(25), 15134-15144.

Matroule, J. Y., Lam, H., Burnette, D. T., & Jacobs-Wagner, C. (2004). Cytokinesis monitoring during development; rapid pole-to-pole shuttling of a signaling protein by localized kinase and phosphatase in Caulobacter. *Cell, 118*(5), 579-590. doi:10.1016/j.cell.2004.08.019

Mayer-Scholl, A., Draeger, A., Gollner, C., Scholz, H. C., & Nockler, K. (2010). Advancement of a multiplex PCR for the differentiation of all currently described Brucella species. *J Microbiol Methods, 80*(1), 112-114. doi:10.1016/j.mimet.2009.10.015

Mechold, U., Murphy, H., Brown, L., & Cashel, M. (2002). Intramolecular regulation of the opposing (p)ppGpp catalytic activities of Rel(Seq), the Rel/Spo enzyme from Streptococcus equisimilis. *J Bacteriol, 184*(11), 2878-2888. doi:10.1128/jb.184.11.2878-2888.2002

Mechold, U., Potrykus, K., Murphy, H., Murakami, K. S., & Cashel, M. (2013). Differential regulation by ppGpp versus pppGpp in Escherichia coli. *Nucleic Acids Res, 41*(12), 6175-6189. doi:10.1093/nar/gkt302

Merker, R. I., & Smit, J. (1988). Characterization of the adhesive holdfast of marine and freshwater caulobacters. *Appl Environ Microbiol, 54*(8), 2078-2085.

Messer, W., Blaesing, F., Majka, J., Nardmann, J., Schaper, S., Schmidt, A., . . . Zakrzewska-Czerwinska, J. (1999). Functional domains of DnaA proteins. *Biochimie, 81*(8-9), 819-825. doi:10.1016/s0300-9084(99)00215-1

Michaux, S., Paillisson, J., Carles-Nurit, M. J., Bourg, G., Allardet-Servent, A., & Ramuz, M. (1993). Presence of two independent chromosomes in the Brucella melitensis 16M genome. *J Bacteriol, 175*(3), 701-705. doi:10.1128/jb.175.3.701-705.1993

Miller, C. N., Smith, E. P., Cundiff, J. A., Knodler, L. A., Bailey Blackburn, J., Lupashin, V., & Celli, J. (2017). A Brucella Type IV Effector Targets the COG Tethering Complex to Remodel Host Secretory Traffic and Promote Intracellular Replication. *Cell Host Microbe, 22*(3), 317-329 e317. doi:10.1016/j.chom.2017.07.017

Moreno, E., & Moriyon, I. (2002). Brucella melitensis: a nasty bug with hidden credentials for virulence. *Proc Natl Acad Sci U S A, 99*(1), 1-3. doi:10.1073/pnas.022622699

Moreno E., Moriyón I. (2006) The Genus Brucella. In: Dworkin M., Falkow S., Rosenberg E., Schleifer KH., Stackebrandt E. (eds) The Prokaryotes. Springer, New York, NY

Morigen, Lobner-Olesen, A., & Skarstad, K. (2003). Titration of the Escherichia coli DnaA protein to excess datA sites causes destabilization of replication forks, delayed replication initiation and delayed cell division. *Mol Microbiol, 50*(1), 349-362. doi:10.1046/j.1365-2958.2003.03695.x

Myka, K. K., Kusters, K., Washburn, R., & Gottesman, M. E. (2019). DksA-RNA polymerase interactions support new origin formation and DNA repair in Escherichia coli. *Mol Microbiol, 111*(5), 1382-1397. doi:10.1111/mmi.14227

Nanamiya, H., Kasai, K., Nozawa, A., Yun, C. S., Narisawa, T., Murakami, K., . . . Tozawa, Y. (2008). Identification and functional analysis of novel (p)ppGpp synthetase genes in Bacillus subtilis. *Mol Microbiol, 67*(2), 291-304. doi:10.1111/j.1365-2958.2007.06018.x

Nascimento, M. M., Lemos, J. A., Abranches, J., Lin, V. K., & Burne, R. A. (2008). Role of RelA of Streptococcus mutans in global control of gene expression. *J Bacteriol, 190*(1), 28-36. doi:10.1128/JB.01395-07

Nozaki, S., Niki, H., & Ogawa, T. (2009). Replication initiator DnaA of Escherichia coli changes its assembly form on the replication origin during the cell cycle. *J Bacteriol, 191*(15), 4807-4814. doi:10.1128/JB.00435-09

Ohta, N., Lane, T., Ninfa, E. G., Sommer, J. M., & Newton, A. (1992). A histidine protein kinase homologue required for regulation of bacterial cell division and differentiation. *Proc Natl Acad Sci U S A, 89*(21), 10297-10301. doi:10.1073/pnas.89.21.10297

Okumura, H., Yoshimura, M., Ueki, M., Oshima, T., Ogasawara, N., & Ishikawa, S. (2012). Regulation of chromosomal replication initiation by oriC-proximal DnaA-box clusters in Bacillus subtilis. *Nucleic Acids Res, 40*(1), 220-234. doi:10.1093/nar/gkr716

Oliva, G., Sahr, T., & Buchrieser, C. (2018). The Life Cycle of L. pneumophila: Cellular Differentiation Is Linked to Virulence and Metabolism. *Front Cell Infect Microbiol, 8*, 3. doi:10.3389/fcimb.2018.00003

Park, Y. H., Lee, C. R., Choe, M., & Seok, Y. J. (2013). HPr antagonizes the anti-sigma70 activity of Rsd in Escherichia coli. *Proc Natl Acad Sci U S A, 110*(52), 21142-21147. doi:10.1073/pnas.1316629111

Paul, B. J., Barker, M. M., Ross, W., Schneider, D. A., Webb, C., Foster, J. W., & Gourse, R. L. (2004). DksA: a critical component of the transcription initiation machinery that potentiates the regulation of rRNA promoters by ppGpp and the initiating NTP. *Cell, 118*(3), 311-322. doi:10.1016/j.cell.2004.07.009

Plommet, M. (1991). Minimal requirements for growth of Brucella suis and other Brucella species. *Zentralbl Bakteriol, 275*(4), 436-450. doi:10.1016/s0934-8840(11)80165-9

Polaczek, P., & Wright, A. (1990). Regulation of expression of the dnaA gene in Escherichia coli: role of the two promoters and the DnaA box. *New Biol, 2*(6), 574-582.

Poncin, K., Roba, A., Jimmidi, R., Potemberg, G., Fioravanti, A., Francis, N., . . . De Bolle, X. (2019). Occurrence and repair of alkylating stress in the intracellular pathogen Brucella abortus. *Nat Commun, 10*(1), 4847. doi:10.1038/s41467-019-12516-8

Porte, F., Liautard, J. P., & Kohler, S. (1999). Early acidification of phagosomes containing Brucella suis is essential for intracellular survival in murine macrophages. *Infect Immun, 67*(8), 4041-4047.

Quon, K. C., Marczynski, G. T., & Shapiro, L. (1996). Cell cycle control by an essential bacterial two-component signal transduction protein. *Cell, 84*(1), 83-93. doi:10.1016/s0092-8674(00)80995-2

Quon, K. C., Yang, B., Domian, I. J., Shapiro, L., & Marczynski, G. T. (1998). Negative control of bacterial DNA replication by a cell cycle regulatory protein that binds at the chromosome origin. *Proc Natl Acad Sci U S A, 95*(1), 120-125. doi:10.1073/pnas.95.1.120

Rajashekara, G., Glasner, J. D., Glover, D. A., & Splitter, G. A. (2004). Comparative whole-genome hybridization reveals genomic islands in Brucella species. *J Bacteriol, 186*(15), 5040-5051. doi:10.1128/JB.186.15.5040-5051.2004

Raskin, D. M., Judson, N., & Mekalanos, J. J. (2007). Regulation of the stringent response is the essential function of the conserved bacterial G protein CgtA in Vibrio cholerae. *Proc Natl Acad Sci U S A, 104*(11), 4636-4641. doi:10.1073/pnas.0611650104

Reyes-Lamothe, R., & Sherratt, D. J. (2019). The bacterial cell cycle, chromosome inheritance and cell growth. *Nat Rev Microbiol, 17*(8), 467-478. doi:10.1038/s41579-019-0212-7

Richter, D., Erdmann, V. A., & Sprinzl, M. (1973). Specific recognition of GTpsiC loop (loop IV) of tRNA by 50S ribosomal subunits from E. coli. *Nat New Biol, 246*(153), 132-135. doi:10.1038/newbio246132a0

Robertson, G. T., Reisenauer, A., Wright, R., Jensen, R. B., Jensen, A., Shapiro, L., & Roop, R. M., 2nd. (2000). The Brucella abortus CcrM DNA methyltransferase is essential for viability, and its overexpression attenuates intracellular replication in murine macrophages. *J Bacteriol, 182*(12), 3482-3489. doi:10.1128/jb.182.12.3482-3489.2000

Ronneau, S., Caballero-Montes, J., Coppine, J., Mayard, A., Garcia-Pino, A., & Hallez, R. (2019). Regulation of (p)ppGpp hydrolysis by a conserved archetypal regulatory domain. *Nucleic Acids Res, 47*(2), 843-854. doi:10.1093/nar/gky1201

Ronneau, S., & Hallez, R. (2019). Make and break the alarmone: regulation of (p)ppGpp synthetase/hydrolase enzymes in bacteria. *FEMS Microbiol Rev, 43*(4), 389-400. doi:10.1093/femsre/fuz009

Ronneau, S., Petit, K., De Bolle, X., & Hallez, R. (2016). Phosphotransferase-dependent accumulation of (p)ppGpp in response to glutamine deprivation in Caulobacter crescentus. *Nat Commun, 7*, 11423. doi:10.1038/ncomms11423

Roop, R. M., 2nd, Gaines, J. M., Anderson, E. S., Caswell, C. C., & Martin, D. W. (2009). Survival of the fittest: how Brucella strains adapt to their intracellular niche in the host. *Med Microbiol Immunol, 198*(4), 221-238. doi:10.1007/s00430-009-0123-8

Ross, W., Sanchez-Vazquez, P., Chen, A. Y., Lee, J. H., Burgos, H. L., & Gourse, R. L. (2016). ppGpp Binding to a Site at the RNAP-DksA Interface Accounts for Its Dramatic Effects on Transcription Initiation during the Stringent Response. *Mol Cell, 62*(6), 811-823. doi:10.1016/j.molcel.2016.04.029

Ross, W., Vrentas, C. E., Sanchez-Vazquez, P., Gaal, T., & Gourse, R. L. (2013). The magic spot: a ppGpp binding site on E. coli RNA polymerase responsible for regulation of transcription initiation. *Mol Cell, 50*(3), 420-429. doi:10.1016/j.molcel.2013.03.021

Rowbotham, T. J. (1986). Current views on the relationships between amoebae, legionellae and man. *Isr J Med Sci, 22*(9), 678-689.

Sakiyama, Y., Nishimura, M., Hayashi, C., Akama, Y., Ozaki, S., & Katayama, T. (2018). The DnaA AAA+ Domain His136 Residue Directs DnaB Replicative Helicase to the Unwound Region of the Replication Origin, oriC. *Front Microbiol, 9*, 2017. doi:10.3389/fmicb.2018.02017

Saxena, R., Fingland, N., Patil, D., Sharma, A. K., & Crooke, E. (2013). Crosstalk between DnaA protein, the initiator of Escherichia coli chromosomal replication, and acidic phospholipids present in bacterial membranes. *Int J Mol Sci, 14*(4), 8517-8537. doi:10.3390/ijms14048517

Schaper, S., & Messer, W. (1995). Interaction of the initiator protein DnaA of Escherichia coli with its DNA target. *J Biol Chem, 270*(29), 17622-17626. doi:10.1074/jbc.270.29.17622

Schreiber, G., Ron, E. Z., & Glaser, G. (1995). ppGpp-mediated regulation of DNA replication and cell division in Escherichia coli. *Curr Microbiol, 30*(1), 27-32. doi:10.1007/bf00294520

Sedzicki, J., Tschon, T., Low, S. H., Willemart, K., Goldie, K. N., Letesson, J. J., . . . Dehio, C. (2018). 3D correlative electron microscopy reveals continuity of Brucella-containing vacuoles with the endoplasmic reticulum. *J Cell Sci, 131*(4). doi:10.1242/jcs.210799

Sekimizu, K., Bramhill, D., & Kornberg, A. (1987). ATP activates dnaA protein in initiating replication of plasmids bearing the origin of the E. coli chromosome. *Cell, 50*(2), 259-265. doi:10.1016/0092-8674(87)90221-2

Seyfzadeh, M., Keener, J., & Nomura, M. (1993). spoT-dependent accumulation of guanosine tetraphosphate in response to fatty acid starvation in Escherichia coli. *Proc Natl Acad Sci U S A, 90*(23), 11004-11008. doi:10.1073/pnas.90.23.11004

Sherlock, M. E., Sudarsan, N., & Breaker, R. R. (2018). Riboswitches for the alarmone ppGpp expand the collection of RNA-based signaling systems. *Proc Natl Acad Sci U S A, 115*(23), 6052-6057. doi:10.1073/pnas.1720406115

Shyp, V., Tankov, S., Ermakov, A., Kudrin, P., English, B. P., Ehrenberg, M., . . . Hauryliuk, V. (2012). Positive allosteric feedback regulation of the stringent response enzyme RelA by its product. *EMBO Rep, 13*(9), 835-839. doi:10.1038/embor.2012.106

Siam, R., & Marczynski, G. T. (2000). Cell cycle regulator phosphorylation stimulates two distinct modes of binding at a chromosome replication origin. *EMBO J, 19*(5), 1138-1147. doi:10.1093/emboj/19.5.1138

Skerker, J. M., & Laub, M. T. (2004). Cell-cycle progression and the generation of asymmetry in Caulobacter crescentus. *Nat Rev Microbiol, 2*(4), 325-337. doi:10.1038/nrmicro864

Smith, R. W., McAteer, S., & Masters, M. (1997). Autoregulation of the Escherichia coli replication initiator protein, DnaA, is indirect. *Mol Microbiol, 23*(6), 1303-1315. doi:10.1046/j.1365-2958.1997.3121675.x

Smulczyk-Krawczyszyn, A., Jakimowicz, D., Ruban-Osmialowska, B., Zawilak-Pawlik, A., Majka, J., Chater, K., & Zakrzewska-Czerwinska, J. (2006). Cluster of DnaA boxes involved in regulation of Streptomyces chromosome replication: from in silico to in vivo studies. *J Bacteriol, 188*(17), 6184-6194. doi:10.1128/JB.00528-06

Speck, C., Weigel, C., & Messer, W. (1999). ATP- and ADP-dnaA protein, a molecular switch in gene regulation. *EMBO J, 18*(21), 6169-6176. doi:10.1093/emboj/18.21.6169

Starr, T., Ng, T. W., Wehrly, T. D., Knodler, L. A., & Celli, J. (2008). Brucella intracellular replication requires trafficking through the late endosomal/lysosomal compartment. *Traffic, 9*(5), 678-694. doi:10.1111/j.1600-0854.2008.00718.x

Sternon, J. F., Godessart, P., Goncalves de Freitas, R., Van der Henst, M., Poncin, K., Francis, N., . . . De Bolle, X. (2018). Transposon Sequencing of Brucella abortus Uncovers Essential Genes for Growth In Vitro and Inside Macrophages. *Infect Immun, 86*(8). doi:10.1128/IAI.00312-18

Sun, D., Lee, G., Lee, J. H., Kim, H. Y., Rhee, H. W., Park, S. Y., . . . Chung, J. (2010). A metazoan ortholog of SpoT hydrolyzes ppGpp and functions in starvation responses. *Nat Struct Mol Biol, 17*(10), 1188-1194. doi:10.1038/nsmb.1906

Swinger, K. K., & Rice, P. A. (2004). IHF and HU: flexible architects of bent DNA. *Curr Opin Struct Biol, 14*(1), 28-35. doi:10.1016/j.sbi.2003.12.003

Tsokos, C. G., Perchuk, B. S., & Laub, M. T. (2011). A dynamic complex of signaling proteins uses polar localization to regulate cell-fate asymmetry in Caulobacter crescentus. *Dev Cell, 20*(3), 329-341. doi:10.1016/j.devcel.2011.01.007

Van der Henst, C., Beaufay, F., Mignolet, J., Didembourg, C., Colinet, J., Hallet, B., . . . De Bolle, X. (2012). The histidine kinase PdhS controls cell cycle progression of the pathogenic alphaproteobacterium Brucella abortus. *J Bacteriol, 194*(19), 5305-5314. doi:10.1128/JB.00699-12

Vinella, D., Albrecht, C., Cashel, M., & D'Ari, R. (2005). Iron limitation induces SpoT-dependent accumulation of ppGpp in Escherichia coli. *Mol Microbiol, 56*(4), 958-970. doi:10.1111/j.1365-2958.2005.04601.x

Waldminghaus, T., & Skarstad, K. (2009). The Escherichia coli SeqA protein. *Plasmid, 61*(3), 141-150. doi:10.1016/j.plasmid.2009.02.004

Wang, J. D., Sanders, G. M., & Grossman, A. D. (2007). Nutritional control of elongation of DNA replication by (p)ppGpp. *Cell, 128*(5), 865-875. doi:10.1016/j.cell.2006.12.043

Wang, S. P., Sharma, P. L., Schoenlein, P. V., & Ely, B. (1993). A histidine protein kinase is involved in polar organelle development in Caulobacter crescentus. *Proc Natl Acad Sci U S A, 90*(2), 630-634. doi:10.1073/pnas.90.2.630

Wargachuk, R., & Marczynski, G. T. (2015). The Caulobacter crescentus Homolog of DnaA (HdaA) Also Regulates the Proteolysis of the Replication Initiator Protein DnaA. *J Bacteriol, 197*(22), 3521-3532. doi:10.1128/JB.00460-15

Wheeler, R. T., & Shapiro, L. (1999). Differential localization of two histidine kinases controlling bacterial cell differentiation. *Mol Cell, 4*(5), 683-694. doi:10.1016/s1097-2765(00)80379-2

Wolz, C., Geiger, T., & Goerke, C. (2010). The synthesis and function of the alarmone (p)ppGpp in firmicutes. *Int J Med Microbiol, 300*(2-3), 142-147. doi:10.1016/j.ijmm.2009.08.017

Wu, X., Haakonsen, D. L., Sanderlin, A. G., Liu, Y. J., Shen, L., Zhuang, N., . . . Zhang, Y. (2018). Structural insights into the unique mechanism of transcription activation by Caulobacter crescentus GcrA. *Nucleic Acids Res, 46*(6), 3245-3256. doi:10.1093/nar/gky161

Xiao, H., Kalman, M., Ikehara, K., Zemel, S., Glaser, G., & Cashel, M. (1991). Residual guanosine 3',5'-bispyrophosphate synthetic activity of relA null mutants can be eliminated by spoT null mutations. *J Biol Chem, 266*(9), 5980-5990.

Zyskind, J. W., & Smith, D. W. (1992). DNA replication, the bacterial cell cycle, and cell growth. *Cell, 69*(1), 5-8. doi:10.1016/0092-8674(92)90112-p

Appendix

AMERICAN SOCIETY FOR MICROBIOLOGY | Infection and Immunity®

MOLECULAR GENOMICS

Transposon Sequencing of *Brucella abortus* Uncovers Essential Genes for Growth *In Vitro* and Inside Macrophages

Jean-François Sternon,[a] Pierre Godessart,[a] Rosa Gonçalves de Freitas,[a] Mathilde Van der Henst,[a] Katy Poncin,[a] Nayla Francis,[a] Kevin Willemart,[a] Matthias Christen,[b] Beat Christen,[b] Jean-Jacques Letesson,[a] Xavier De Bolle[a]

[a]Research Unit in Microorganisms Biology (URBM), Narilis, University of Namur, Namur, Belgium
[b]Institute of Molecular Systems Biology, ETH Zürich, Zurich, Switzerland

ABSTRACT *Brucella abortus* is a class III zoonotic bacterial pathogen able to survive and replicate inside host cells, including macrophages. Here we report a multidimensional transposon sequencing analysis to identify genes essential for *Brucella abortus* growth in rich medium and replication in RAW 264.7 macrophages. The construction of a dense transposon mutant library and mapping of 929,769 unique mini-Tn*5* insertion sites in the genome allowed identification of 491 essential coding sequences and essential segments in the *B. abortus* genome. Chromosome II carries a lower proportion (5%) of essential genes than chromosome I (19%), supporting the hypothesis of a recent acquisition of a megaplasmid as the origin of chromosome II. Temporally resolved transposon sequencing analysis as a function of macrophage infection stages identified 79 genes with a specific attenuation phenotype in macrophages, at either 2, 5, or 24 h postinfection, and 86 genes for which the attenuated mutant phenotype correlated with a growth defect on plates. We identified 48 genes required for intracellular growth, including the *virB* operon, encoding the type IV secretion system, which supports the validity of the screen. The remaining genes encode amino acid and pyrimidine biosynthesis, electron transfer systems, transcriptional regulators, and transporters. In particular, we report the need of an intact pyrimidine nucleotide biosynthesis pathway in order for *B. abortus* to proliferate inside RAW 264.7 macrophages.

KEYWORDS *Brucella*, RAW264.7 macrophage, Tn-seq

Brucella abortus is a class III bacterial pathogen from the *Brucella* genus known for being the causative agent of brucellosis, a worldwide anthropozoonosis generating major economic losses and public health issues (1). These bacteria are Gram negative and belong to the *Rhizobiales* order within the class *Alphaproteobacteria* and share common characteristics such as the DivK-CtrA regulation network which governs cell cycle regulation (2) and unipolar growth, as observed in *Agrobacterium tumefaciens* and *Sinorhizobium meliloti* (3). A specific feature of *B. abortus* in comparison to other *Alphaproteobacteria* is its multipartite genome, composed of two replicons of 2.1 and 1.2 Mb named chromosome 1 (chr I) and chromosome 2 (chr II), respectively (4). The chr I replication origin is similar to the one of *Caulobacter crescentus*, while the chr II replication origin resembles those found in megaplasmids of the *Rhizobiales* (5, 6).

One main aspect of *B. abortus* infections is the ability of the bacteria to invade, survive, and proliferate within host cells, including macrophages (7). Recently, the cellular infection process of *B. abortus* in both RAW 264.7 macrophages and HeLa cells has been extensively characterized at the single-cell level in terms of growth and genome replication, highlighting a typical biphasic infection profile (5). Indeed, during the course of cellular infections, *Brucella* first enters host cells through the endosomal pathway, where it remains in a "*Brucella*-containing vacuole" (BCV) for several hours without proliferating while preventing the maturation of its compartment into a

Received 25 April 2018 **Returned for modification** 16 May 2018 **Accepted** 22 May 2018

Accepted manuscript posted online 29 May 2018

Citation Sternon J-F, Godessart P, Gonçalves de Freitas R, Van der Henst M, Poncin K, Francis N, Willemart K, Christen M, Christen B, Letesson J-J, De Bolle X. 2018. Transposon sequencing of *Brucella abortus* uncovers essential genes for growth *in vitro* and inside macrophages. Infect Immun 86:e00312-18. https://doi.org/10.1128/IAI.00312-18.

Editor Andreas J. Bäumler, University of California, Davis

Address correspondence to Xavier De Bolle, xavier.debolle@unamur.be.

phagolysosome (7). During that period, typical markers such as LAMP1 are acquired (7). In most cell types, surviving bacteria are able to control the biogenesis of their vacuole into an endoplasmic reticulum (ER)-derived compartment, where they actively proliferate (7–9). This process is dependent on the type IV secretion system called VirB (10, 11). The chemical composition of the replicative BCV is difficult to study directly, but mutant *Brucella* strains may be used as probes to gain a better knowledge of the bacterial environment in these compartments. Screening of collections of transposon mutants for attenuated strains has generated hypotheses, such as the availability of histidine that was proposed to be limited (12), which is consistent with the ability of histidinol dehydrogenase inhibitors to impair growth of *Brucella* in macrophages (13). However, a major drawback of previous screenings for attenuated mutants was the size of the library, typically limited to a few thousand mutants, which does not allow saturation at the genome-wide level and therefore cannot yield quantitative results. Moreover, several interesting hypotheses regarding biosynthetic pathways required for intracellular proliferation have never been investigated.

In the present study, we have performed transposon sequencing (Tn-seq) on *B. abortus* both before and after the infection of RAW 264.7 macrophages by using a highly saturating transposon mutant library. This library was generated by plating *B. abortus* on a rich medium and was subsequently used to infect RAW 264.7 macrophages for 2, 5, and 24 h. At each stage, the transposon insertion sites were mapped to identify genes in which the transposition insertion frequency is low, suggesting that these genes are required for growth and/or survival. This approach allowed identification of genes involved in several essential processes for growth on rich medium. The temporally resolved transposon sequencing analysis allowed the identification of mutants attenuated at three postinfection (p.i.) time points. Complete and near-complete pathways required for trafficking to the ER and intracellular growth in host cells have been identified, including the ability to synthesize pyrimidines when *B. abortus* is growing in RAW 264.7 macrophages.

RESULTS

Identification of essential genes in *B. abortus* 2308. To gain genome-wide insights into the composition of essential genes necessary for growth of *B. abortus* on rich medium, we carried out a Tn-seq analysis. A *B. abortus* 2308 library of 3×10^6 random mutants was constructed using a Kan^r derivative of mini-Tn*5*, a mini-transposon that was previously used with *Brucella* (12, 14). A P*xyl* promoter was present in the mini-Tn*5* derivative to limit the potential polar effects (see Materials and Methods). The mini-Tn*5* derivatives transpose using a conservative mechanism, and a single insertion is found in each mutant (14). Directly after mating, the library was grown on rich medium and transposon insertion sites were identified by deep sequencing (Fig. 1). We identified 929,769 insertion sites from 154,630,306 mapped reads, saturating the *B. abortus* genome with an insertion site every 3.5 bp, on average. To allow a genome-wide analysis independent of gene annotations, we created a simple parameter assessing the transposon insertion frequency termed R200 (see Materials and Methods; see also Fig. S1 in the supplemental material), equal to the $\log_{10}$(number of transposon insertions + 1) found within a 200-bp sliding window (Fig. 2). According to the frequency distribution of R200 values (Fig. S2), a main peak of frequency is centered on an average value of 4.05 with a standard deviation of 0.204. Since average values are strongly influenced by extreme data and because the proportion of essential genes is very different between chr I and chr II (see below), the average R200 values for chr I and II are 3.3 and 3.8, respectively. The theoretical distribution of R200 values (Fig. S2) allows the definition of cutoffs to consider growth alteration, expressed as the number of standard deviations from the average of the main peak of R200 values. Simple statistics can also be applied to compare the R200 values of different genomic regions, as indicated in Fig. 2. As shown in Fig. 2 and the externally hosted supplemental data (SD) files (SD1 to SD14) (see Table 3) showing the transposition tolerance maps (TTMs), the essential genes and genes generating a fitness defect when mutated are very often located in the coding sequences, validating the use of R200 values. One TTM was generated for each chromosome, gener-

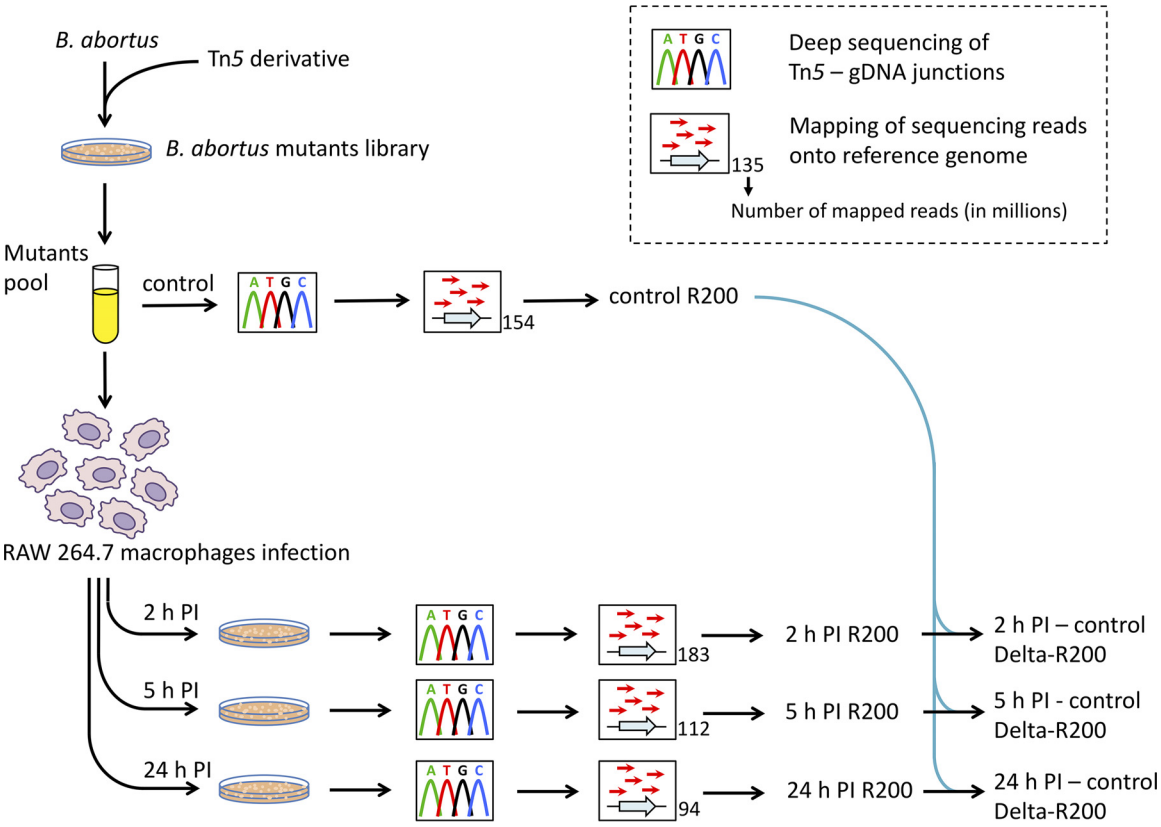

FIG 1 Summary of the Tn-seq approach. A transposon mutant library was initially created in *B. abortus* on plates using a mini-Tn*5* derivative. Three million mutants were then pooled, and the resulting suspension was split in two. The first part of the pool underwent direct sequencing of Tn*5*-gDNA junctions, allowing the identification of mini-Tn*5* insertion sites by mapping on the genomic sequence (see Fig. S1 in the supplemental material for a detailed description of the mapping and the subsequent computing), resulting in the control data set. The second part of the pool was used to infect RAW 264.7 macrophages in three separate infections. At given time points p.i. (2 h, 5 h, and 24 h), bacteria were extracted and grown on plates, colonies were collected, and their gDNA was subsequently extracted to be sequenced as for the control, resulting in 2-, 5-, and 24-h-p.i.-specific data sets. Transposon tolerance maps (TTMs) in the form of R200 values and all postinfection lists were separately compared to the control list using the Delta-R200 method (see Materials and Methods). The number of mapped read (in millions) for each data set is displayed besides its respective mapping icon, and the numbers of insertion sites are 929×10^3 for the control condition and 742×10^3, 713×10^3, and 579×10^3 for the 2-, 5-, and 24-h-p.i. data sets, respectively.

ating SD1 for chr I (https://figshare.com/s/bd0d4fa73ad8cf7737fe) and SD2 for chr II (https://figshare.com/s/3219dfa7ac60d1cda34f). Moreover, R200 and dense coverage offer an analysis with high resolution to identify new essential genes and domains (see below).

We considered essential all genes where at least one R200 value was equal to 0 under the control condition (growth on rich medium), since the probability of such events to happen randomly was estimated to be approximately 4.10^{-15} (see Materials and Methods) (15). In order to test the validity of this analysis, we checked that genes required for supposedly essential processes were indeed scored as essential if they do not have functional paralogs. As expected, genes coding for all four RNA polymerase core subunits (α, β, β', and ω), the housekeeping σ^{70}, and 51 out of the 54 ribosomal proteins were found to be essential. Additionally, the previously established essentiality of *pdhS*, *ccrM*, *omp2b*, *divK*, *cckA*, and *chpT* genes (16–20) was also confirmed.

Of the 3,419 predicted genes annotated on the *B. abortus* genome, 491 genes were found to be essential for *in vitro* culture, i.e., 14.4% of the predicted genes. This percentage is in agreement with those previously reported for other *Alphaproteobacteria* such as *C. crescentus* (12.4%), *Brevundimonas subvibrioides* (13.4%), and *Agrobacterium tumefaciens* (6.9%) (15, 21). A list of all essential genes for *in vitro* culture is available in Table S1 in the supplemental material.

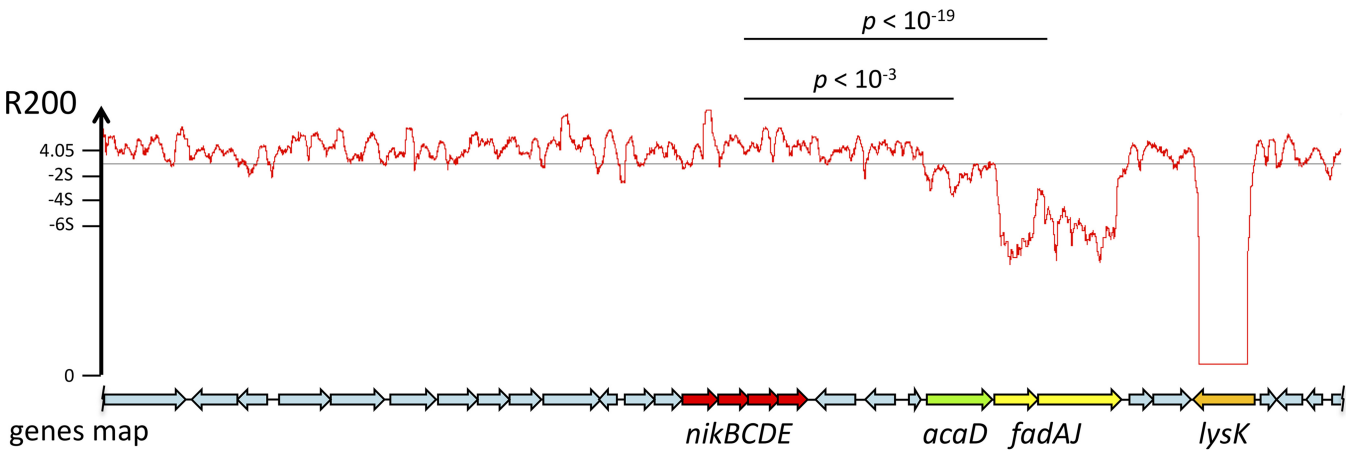

FIG 2 Sliding R200 values along a gene map. Statistical analysis of the R200 values is indicated in Fig. S2 in the supplemental material. This analysis indicates a main peak of R200 centered on a value of 4.05. Values of 2 (−2S), 4 (−4S), and 6 (−6S) standard deviations below 4.05 are indicated on the *y* axis. The region shown here is an example in which nonessential genes such as the *nikBCDE* operon (red) are found close to the *acaD* gene (BAB2_0442; green) and the *fadAJ* operon (yellow), contributing to fitness. In the same region, an essential gene (*lysK*) is also identified. The R200 values of *nikBCDE* are statistically different from those of *acaD* ($P < 10^{-3}$) and *fadAJ* ($P < 10^{-19}$), according to a Scheffé pairwise comparison test with independent samples (9 and 16 nonoverlapping windows for the *nikBCDE*-to-*acaD* and *nikBCDE*-to-*fadAJ* comparisons, respectively). The light gray horizontal line is the average R200 for chr II (3.8).

Based on the presence of a plasmid-like replication and segregation system on chr II and differences in gene content, it has been postulated that chr II might originate from an ancestrally acquired megaplasmid (5, 22). We thus tested the distribution of essential genes between the two chromosomes of *B. abortus*. Accordingly, 429 out of the 2,236 genes (19%) of chr I were essential. This is 3.7 times more than the 5% found on chr II, with 62 essential genes out of 1,183. This result further supports the megaplasmid hypothesis. One can thus hypothesize that essential genes have started to be transferred from chr I to chr II but that the frequency of this transfer is not sufficient to equilibrate the proportion of essential genes on both chromosomes yet. Besides the *repABC* operon, essential for replication initiation and segregation (5, 6), many essential genes of chr II could have been gained by recombination events with chr I. In agreement with this hypothesis, a fraction of the essential genes of chr II are clustered, such as the BAB2_0983 to BAB2_1013 region which contains 10 essential genes potentially involved in housekeeping functions like diaminopimelate biosynthesis (*dapD* and *dapE*), cell division (*fzlA*), and lipopolysaccharide (LPS) export (*msbA*).

The high resolution of the mapping (200 bp) due to the high number of reads aligned to many unique sites allows the identification of previously unannotated essential coding sequences. Indeed, since R200 values clearly map to the position of coding sequences in many instances in the genome, a drop in R200 values in a region where no gene has been predicted could indicate that a gene is indeed present and functionally relevant. This is conceptually validated by two examples shown in Fig. 3A. Interestingly, one of the two newly identified genes codes for the antitoxin component of a homologue of the SocAB system first identified in *C. crescentus* (Fig. 3A) (23). In *C. crescentus*, SocA is a proteolytic adaptor for the degradation of the SocB toxin by the ClpXP machinery (23). The essentiality of ClpXP in *C. crescentus* is due to the presence of the SocAB system (23). Therefore, the essentiality of *clpXP* genes in *B. abortus* (Fig. S3) could also be due to the presence of a SocAB homologue in *B. abortus*. Moreover, this method also allows for the reannotation of genes as exemplified by *ftsK*, where the open reading frame extends beyond the current *ftsK* locus in 5′ and matches an essentiality region (Fig. 3B). Furthermore, thanks to the high coverage of this Tn-seq, our analysis also permits the mapping of essentiality regions in genes corresponding to protein domains, as displayed by genes showing essentiality on a fraction of their coding sequence (Fig. 3C). Taken together, these observations show that high-resolution Tn-seq could support genomic reannotations and identification of essential protein domains.

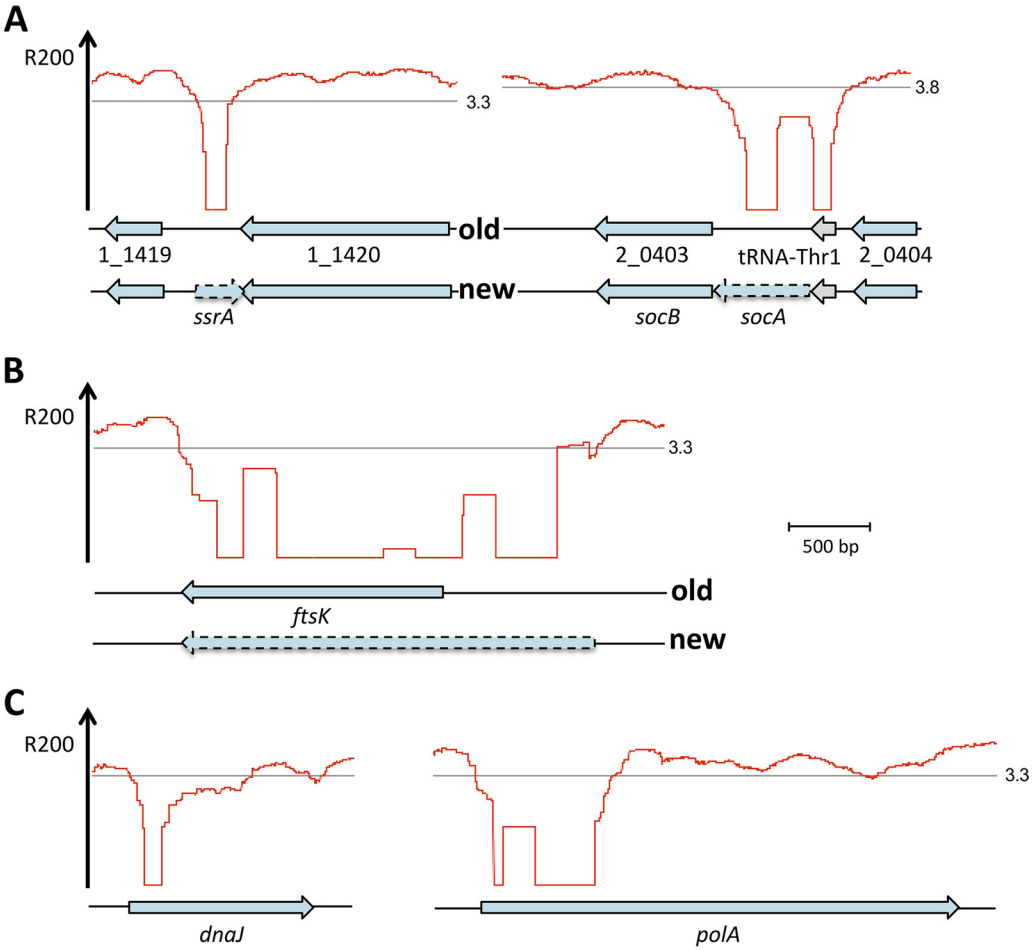

FIG 3 Genomic reannotations and identification of essential domains according to Tn-seq. The red line represents R200 values across the genome, the thin gray line represents the mean R200 per chromosome, and the black size marker corresponds to 0.5 kb. (A) Tn-seq has allowed the identification of two previously unannotated essential genes, as exemplified by the *ssrA* gene (encoding transfer-messenger RNA [tmRNA], allowing proteolysis of incomplete proteins) (67) between BAB1_1419 and BAB1_1420. A coding sequence located between BAB2_0403 and BAB2_0404, carrying a DUF4065 domain and well conserved (>90% identities at the protein level) within *Rhizobiales*, was also found to be essential. This gene encodes the antitoxin component of a toxin/antitoxin system called SocAB in *C. crescentus* (see the text), and BAB2_0403 is homologous to *socB*. Proposed reannotations are shown with a hatched line. Old and new proposed annotations are shown. (B) Open reading frame extension and matching essentiality region strongly suggest that *ftsK* (BAB1_1895) was misannotated. It should be noted that this corrected annotation is supported by BLASTP of the resulting extended *ftsK* gene against the alphaproteobacterium model *C. crescentus*. Examples in panels A and B are also supported by correct annotation in other genomic sequences. (C) Tn-seq is able to identify domain-specific essentiality as shown for *polA* (BAB1_0120) and *dnaJ* (BAB1_2130). In *dnaJ*, the Hsp70 interaction site seems essential, while in *polA*, encoding the DNA polymerase I, the 5′-3′ exonuclease domain is proposed to be essential.

Tn-seq allows for the reconstruction of essential pathways, complexes, and systems. Here, we specifically focused on pathways relative to the *B. abortus* cell cycle, which will be divided into four categories, the replication of DNA, the growth of the envelope, the cell division, and the cell cycle regulation network. Regarding the replication of DNA, α, β, γ, δ, χ, and τ subunits of the DNA polymerase III as well as the helicase *dnaB* and the primase *dnaG* are essential for growth. None of the three ε subunits (BAB1_2072, BAB2_0617, and BAB2_0967) were scored essential, which is likely due to functional redundancy. Genes responsible for the initiation of DNA replication for chromosome I (*dnaA*) and for chromosome II (*repC*) and for the segregation of chromosome I (*parA* and *parB*) and chromosome II (*repA* and *repB*) origins were also essential. Interestingly, only one homolog of the structural maintenance of chromosome gene (*smc*, BAB1_0522) could be found in the genome and was not essential in our Tn-seq, suggesting either that a functional analog is present or that this function is not essential

in *B. abortus*. Genes responsible for the synthesis of peptidoglycan precursors from fructose-6-phosphate and their export to the periplasm (namely, *glmS*, *glmM*, *glmU*, *murA*, *murB*, *murC*, *murD*, *murE*, *murF*, *murG*, *mraY*, and *ftsW*) were all scored essential. Out of three predicted class A penicillin-binding proteins (PBPs), only one (BAB1_0932) was found to be essential for growth on rich medium, as well as the only predicted class B PBP, the FtsI protein. The two other class A PBPs were either only needed for optimal growth on rich medium while not being strictly essential (BAB1_0607) or not required at all (BAB1_0114).

The entire pathway responsible for the synthesis of LPS lipid A from UDP-GlcNAc (namely, *lpxA*, *lpxB*, *lpxC*, *lpxD*, *lpxK*, *lpxXL*, and *kdtA*), as well as the pathway responsible for its export to the outer membrane (namely, *msbA*, *lptA*, *lptB*, *lptC*, *lptD*, *lptE*, *lptF*, and *lptG*), appears to be essential for growth on rich medium. Conversely, no gene known for being involved in the LPS core synthesis (24) was scored essential for culture on plates. Moreover, none of the genes responsible for the LPS O-chain synthesis were scored essential, with the exception of *wbkC* (see Discussion).

Genes involved in the export of outer membrane proteins (OMPs), such as *bamA*, *bamD*, and *bamE*, were essential for growth on rich medium (see Discussion). However, no predicted homolog of *bamB* or *bamC* could be found. Interestingly, none of the three homologs of the OMP periplasmic chaperone *degP* were scored essential, which is probably due to functional redundancy. It should be noted that no clear predicted homolog of the OMP periplasmic chaperones *skp* and *surA* could be identified *in silico*. Additionally, among the genes responsible for lipoprotein export to the outer membrane, both *lgt* and *lspA* were essential, but surprisingly, *lnt* was not. Lnt is the phospholipid/apolipoprotein transacylase that is N-acylating the N-terminal cysteine in the biogenesis of lipoproteins. The *lnt* gene is also not essential in *B. subvibrioides*, suggesting that the dispensability of *lnt* could be a shared feature among *Alphaproteobacteria*.

Genes coding for the divisome proteins, i.e., *ftsZ*, *ftsA*, *ftsQ*, *ftsK*, *ftsW*, *ftsY*, and *ftsI*, as well as those coding for the outer membrane invagination system, *tolQRAB-pal*, were all essential on plates. The cell division regulatory operon *minCDE* as well as *ftsEX* was not essential, and no predicted homologs could be found for *ftsB*, *ftsN*, and *zipA*.

Regarding the regulation of the bacterial cell cycle in *Brucella*, one of the key features of the *Brucella* cell cycle is the DivK-CtrA pathway, conserved among many *Alphaproteobacteria* (25). Most but not all members of the DivK-CtrA pathway were found to be essential for growth on plates in Tn-seq. Indeed, *pdhS*, *divK*, *divL*, *cckA*, *chpT*, *ctrA*, *cpdR*, and *clpXP* were found to be essential (Fig. S3). Presumably redundant genes for c-di-GMP synthesis (*pdeA* and *pleD*) and for DivK phosphorylation (*pleC* and *divJ*) were not essential (Fig. S3).

Taken together, these data demonstrate that Tn-seq enables the reconstitution of essential pathways in a single experiment. In particular, it allows the identification of a crucial homolog within a family of several potential paralogs.

Screening for genes required for macrophage infection. Another main objective of this study was to identify genes specifically required for macrophage infection. For this purpose, three large-scale infections of RAW 264.7 macrophages were carried out in parallel using the transposon mutant library described above (Fig. 1). For each infection, a specific postinfection (p.i.) time point was selected in order to have a better understanding of the specific gene requirement at different stages of the cellular infection process. After each time point, bacteria were extracted from infected macrophages and grown on rich medium prior to transposon insertion site identification and R200 calculation, as explained above (Fig. 1).

Attenuation corresponds to a decrease of fitness specific to infection. Therefore, in the context of an attenuated mutant, one expects that the R200 values for the mutated gene would be lower after infection than under the control condition. Consequently, for analyzing p.i. data, the control R200 values were subtracted from the corresponding p.i. R200 for each p.i. data set. This resulted in three lists of Delta-R200 values, namely,

"2 h p.i. R200 − control R200," "5 h p.i. R200 − control R200," and "24 h p.i. R200 − control R200," corresponding to Delta-R200 2 h p.i. (SD3 [https://figshare.com/s/77195e0a2cc1a1933b7f] and SD4 [https://figshare.com/s/2475d4b00e6a58226e40]), Delta-R200 5 h p.i. (SD5 [https://figshare.com/s/93ce83ccea559a0de2f7] and SD6 [https://figshare.com/s/6f604b5eba5934c392f1]) and Delta-R200 24 h p.i. (SD7 [https://figshare.com/s/ea7871157f284d31eaed] and SD8 [https://figshare.com/s/958e728387a31b8ce139]), respectively. A total of 165 candidates have been identified using the Delta-R200 analysis Among these candidates, 75 were found at 2 h p.i., 98 were found at 5 h p.i., and 165 were found at 24 h p.i. (Tables 1 and 2).

In order to validate the Delta-R200 analysis, we checked for genes known to cause an attenuation during a cellular infection when mutated. For this purpose, we have chosen one control for 2 h p.i., the response regulator *bvrR*, and two controls for 24 h p.i., the type IV secretion system operon *virB* (10, 26), required for intracellular proliferation, and *vjbR*, an important transcriptional activator of *virB* which is not part of the *virB* operon (27, 28). As expected, the *bvrR* mutants were strongly attenuated from 2 h p.i., and both *virB* and *vjbR* mutants were attenuated only at 24 h p.i. (Table 1; Fig. S4), which is in agreement with the timing required by the bacterium to reach its replicative niche and proliferate. Taken together, these data lean toward the validation of the candidates identified by the Delta-R200 analysis.

We decided to assess the validity of our data sets by testing for the reproducibility of the observed phenotypes by mutating candidate genes and testing mutant survival by the counting of CFU after infection of RAW 264.7 macrophages for 2 h. We chose four candidates, two that displayed no attenuation in Tn-seq as negative controls (*omp2a* and *ftsK*-like, corresponding to BAB1_0659 and BAB2_0709 coding sequences, respectively) and two that displayed attenuation in Tn-seq as positive controls (*wadB* and *pgk*, corresponding to BAB1_0351 and BAB1_1742, respectively). As expected, the two negative-control strains did not show any sign of attenuation in comparison to the wild-type strain, while the positive-control strains exhibited a statistically significant attenuation phenotype (Fig. 4A).

One can distinguish two categories of attenuated mutants. On the one hand, mutants can be attenuated due to a failure to perform a successful infection, but on the other hand, mutants can be attenuated due to growth impairments that are actually already observed when grown on rich medium and amplified during infection. In fact, as opposed to candidates displaying a typical attenuation profile such as the *wadB* mutant, others displayed attenuation in conjunction with low control R200 values, as exemplified by the *pgk* mutant (Fig. 4B). This second type of profile suggested growth deficiencies independent of infection. In addition, while the *pgk* mutant strain displayed a small but significant decrease in CFU (Fig. 4A), it was clear that the colonies were smaller in size than the wild-type colonies (Fig. 4C). Therefore, the attenuation of candidates sharing a *pgk*-like profile in Tn-seq is likely to be due, at least in part, to growth impairments already present under the control condition. Actually, the second round of culture taking place after the infection might simply amplify the disadvantage of clones that already display growth delays on plates.

In order to investigate the effect of replating on Tn-seq candidates, we performed a new Tn-seq experiment in which the colonies of the library of transposon mutants were collected and replated prior to sequencing instead of infecting host cells. The TTMs obtained for this control condition (SD9 [https://figshare.com/s/519aecf6ea1bea563510] and SD10 [https://figshare.com/s/266012d35d5780c5a1b3]) and the replating (SD11 [https://figshare.com/s/9282c05218ec976c4286] and SD12 [https://figshare.com/s/c5318e37bf294ff0cdde]) are available at the indicated URLs. Despite a large difference in the average R200 values between the two control experiments (3.47 for the first control and 5.21 for the second), a good correlation ($r = 0.86$) was found between the two data sets. By comparing the control condition with the replating, we were able to monitor the fitness loss of mutants due to a second growth on the plate, independently of any infection. Surprisingly, 54% of the candidates harboring attenuation at 2, 5, or 24 h p.i. in our initial Tn-seq also displayed a similar attenuation after replating, thus

TABLE 1 Attenuated *B. abortus* mutants in RAW 264.7 infection at 2, 5, or 24 h p.i.[a]

ORF[b]	Gene name	Change in R200 value[c]			Predicted function
		2 h p.i.	5 h p.i.	24 h p.i.	
Secretion					
BAB2_0068	*virB1*	−	−	+	Type IV secretion system
BAB2_0067	*virB2*	−	−	+	Type IV secretion system
BAB2_0066	*virB3*	−	−	+	Type IV secretion system
BAB2_0065	*virB4*	−	−	+	Type IV secretion system
BAB2_0064	*virB5*	−	−	+	Type IV secretion system
BAB2_0063	*virB6*	−	−	+	Type IV secretion system
BAB2_0062	*virB7*	−	−	+	Type IV secretion system
BAB2_0061	*virB8*	−	−	+	Type IV secretion system
BAB2_0060	*virB9*	−	−	+	Type IV secretion system
BAB2_0059	*virB10*	−	−	+	Type IV secretion system
BAB2_0058	*virB11*	−	−	+	Type IV secretion system
BAB1_0045	*tamA*	−	−	+	Export of autotransporters (type V secretion system)
BAB1_0046	*tamB*	−	−	+	Export of autotransporters (type V secretion system)
Protein synthesis and degradation					
BAB1_2087	*hisE*	−	−	+	Histidine biosynthesis
BAB1_2082	*hisB*	−	−	+	Histidine biosynthesis
BAB1_1988	*hisC*	−	−	+	Histidine biosynthesis
BAB1_0285	*hisD*	−	−	+	Histidine biosynthesis
BAB1_1399	*ilvC*	−	−	+	Isoleucine, leucine, and valine biosynthesis
BAB1_0096	*ilvD*	−	−	+	Isoleucine, leucine, and valine biosynthesis
BAB1_2158	*lnt*	+	+	+	Lipoprotein synthesis
BAB1_1437	*pepP*	+	+	+	Peptidase, Xaa-Pro aminopeptidase
BAB1_0162	*ibpA*	−	−	+	Chaperone
BAB1_2025		+	+	+	DnaJ-like chaperone
BAB1_1115	*tgt*	+	+	+	tRNA modification
BAB1_0477	*rplI*	−	+	+	Ribosomal protein L9
BAB1_0427		−	+	+	tRNA1(Val) A37 N6-methylase TrmN6
Nucleic acid synthesis and degradation					
BAB2_0641	*pyrB*	−	−	+	Pyrimidine biosynthesis
BAB2_0640	*pyrC*	−	−	+	Pyrimidine biosynthesis
BAB1_0341	*pyrD*	−	−	+	Pyrimidine biosynthesis
BAB1_0673	*pyrE*	−	−	+	Pyrimidine biosynthesis
BAB1_2132	*pyrF*	−	−	+	Pyrimidine biosynthesis
BAB1_0688	*pyrC2*	−	+	+	Pyrimidine biosynthesis
BAB1_1695	*purA*	−	−	+	Purine biosynthesis
BAB1_1757	*purE*	+	+	+	Purine biosynthesis
BAB1_0861	*purS*	−	−	+	Purine biosynthesis
BAB1_0024	*cmk*	+	+	+	CDP synthesis from CMP
BAB1_0168	*ydjH*	−	−	+	Adenosine kinase (AK)
BAB1_0172	*rph*	−	−	+	RNase
BAB2_0643	*yqgF*	−	+	+	Endonuclease, resolvase family
BAB1_0003	*recF*	−	−	+	Recombination in response to DNA damage
BAB1_1206	*queF*	−	−	+	Dehydrogenase, involved in queuosine biosynthesis
Electron transfer and redox					
BAB2_0727	*cydB*	−	−	+	Cytochrome *bd*
BAB2_0728	*cydA*	−	−	+	Cytochrome *bd*
BAB2_0729	*cydC*	−	−	+	ABC transporter, cytochrome *bd* biogenesis
BAB2_0730	*cydD*	−	−	+	ABC transporter, cytochrome *bd* biogenesis
BAB1_1435		−	+	+	Related to cytochrome *c* oxidase synthesis
BAB1_0051	*pcuC*	−	+	+	Incorporation of Cu(I) in cytochrome *c* oxidase
BAB1_0139	*nfuA*	−	−	+	Fe-S cluster biogenesis protein
Cell envelope					
BAB1_0351	*wadB*	+	+	+	Envelope, LPS core synthesis
BAB1_1217	*murI*	−	−	+	Glutamate racemase
BAB1_1462	*ampD*-like	−	+	+	*N*-acetyl-anhydromuramyl-L-alanine amidase
Regulation					
BAB1_2092	*bvrR*	+	+	+	Two-component regulator
BAB1_1665	*rpoH2*	+	+	+	RNA polymerase sigma factor
BAB1_1669		+	+	+	Signal transduction, HWE family histidine kinase

(Continued on next page)

TABLE 1 (Continued)

ORF[b]	Gene name	Change in R200 value[c]			Predicted function
		2 h p.i.	5 h p.i.	24 h p.i.	
BAB2_0678	*rirA*	−	+	+	Transcriptional regulator, iron responsive
BAB1_1517	*vtlR*	−	−	+	LysR transcriptional regulator controlling sRNA expression
BAB2_0118	*vjbR*	−	−	+	Quorum-sensing transcriptional regulator
BAB2_0143	*deoR1*	−	−	+	Transcriptional regulator
BAB1_0160	*ptsN*	+	+	+	Phosphotransferase system (PTS), IIA component
BAB1_0638	*glnE*	−	−	+	Glutamine pool regulation
Transport					
BAB1_1460	*mntH*	+	+	+	Manganese transport, ion transport
BAB2_0699	*oppA*	+	+	+	ABC transporter, substrate binding, oligopeptide transport
BAB2_0701	*oppB*	+	+	+	ABC transporter, permease, oligopeptide transport
BAB2_0702	*oppC*	+	+	+	ABC transporter, permease, oligopeptide transport
BAB2_0703	*oppD*	+	+	+	ABC transporter, ATPase
BAB1_2145	*phoU*	−	+	+	Phosphate transport control
BAB1_1345		−	−	+	Kef-type potassium/proton antiport protein
Metabolism					
BAB2_1010	*glk*	−	−	+	Glucokinase
BAB1_0435	*glcD*	+	+	+	Glycolate oxidase
BAB1_1918	*lpd*	+	+	+	Dihydrolipoyl dehydrogenase
BAB1_0898	*bglX*	−	+	+	Beta-glucosylase-related glycosidase
BAB1_1476	*pldB*	−	+	+	Lysophospholipase L2
BAB1_0113	*fabG*	−	−	+	3-Oxoacyl-ACP reductase
BAB1_0318	*gph*	−	−	+	Phosphoglycolate phosphatase
Unknown functions					
BAB1_1485		+	+	+	Inner membrane conserved protein (DUF475)
BAB1_1766	*hfaC*	+	+	+	Duplicated ATPase domains
BAB1_0478		−	−	+	Inner membrane conserved protein (DUF2232)
BAB1_1283		−	−	+	Conserved periplasmic protein (DUF192)
BAB1_2069	*maf-2*	−	−	+	Maf-like nucleotide binding protein

[a]The R200 values (TTMs) and the genomic maps are available as supplemental data sets (see Table 3 for a complete list).
[b]The coding sequences (ORFs) untouched by previous screenings of mutant libraries are shown in bold, including some (like those for *mntH*, *rirA*, *wadB*, and *rpoH2*) that were investigated by targeted mutagenesis (63–66).
[c]For each coding sequence (ORF), a reduced R200 value is indicated by a plus. If the corresponding mutants also displayed a lower R200 after replating on rich medium, they are reported in Table 2. If a similar R200 value was found between a given time p.i. and the control, a minus is shown.

indicating that the fitness loss of those mutants could be due to a growth defect detectable after a simple replating instead of infection. Consequently, attenuated candidates displaying preexisting growth impairments (listed in Table 2) should be carefully analyzed in future investigations (see Discussion). It is striking that complete or almost complete pathways fall into this category, like the purine biosynthesis (*purB*, *purC*, *purD*, *purF*, *purH*, *purL*, *purMN*, and *purQ*) and the cytochrome *c* maturation (*ccmABC* and *ccmIEFH*) pathways (Table 2).

Identification of hyperinvasive mutants. Tn-seq can theoretically highlight hyperinvasive mutants in addition to attenuated mutants. Indeed, such mutants would be expected to display higher R200 values than the control, meaning that proportionally more mutant bacteria would be found inside host cells when such genes are disrupted, thus resulting in positive Delta-R200 values. Using this criterion, only nine genes (namely *wbkD*, *wbkF*, *per*, *gmd*, *wbkA*, *wbkE*, *wboA*, *wboB*, and $manB_{core}$ [BAB2_0855]) were identified, and remarkably, all of them are part of the lipopolysaccharide O-chain synthesis pathway (24). Indeed, such mutants have a rough LPS, and rough mutants are known to be more invasive than the smooth parental strain (29, 30). To confirm this using our settings, a mutant of the GDP-mannose dehydratase gene (*gmd*) was constructed, and CFU were counted after infection of RAW 264.7 macrophages for 2 h. As expected, the resulting strain displayed increased invasiveness, which is typical of rough strains (Fig. S5).

Identification of genes required for growth in RAW 264.7 macrophages. The 24-h-p.i.-specific candidates mainly include genes predicted to be involved in traffick-

TABLE 2 Attenuated *B. abortus* mutants in RAW 264.7 infection at 2, 5, or 24 h p.i. with a growth defect on plates[a]

ORF	Gene name	Change in R200 value[b]			Predicted function
		2 h p.i.	5 h p.i.	24 h p.i.	
Protein synthesis and degradation					
BAB1_1846		−	+	+	Membrane-bound metallopeptidase
BAB1_1191	*clpA*	+	+	+	Protease-associated factor
BAB2_0183	*hisG*	−	−	+	Histidine biosynthesis, first part of the pathway
BAB2_0182	*hisZ*	−	−	+	Histidine biosynthesis, first part of the pathway
BAB1_1098	*hisI*	−	−	+	Histidine biosynthesis, first part of the pathway
BAB1_2085	*hisA*	+	+	+	Histidine biosynthesis, first part of the pathway
BAB1_2084	*hisH*	+	+	+	Histidine biosynthesis, first part of the pathway
BAB1_2086	*hisF*	+	+	+	Histidine biosynthesis, first part of the pathway
BAB1_0704	*ksgA*	−	+	+	16S rRNA methyltransferase
BAB1_1553	*ychF*	+	+	+	Translation-associated GTPase
BAB1_2167	*truB*	−	+	+	tRNA modification
BAB1_1019	*rluA*	−	−	+	Pseudouridylate synthase, 23S RNA-specific
BAB1_1657	*dsbB*	−	−	+	Disulfide bond formation in periplasm
BAB1_0962		+	+	+	Protein-L-isoAsp *O*-methyltransferase
Nucleic acid synthesis and degradation					
BAB1_0442	*purD*	+	+	+	Purine biosynthesis
BAB1_0730	*purN*	+	+	+	Purine biosynthesis
BAB1_0857	*purL*	+	+	+	Purine biosynthesis
BAB1_0860	*purQ*	+	+	+	Purine biosynthesis
BAB1_0731	*purM*	+	+	+	Purine biosynthesis
BAB1_0862	*purC*	+	+	+	Purine biosynthesis
BAB1_0868	*purB*	+	+	+	Purine biosynthesis
BAB1_1824	*purH*	+	+	+	Purine biosynthesis
Electron transfer and redox					
BAB1_0091	*ccmA*	+	+	+	Cytochrome *c* maturation
BAB1_0092	*ccmB*	+	+	+	Cytochrome *c* maturation
BAB1_0093	*ccmC*	+	+	+	Cytochrome *c* maturation
BAB1_0632	*ccmE*	+	+	+	Cytochrome *c* maturation
BAB1_0633	*ccmF*	+	+	+	Cytochrome *c* maturation
BAB1_0634	*ccmH*	+	+	+	Cytochrome *c* maturation
BAB1_0631	*ccmI*	+	+	+	Cytochrome *c* maturation
BAB2_0656	*ccdA*	+	+	+	Cytochrome *c* maturation (*dsbD* homolog)
BAB1_0388	*ccoG*	−	+	+	Cytochrome *c* oxidase
BAB1_0389	*ccoP*	−	+	+	Cytochrome *c* oxidase
BAB1_0392	*ccoN*	−	+	+	Cytochrome *c* oxidase
BAB1_1557		−	+	+	Cytochrome c_1 family
BAB1_1559		−	+	+	Ubiquinol cytochrome *c* reductase, iron-sulfur component
BAB1_0739		+	+	+	Electron transport chain (ETC)-complex I subunit
BAB1_1030	*gor*	+	+	+	Glutathione reductase
BAB2_0476	*gshA*	+	+	+	Gamma-glutamylcysteine synthetase
BAB1_2135	*gshB*	+	+	+	Glutathione synthetase
BAB1_0855		+	+	+	Glutaredoxin-like protein
Cell envelope					
BAB1_1041	*mlaA*	+	+	+	Predicted lipoprotein
BAB1_1040	*mlaD*	+	+	+	ABC transporter-associated inner membrane protein
BAB1_1038	*mlaE*	+	+	+	ABC transporter, permease
BAB1_1039	*mlaF*	+	+	+	ABC transporter, ATPase
BAB2_0076	*omp10*	+	+	+	Outer membrane lipoprotein
BAB1_1930	*omp19*	−	−	+	Outer membrane lipoprotein
BAB1_0491		+	+	+	Invasion protein B (conserved periplasmic protein)
Regulation					
BAB1_0143	*glnD*	+	+	+	Glutamine pool regulation
BAB1_0304	*cenR*	+	+	+	Regulator for envelope composition
BAB1_2006	*cenR*	+	+	+	Transcriptional regulator (also called *otpR*)
BAB1_1962	*gntR13*	−	+	+	Transcriptional regulator
BAB1_0640	*pleC*	−	−	+	Histidine kinase, regulation of cell cycle
BAB1_2093	*bvrS*	+	+	+	Histidine kinase for BvrR regulator
BAB1_2094	*hprK*	+	+	+	Kinase, regulator of phosphotransferase system (PTS)
BAB1_2159	*hipB*	+	+	+	Transcriptional regulator
BAB1_2175	*irr*	+	+	+	Transcriptional regulator, ferric uptake regulator

(Continued on next page)

TABLE 2 (Continued)

ORF	Gene name	Change in R200 value[b] 2 h p.i.	5 h p.i.	24 h p.i.	Predicted function
Transport and storage					
BAB1_0386	*copA*	+	+	+	Cation metal exporter, ATPase
BAB1_0387		+	+	+	Cation exporter-associated protein
BAB2_1079	*znuA*	−	−	+	ABC transporter for zinc
BAB2_1080	*znuC*	−	−	+	ABC transporter for zinc
BAB2_1081	*znuB*	−	−	+	ABC transporter for zinc
BAB2_0411		+	+	+	Conserved hypothetical
BAB2_0412	*tauE*	+	+	+	Sulfite exporter
BAB1_1589		−	+	+	Major facilitator superfamily (transporter)
BAB1_1045	*fdx*	+	+	+	Ferredoxin
Metabolism					
BAB2_0366	*eryI*	+	+	+	Erythritol metabolism (also called *rpiB*)
BAB2_0367	*eryH*	+	+	+	Erythritol metabolism (also called *tpiA2*)
BAB2_0370	*eryC*	+	+	+	Erythritol metabolism
BAB2_1013	*gpm*	+	+	+	Phosphoglycerate mutase
BAB1_1761	*pykM*	−	−	+	Pyruvate kinase
BAB2_0513	*gcvT*	−	−	+	Glycine cleavage system
BAB2_0514	*gcvH*	−	−	+	Glycine cleavage system
BAB2_0515	*gcvP*	−	−	+	Glycine cleavage system
BAB1_2022	*cobT*	−	−	+	Cobalamin biosynthesis
BAB1_2023	*cobS*	−	−	+	Cobalamin biosynthesis
BAB2_1012	*dapB*	+	+	+	Dihydrodipicolinate reductase
BAB1_0773	*gppA*	+	+	+	Exopolyphosphatase
BAB1_2103		+	+	+	Nucleotidyl transferase
BAB2_0442	*acaD*	+	+	+	Acyl coenzyme A dehydrogenase
BAB2_0511		+	+	+	Reductase
BAB2_0668	*pssA*	+	+	+	Phosphatidylserine synthase
BAB1_0471		−	+	+	Oxoacyl-(acyl carrier protein) reductase
BAB2_1027	*upp*	−	+	+	Phosphoribosyl transferase
Unknown functions					
BAB1_0084	*yccA*	−	−	+	Inner membrane protein
BAB1_1670		−	−	+	Hypothetical protein
BAB1_1092		−	−	+	Hypothetical protein

[a]The R200 values (TTMs) and the genomic maps are available as supplemental data sets (see Table 3 for a complete list).
[b]For each coding sequence (ORF), a reduced R200 value is indicated by a plus. If a similar R200 value was found between a given time p.i. and the control, a minus is shown. These mutants also displayed a lower R200 after replating on rich medium.

ing, regulation, transport, and metabolism, including amino acid and nucleic base biosynthesis (Table 1). The biosynthesis of histidine seems to be crucial, as well as the synthesis of pyrimidines, suggesting that *B. abortus* cannot find or take up enough of these compounds from the ER compartments in which it is proliferating. The 24-h-p.i.-specific candidates also comprise expected virulence genes such as the *virB* operon (11), transcriptional regulators like *vjbR* (28) and *vtlR* (31), and the cytochrome *bd* biosynthesis operon *cydABCD* (32). When our data are compared with the list of attenuated transposon mutants from previous studies performed using various infection models and *Brucella* species (33–37), it is striking that only 42% of the attenuated mutants identified here had already been identified. Indeed, 33 of the 79 candidates attenuated in our time-resolved Tn-seq analysis were part of the 257 candidates compiled from the previous studies. Therefore, the Tn-seq approach reported here has generated 46 new candidates, suggesting that the comprehensive analysis of the *Brucella* genome might yield new insights into the genes required for a macrophage infection (see Discussion).

The pyrimidine biosynthesis pathway allows intracellular proliferation. One of the major hits of the 24-h-p.i. data set is the pyrimidine biosynthesis (here called "pyr") pathway. In fact, with the exception of genes already essential for culture on rich medium, all pyr biosynthesis genes became strongly attenuated at 24 h p.i. (namely, *pyrB*, *pyrC*, *pyrD*, *pyrE*, and *pyrF*), while none of them were affected when replated.

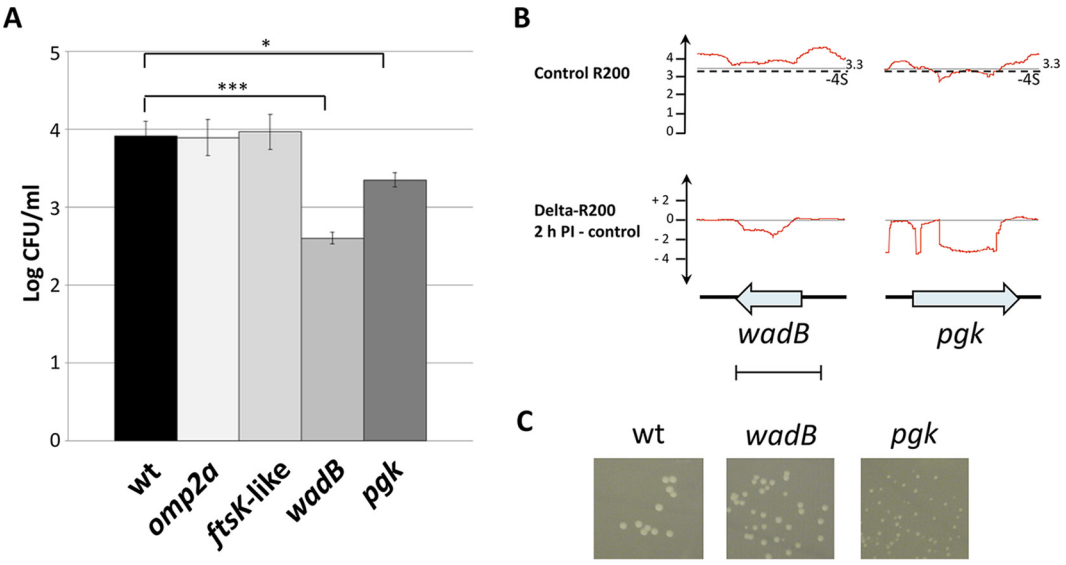

FIG 4 Validation of Tn-seq data using reconstructed mutants. (A) CFU counting after a 2-h infection of RAW 264.7 macrophages with individual *omp2a*, *ftsK*-like, *wadB*, and *pgk* mutants. The Tn-seq data indicate that *omp2a* and *ftsK*-like mutants are fully virulent at 2 h p.i., while the *wadB* and *pgk* mutants are attenuated. The wild-type (wt) strain was used as a virulent control. *, $P < 0.05$; ***, $P < 0.001$. (B) Comparison of the Tn-seq profiles of the *wadB* and *pgk* mutants, highlighting the growth defect of the *pgk* mutant (below the −4S threshold shown as a hatched line, i.e., 4 standard deviations under the average of the theoretical distribution of R200 values [see Fig. S2 in the supplemental material]). The gray lines correspond to the average R200 or average Delta-R200 for the whole chromosome. (C) Images of the wild-type strain, *wadB* mutant, and *pgk* mutant colonies on rich medium, supporting the hypothesis of the *pgk* growth defect.

We further investigated the pyr pathway by creating a deletion mutant of its first nonessential gene, the Δ*pyrB* strain. The Δ*pyrB* mutant grew like the wild-type strain in rich medium (Fig. S6). We then evaluated the infectious potential of the Δ*pyrB* strain and its complementation strain by enumerating CFU in RAW 264.7 macrophages at both 2 h p.i. and 24 h p.i. Estimation of the intracellular growth ratio (CFU at 24 h p.i. divided by CFU at 2 h p.i.) clearly showed that the Δ*pyrB* strain is strongly attenuated in comparison to the wild type and the complementation strains, validating the Tn-seq profile of the mutant (Fig. 5). Consistently, deletion mutants for all other *pyr* genes (Δ*pyrC*, Δ*pyrD*, Δ*pyrE*, and Δ*pyrF*) behaved like the wild type when cultured in rich medium (Fig. S6) and were impaired for intracellular growth, further validating the involvement of the pyr pathway for proliferation inside RAW 264.7 macrophages (Fig. 5).

DISCUSSION

In this work, a multidimensional Tn-seq analysis was performed with *B. abortus* to identify genes essential for growth on rich medium as well as genes required for replication in RAW 264.7 macrophages. The analysis of mutants at different times p.i. as well as the analysis of the replated library allowed the identification of genes specifically involved in the infection model tested here, by comparison with the control condition (growth on rich medium). A similar approach could be successfully applied to many other bacterial pathogens.

As most of the current therapies against bacterial pathogens aim at targeting essential processes such as translation or cell wall biosynthesis, the collection of all essential genes for growth on rich medium generates a baseline to identify novel therapeutic targets. In this study, a total of 491 candidate genes were qualified as essential for growth on rich medium plates. Interestingly, our quantitative analysis also highlights genome sections that show a reduced fitness, and statistical comparison of any regions (inside or outside predicted genes) in the genome is thus also feasible (Fig. 2). The quantitative analysis also allows the identification of regions in which mutagenesis generates a growth defect on the control plates, and thus a category of attenuated

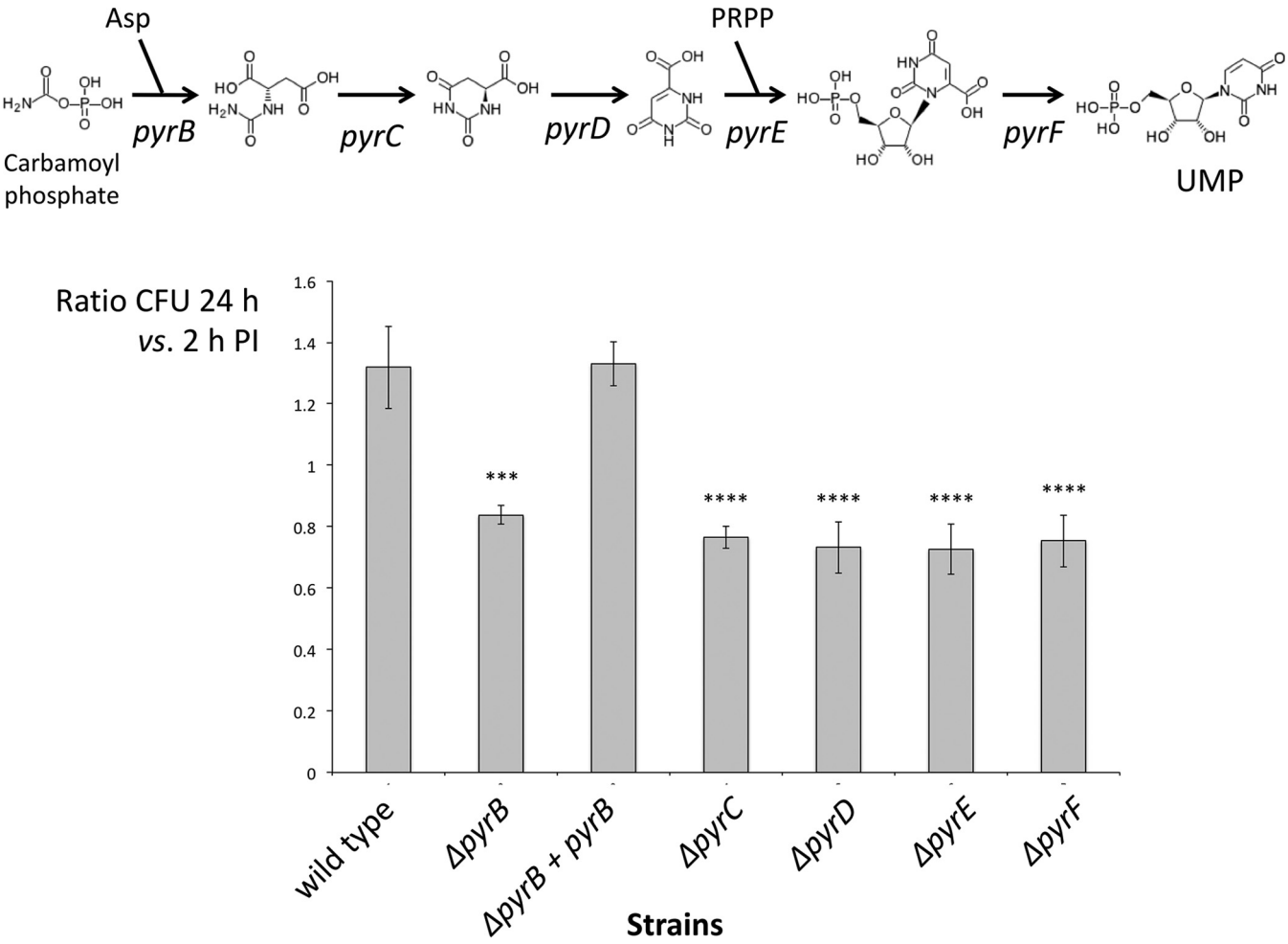

FIG 5 Intracellular growth of *pyr* mutants. The pyrimidine biosynthesis pathway with the corresponding genes for each step, with aspartate (Asp) and phosphoribosylpyrophosphate (PRPP) involved in UMP synthesis. The 24 h p.i./2 h p.i. CFU ratio for each *pyr* mutant after infection of RAW 264.7 macrophages is shown. For each strain, the $\log_{10}$ CFU count after a 24-h infection of RAW 264.7 macrophages was divided by the corresponding $\log_{10}$ CFU count after a 2-h infection, resulting in a ratio depicting the evolution of the bacterial load from 2 h p.i. to 24 h p.i. Accordingly, an increased load will give a ratio of >1. Each strain was compared to the wild-type control using a Scheffé analysis (one-way analysis of variance [ANOVA]), and significant differences are indicated (***, $P < 0.001$; ****, $P < 0.0001$).

mutants with growth defects on plates (Table 2) should be distinguished from specifically attenuated mutants (Table 1). This type of discrimination is supported by the possibility that a fraction of the attenuated mutants with growth defects on plates might be nonspecifically affected during the infection process. On the other hand, the specificity of the attenuated mutants reported in Table 1 is expected to be medium dependent and could thus be challenged by other screenings. Additionally, it would be interesting to apply Tn-seq analysis to *B. abortus* grown in different media. In particular, it would be informative to test chemically defined media.

While peptidoglycan biosynthesis is obviously essential, only one of the three predicted class-A penicillin-binding proteins, BAB1_0932, was found to be essential for growth on rich medium, showing that Tn-seq could allow the identification of the main functional gene among a group of paralogs. As expected, BAB1_0932 is the ortholog of Atu1341, which was also identified as essential in *A. tumefaciens* (21). A comparison of essential genes in *B. abortus*, *A. tumefaciens*, and *B. subvibrioides* also reveals interesting observations. The D-Ala-D-Ala ligase-encoding gene *ddl* (BAB1_1447) located near the *murB-murG* gene cluster involved in cell wall synthesis is not essential in *B. abortus*, while it is essential in *A. tumefaciens* and *B. subvibrioides*. This could be explained by the presence of a paralog for *ddl* (BAB1_1291, also not essential) in *B. abortus*. MurI, a glutamate racemase that was found to be essential in *C. crescentus* (15) and nonessen-

tial in *A. tumefaciens* (21), is actually required for *B. abortus* growth in RAW 264.7 macrophages but not in rich medium (see below; Table 1). Tn-seq also allowed the reshaping of essential processes in comparison to those of other bacteria, as exemplified by the *bam* genes, responsible for the OMP export system. *Brucella* possesses an incomplete OMP export system composed of only *bamADE* and lacking *bamB* and *bamC*, and here we showed that *bamE* was scored essential by Tn-seq, whereas it is not essential in *Escherichia coli* (38). One possibility is that *bamE* is functionally redundant with another gene in *E. coli*, while this redundancy is absent in *B. abortus*. At the level of the regulation network involving CtrA (see Fig. S1 in the supplemental material), it is interesting to note that *cpdR*, *sciP*, *gcrA*, and *ccrM* are identified here as essential genes, which is consistent with the previous identification of *ccrM* as an essential gene in *B. abortus* (18) but surprisingly different from that for *A. tumefaciens*, where they are all nonessential, except for *gcrA*, which is absent in *A. tumefaciens* C58 (21). In *C. crescentus*, *cpdR* and *sciP* are not essential (39, 40), while *gcrA* and *ccrM* were first reported as essential (41, 42), which was later questioned by the observation of a slow growth phenotype for *C. crescentus* Δ*gcrA* and Δ*ccrM* strains (43). The essentiality of *cpdR*, *sciP*, *gcrA*, and *ccrM* genes might indicate that this part of the regulation network is less redundant with other cell cycle control systems in *B. abortus* than in *C. crescentus*.

Intriguingly, a few genes (*mucR*, *sodA*, *pgm*, and *wbkC*) for which a viable deletion mutant has been previously reported (44–49) are actually scored as essential in our Tn-seq analysis. A *pssA* gene (BAB1_0470) was also scored as essential, but the corresponding viable mutant was previously characterized (50). Interestingly, mutants for another *pssA* homolog (BAB2_0668) were found to be attenuated from 2 h p.i. (Table 2), suggesting that these enzymes are playing distinct roles. The absence of a mini-transposon in dispensable genes has already been observed in previous Tn-seq experiments performed on other bacterial species (51). It is also possible that in the Tn-seq protocol, suppressor mutations do not have the time to be selected, and thus these genes appear as essential only in Tn-seq. Another possibility is that these mutants have a long lag phase for growth on plates or a very low growth speed and are thus wrongly detected as essential in the Tn-seq analysis.

Remarkably, a second Tn-seq analysis assessing the effects of replating revealed that 54% of these candidates displayed fitness decreases similar to those found in infection during a second round of culture. Strikingly, 55 out of the 75 initial candidates identified at 2 h p.i. are in the second category (Table 2), since they were already affected by replating. Such observations suggest that it could be important to take into account a growth defect in culture before proposing a "specific" virulence attenuation for mutant strains. Interestingly, this does not rule out that particular mutants might have an exacerbated growth defect phenotype inside host cells. Analysis of the difference between R200 values at 24 and 5 h p.i. (SD13 [https://figshare.com/s/44d2126e6c24ca1214d1] and SD14 [https://figshare.com/s/c6a0d65386f6edb2202b]) indicates that several *pur* genes (*purA*, *purB*, *purC*, *purD*, *purF*, *purH*, *purL*, *purM*, *purN*, and *purQ*) have lower R200 values at 24 h p.i. than at 5 h p.i. These data suggest that even if a mutant has growth problems in a given culture medium, Tn-seq analysis at different times postinfection allows the generation of hypotheses regarding attenuation at different times postinfection. Additionally, the reference culture medium is of course important, and it would be interesting to test several rich media for growth colonies before and after infection.

When comparing our candidates to the list of 257 attenuated mutants previously available from different infection models (33–37), it was surprising that only 33 genes could be found in common (Table S3). This means that 46 additional candidates were identified by Tn-seq analysis. However, this also means that 214 attenuated mutants previously reported were not identified using Tn-seq in a RAW 264.7 macrophage infection, which is not surprising, since these screenings were done with different strains/species and different infection models. However, it should be noted that, intriguingly, out of the remaining 214 candidates, 80 were categorized here as either strictly essential for growth on rich medium or essential when replated (Table S3). It is

thus possible that different strains and different culture media generate different collections of essential genes or that several attenuated mutants previously reported are actually suppressors of mutants in essential genes that display a growth defect in the infection model.

The 24-h-p.i. time point revealed several pathways involved in trafficking and metabolism. The type IV secretion system VirB was needed, but the effectors proposed to be translocated to the host cell (52) were untouched in our Tn-seq analysis, which is probably the result of functional redundancy between effectors. Indeed, under the infection conditions used here, there is usually one bacterium per infected cell, and thus *trans*-complementation (53) is unlikely, although it cannot be completely ruled out. Regarding metabolism, *glk* mutants were attenuated at 24 h p.i. (Table 2), suggesting that *B. abortus* might need to utilize glucose in the replication niche of RAW 264.7 macrophages, which is consistent with the requirement of glucose uptake in alternatively activated macrophages (54). The biosynthesis of histidine was strongly impacted at 24 h p.i., as previously suggested (55), and we found here that it is more specifically the second part of the pathway that is important for bacterial proliferation inside RAW 264.7 macrophages (namely, *hisB*, *hisC*, and *hisD*). This could be due to the fact that the first half of the histidine biosynthesis pathway (composed of *hisZ*, *hisG*, *hisE*, *hisI*, *hisA*, *hisH*, and *hisF*) is also responsible for the production of 5′-phosphoribosyl-4-carboxamide-5-aminoimidazole (AICAR) that contributes to purine biosynthesis. The first half of the histidine biosynthesis pathway and the purine biosynthesis pathway are both impacted when colonies are replated (Table 2). Therefore, Tn-seq suggests that genes responsible for the synthesis of histidine, at least from imidazole-glycerol-3-phosphate, are required for the proliferation of *B. abortus* in the endoplasmic reticulum of RAW 264.7 macrophages. The *ilvC* and *ilvD* genes, coding for enzymes involved in the biosynthesis of isoleucine and valine, are also scored as required for growth in RAW 264.7 macrophages. It is also noticeable that the glutamate racemase (MurI) is required for growth in these macrophages. This enzyme converts L-Glu to D-Glu, presumably to allow the synthesis of PG. The late attenuation of these *murI* mutants is consistent with a late growth of *B. abortus* in RAW 264.7 macrophages (5). Another major hit is the biosynthesis of pyrimidines. Indeed, Tn-seq showed that all nonessential pyr biosynthesis genes (i.e., *pyrB*, *pyrC*, *pyrD*, *pyrE*, and *pyrF*) were consistently attenuated at 24 h p.i. in RAW 264.7 macrophages, while none of the associated mutants displayed growth defects on rich medium. Interestingly, none of the *pyr* genes were impacted when replated in comparison to most genes involved in purine biosynthesis (i.e., *purB*, *purC*, *purD*, *purH*, *purN*, *purM*, and two *purL* homologs). This is likely due to the composition of the culture medium and the heat resistance of purines and pyrimidines during medium sterilization. The *hisD*, *hisF*, *pyrB*, *pyrC*, and *pyrD* genes were already hit in previous screenings for attenuated mutants (12, 56), but the *pyr* mutants have not been complemented and the pyrimidines biosynthesis pathway has never been investigated in *B. abortus*. Here we show that all the mutants in genes of the pyr pathway are attenuated for growth inside macrophages, hence validating the Tn-seq data. It should be noted that a second homolog was found for *pyrC* (BAB1_0688); however, a *B. abortus* ΔBAB1_0688 strain displays a growth defect in rich medium (Fig. S7) and attenuation at 5 h p.i. in Tn-seq (Table 1), suggesting pleiotropic defects in this mutant in comparison to the *pyr* mutants characterized in this work. Altogether, these results strongly suggest that the ability of *B. abortus* to synthesize pyrimidines in the host cell is decisive for its proliferation inside macrophages. It would be interesting to investigate the survival, trafficking, and proliferation of *pyr* mutants in different cell types as well as in other infection models. If the inability of the *pyrB* mutant to proliferate inside several intracellular niches is confirmed, this mutant might be a good candidate to start vaccinal tests.

Tn-seq data also generate unexpected observations, such as the attenuation of the *lnt* mutants at 2 h p.i., while *lnt* is not required for growth on rich medium, suggesting that a redundant function is present for growth on plates but not for short-term survival in RAW 264.7 macrophages. Alternatively, it is also possible that the activity of Lnt is dispensable in *B. abortus*, at least under the control condition. It is noticeable that *lnt*

is also dispensable for growth in *Francisella tularensis* (57), suggesting that the dispensability of Lnt is widespread. Interestingly, our screening also revealed a role for a TamAB (BAB1_0045 and BAB1_0046) system homolog for intracellular proliferation, TamAB being proposed to be involved in the translocation of outer membrane proteins (58). These data thus open new investigation pathways to better understand the molecular processes required for *B. abortus* survival and growth inside host macrophages.

In conclusion, Tn-seq is a comprehensive method that allowed the identification of attenuated *B. abortus* mutants for macrophage infection. The high coverage of the genome with transposons has allowed the identification of essential, attenuated, and nonessential genes, as well as genes or operons required for full growth on rich medium. It would be interesting to perform such experiments on other *Brucella* strains as well as other host cell types (including activated macrophages and trophoblasts [59]) and using more complex infection models such as animal models, e.g., a mouse intranasal infection model (60). This would generate a fundamental knowledge of the molecular arsenal required for *Brucella* survival and growth in the course of infections.

MATERIALS AND METHODS

Bacterial strains and media. The wild-type strain *Brucella abortus* 2308 Nal^r was cultivated in 2YT (1% yeast extract, 1.6% peptone, 0.5% NaCl). The conjugative *Escherichia coli* S17-1 strain was cultivated in rich medium (Luria-Bertani broth). When required, antibiotics were used at the following concentrations: ampicillin, 100 μg ml^{-1}; kanamycin, 50 μg ml^{-1} for *E. coli* and 10 μg ml^{-1} for *B. abortus*; nalidixic acid, 25 μg ml^{-1}.

RAW 264.7 macrophage culture. Macrophages were cultivated in Dulbecco modified Eagle medium (DMEM) (Invitrogen) supplemented with 10% fetal bovine serum (Gibco), 4.5 g liter^{-1} glucose, 1.5 g liter^{-1} $NaHCO_3$, and 4 mM glutamine at 37°C with 5% CO_2.

Mini-Tn*5* Kan^r plasmid construction. The pXMCS-2 mini-Tn*5* Genta^R plasmid (61) was manipulated to exchange the gentamicin resistance cassette (Genta^R) with a Kan^r gene, using a dual joining PCR strategy. The region upstream of the Genta^R cassette was amplified by PCR from the pXMCS-2 mini-Tn*5* Genta^R plasmid using primers Tn-Kan part 1 F and Tn-Kan part 1 R and fused by overlapping PCR to the Kan^r coding sequence, amplified from the pNPTS138 plasmid using primers Tn-Kan part 2 F and Tn-Kan part 2 R. This DNA fragment was then fused to the region downstream of the Genta^R cassette amplified by PCR using primers Tn-Kan part 3 F and Tn-Kan part 3 R from the pXMCS-2 mini-Tn*5* Genta^R plasmid. In parallel, the pXMCS-2 mini-Tn*5* Genta^R plasmid was restricted using EcoRI and NdeI to excise the Genta^R fragment. The DNA fragment bearing the new Kan^r cassette was digested with EcoRI, and NdeI was then ligated in the previously restricted pXMCS-2 mini-Tn*5* Genta^R plasmid. Primers used for this construct are listed in Table S2 in the supplemental material.

Mutant library generation. One milliliter of an overnight culture of *B. abortus* 2308 was mixed with 50 μl of an overnight culture of the conjugative *E. coli* S17-1 strain carrying the pXMCS-2 mini-Tn*5* Kan^r plasmid. This plasmid possesses a hyperactive Tn*5* transposase allowing the straightforward generation of a high number of transposon mutants. The resulting *B. abortus* transposon mutants were selected on 2YT plates (2% agar) supplemented with both kanamycin and nalidixic acid. Tn*5* mutagenesis generates insertion of the transposon in only one locus per genome, as demonstrated previously for *Brucella* (14). Each Tn*5* derivative contains a *C. crescentus xyl* promoter that is constitutively active in *B. abortus*, since when it is fused to yellow fluorescent protein (YFP) coding sequence on a pBBR1-derived plasmid, it generates a fluorescent signal of uniform intensity similar to the *E. coli lac* promoter fused to YFP coding sequence.

RAW 264.7 macrophage infection using the transposon mutant library. Transposon mutants were pooled using 2YT medium, diluted in RAW 264.7 macrophage culture medium to reach a multiplicity of infection (MOI) of 50, and added to the macrophages, which were previously seeded in 6-well plates to a concentration of 1.5×10^5 cells per ml. A total of 16 6-well plates were planned per time point. Macrophages were then centrifuged for 10 min at 400 $\times$ *g* at 4°C and subsequently incubated for 1 h at 37°C with 5% CO_2. The culture medium was then removed and replaced with fresh medium containing gentamicin at 50 μg ml^{-1} in order to kill extracellular bacteria, and macrophages were then further incubated for 1, 4, and 23 h at 37°C with 5% CO_2. For each time postinfection (2 h, 5 h, or 24 h), culture medium was removed, each well was washed twice with phosphate-buffered saline (PBS), and macrophages were lysed using PBS–0.1% Triton X-100 for 10 min at 37°C. Macrophage lysates were then plated on 100 2YT plates per time point, each supplemented with kanamycin and incubated at 37°C for 4 days in order to obtain colonies that were collected for genomic DNA (gDNA) preparation and sequencing of Tn*5*-gDNA junctions.

RAW 264.7 macrophage infection and CFU counting. The infection protocol for performing CFU counting is identical to the one described above, with the exception of the inoculum, which originates from an overnight liquid culture. After infection, infected macrophages are lysed, and the resulting extracts are cultivated on 2YT plates supplemented with kanamycin. Once grown, colonies were counted to calculate the number of colonies per ml of lysate.

Analysis of essential genes for growth on plates. In order to assess the overall transposon insertion across the *B. abortus* genome, we have created a parameter called R200, defined by the

TABLE 3 Externally hosted supplemental data

Supplemental data no.	Name	Description	Link
SD1	TTM_ctrl_chrI.txt	Transposon tolerance map (R200) for chromosome I when grown on rich medium	https://figshare.com/s/bd0d4fa73ad8cf7737fe
SD2	TTM_ctrl_chrII.txt	Transposon tolerance map (R200) for chromosome II when grow on rich medium	https://figshare.com/s/3219dfa7ac60d1cda34f
SD3	Delta-R200_2hPI_chrI.txt	Attenuation profile at 2 h p.i. for chromosome I	https://figshare.com/s/77195e0a2cc1a1933b7f
SD4	Delta-R200_2hPI_chrII.txt	Attenuation profile at 2 h p.i. for chromosome II	https://figshare.com/s/2475d4b00e6a58226e40
SD5	Delta-R200_5hPI_chrI.txt	Attenuation profile at 5 h p.i. for chromosome I	https://figshare.com/s/93ce83ccea559a0de2f7
SD6	Delta-R200_5hPI_chrII.txt	Attenuation profile at 5 h p.i. for chromosome II	https://figshare.com/s/6f604b5eba5934c392f1
SD7	Delta-R200_24hPI_chrI.txt	Attenuation profile at 24 h p.i. for chromosome I	https://figshare.com/s/ea7871157f284d31eaed
SD8	Delta-R200_24hPI_chrII.txt	Attenuation profile at 24 h p.i. for chromosome II	https://figshare.com/s/958e728387a31b8ce139
SD9	TTM_replated_ctrl_chrI.txt	Transposon tolerance map (R200) for chromosome I when grown on rich medium (prior to replating)	https://figshare.com/s/519aecf6ea1bea563510
SD10	TTM_replated_ctrl_chrII.txt	Transposon tolerance map (R200) for chromosome II when grown on rich medium (prior to replating)	https://figshare.com/s/266012d35d5780c5a1b3
SD11	TTM_replated_chrI.txt	Transposon tolerance map (R200) for chromosome I when replated on rich medium	https://figshare.com/s/9282c05218ec976c4286
SD12	TTM_replated_chrII.txt	Transposon tolerance map (R200) for chromosome II when replated on rich medium	https://figshare.com/s/c5318e37bf294ff0cdde
SD13	DD-R200_24-5hPI_chrI.txt	Attenuation at 24 h p.i. compared to 5 h p.i. for chromosome I	https://figshare.com/s/44d2126e6c24ca1214d1
SD14	DD-R200_24-5hPI_chrII.txt	Attenuation at 24 h p.i. compared to 5 h p.i. for chromosome II	https://figshare.com/s/c6a0d65386f6edb2202b
SD15	ChrI.gb	Annotated chromosome I of *B. abortus* 2308	https://figshare.com/s/ae37affea7e62601b553
SD16	ChrII.gb	Annotated chromosome II of *B. abortus* 2308	https://figshare.com/s/ddee5b11fe553d1a2052

$\log_{10}$(number of Tn*5* insertions + 1) for a 200-bp sliding window. This sliding window was shifted every 5 bp to generate a collection of R200 values spanning the whole genome for the control condition, i.e., bacteria on plates. Given that the *B. abortus* genome is 3,278,307 bp, a list of 655,662 R200 values was created, with an average value of 9,481 transposon insertions mapped per window. As previously published (15), the probability of obtaining a window of a given size with no transposon insertion event can be estimated by the following formula: $P = [1 - (w/g)]^n$, where w is the window size, g is the genome size, and n is the number of independent Tn*5* insertion events. In our case, the resulting probability was 3.8×10^{-15}, with $g = 3{,}278{,}307$, $w = 200$, and $n = 544{,}094$. It should be noted that this value accounts only for a single window, whereas essential genes are typically characterized by a series of overlapping empty windows rather than a single 200-bp window, thus further lowering the probability of finding such profiles fortuitously. Essential genes were defined as all genes having at least one R200 value equal to 0. Defined essential genes usually have many R200 values equal to 0, as indicated in supplemental data (SD) sets 1 to 14. The TTMs can be aligned with the annotated GenBank files for chromosomes I and II (SD15 and SD16) of *B. abortus* 2308 using Artemis (Sanger Institute [http://www.sanger.ac.uk/science/tools/artemis]). A list of the externally hosted supplemental data sets is shown in Table 3.

Statistical analysis is described in Fig. S2. Briefly, a main frequency peak centered on an R200 value of 4.05 was used to predict a theoretical distribution of R200 values from which thresholds corresponding to 2 (−2S), 4 (−4S), and 6 (−6S) standard deviations (S) for the average of the theoretical distribution were computed.

Analysis of the effect of replating on rich medium was tested in an independent Tn-seq analysis in which a new mutant library was constructed with the same mini-Tn*5* derivative as described above. All colonies were collected, and the resulting suspension was used, on the one hand, for control analysis (data in TTM_replated_ctrl_chrI and TTM_replated_ctrl_chrII) and, on the other hand, for replating on the same rich medium. Colonies generated after replating were collected and analyzed by Tn-seq as described above (data in TTM_replated_chrI and TTM_replated_chrII).

Attenuation in infection analysis. For each postinfection sample (2 h, 5 h, and 24 h p.i.), a list of R200 values was calculated as for the control condition. Then, each R200 value from the control sample list was subtracted from each R200 value from the postinfection sample list separately, generating three Delta-R200 data sets, SD3 to SD8. Therefore, regions with a neutral Delta-R200 value have no impact during infection when mutated, while regions with a negative Delta-R200 value are attenuated during infection, and regions with a positive Delta-R200 value depict hyperinvasiveness for the corresponding mutants. For each time postinfection, the frequency distribution of Delta-R200 values was computed to define a normal distribution with an average and a standard deviation covering the main peak of this distribution. The threshold for negative Delta-R200 values was set at -0.75 $\log_{10}$ for the "2 h p.i. R200 − control R200" and "5 h p.i. R200 − control R200" Delta-R200 analyses, selecting, respectively, 5.5% and 6.7% of windows from the total genome. The threshold for negative Delta-R200 values was set at -1 $\log_{10}$ for the "24 h p.i. R200 − control R200" Delta-R200 analysis, allowing selection of 10.3% of the windows. The threshold for positive Delta-R200 values for the "2 h p.i. R200 − control R200" condition was set at $+0.6$ $\log_{10}$, selecting 1.1%

of the windows. The genes covered by selected windows were considered required for the infection, with usually most of their coding sequences covered.

Generation of the *B. abortus* targeted mutants. Unless stated otherwise, all *B. abortus* mutants were generated by insertion of a plasmid in the targeted gene, according to a previously published procedure (62). The primer sequences used to generate PCR products cloned in the disruption plasmids are available in Table S2.

All deletion strains were constructed using a previously described allelic exchange strategy (5). The primers used to amplify upstream and downstream regions of the target genes required for homologous recombination are also available in Table S2.

Growth curves. Growth was monitored in 2YT medium at 37°C for 72 h by measuring the optical density at 600 nm using a permanently shaking plate reader (Epoch2 microplate spectrophotometer; Biotek).

SUPPLEMENTAL MATERIAL

Supplemental material for this article may be found at https://doi.org/10.1128/IAI.00312-18.

SUPPLEMENTAL FILE 1, PDF file, 0.9 MB.

ACKNOWLEDGMENTS

We thank M. Waroquier for his flawless technical support, F. Tilquin for lab management, and F. Renzi, J.-Y. Matroule, and R. Hallez for stimulating and helpful discussions.

This research was supported by funds from the Interuniversity Attraction Poles Programme initiated by the Belgian Science Policy Office (https://www.belspo.be/) to J.-J. Letesson, by grants from Fonds de la Recherche Scientifique-Fonds National de la Recherche Scientifique (FRS-FNRS [http://www.fnrs.be]) (PDR T.0053.13, PDR Brucell-cycle T.0060.15, and CDR J.0091.14) to X. De Bolle, and by grant 31003A_166476 from the Swiss National Science Foundation to B. Christen. We thank UNamur (https://www.unamur.be/) for financial and logistic support. N. Francis held an Aspirant fellowship from FRS-FNRS. J.-F. Sternon, P. Godessart, M. Van der Henst, and K. Poncin are supported by a Ph.D. grant from FRIA (FRS-FNRS).

The funders had no role in study design, data collection, and interpretation or the decision to submit the work for publication.

J.-F.S., P.G., R.G.D.F., M.V.D.H., K.P., N.F., and K.W. performed the experiments, J.-F.S., P.G., M.C., B.C., J.-J.L., and X.D.B. designed the study, and J.-F.S. and X.D.B. wrote the manuscript.

REFERENCES

1. Moreno E, Moriyon I. 2006. The genus *Brucella*. Prokaryotes 5:315–456.
2. De Bolle X, Crosson S, Matroule JY, Letesson JJ. 2015. *Brucella abortus* cell cycle and infection are coordinated. Trends Microbiol 23:812–821. https://doi.org/10.1016/j.tim.2015.09.007.
3. Brown PJ, de Pedro MA, Kysela DT, Van der Henst C, Kim J, De Bolle X, Fuqua C, Brun YV. 2012. Polar growth in the Alphaproteobacterial order Rhizobiales. Proc Natl Acad Sci U S A 109:1697–1701. https://doi.org/10.1073/pnas.1114476109.
4. Michaux-Charachon S, Bourg G, Jumas-Bilak E, Guigue-Talet P, Allardet-Servent A, O'Callaghan D, Ramuz M. 1997. Genome structure and phylogeny in the genus *Brucella*. J Bacteriol 179:3244–3249. https://doi.org/10.1128/jb.179.10.3244-3249.1997.
5. Deghelt M, Mullier C, Sternon JF, Francis N, Laloux G, Dotreppe D, Van der Henst C, Jacobs-Wagner C, Letesson JJ, De Bolle X. 2014. G1-arrested newborn cells are the predominant infectious form of the pathogen *Brucella abortus*. Nat Commun 5:4366. https://doi.org/10.1038/ncomms5366.
6. Pinto UM, Pappas KM, Winans SC. 2012. The ABCs of plasmid replication and segregation. Nat Rev Microbiol 10:755–765. https://doi.org/10.1038/nrmicro2882.
7. Celli J. 2015. The changing nature of the *Brucella*-containing vacuole. Cell Microbiol 17:951–958. https://doi.org/10.1111/cmi.12452.
8. Detilleux PG, Deyoe BL, Cheville NF. 1990. Entry and intracellular localization of *Brucella* spp. in Vero cells: fluorescence and electron microscopy. Vet Pathol 27:317–328. https://doi.org/10.1177/030098589002700503.
9. Sedzicki J, Tschon T, Low SH, Willemart K, Goldie KN, Letesson JJ, Stahlberg H, Dehio C. 2018. 3D correlative electron microscopy reveals continuity of *Brucella*-containing vacuoles with the endoplasmic reticulum. J Cell Sci 131:jcs210799. https://doi.org/10.1242/jcs.210799.
10. Comerci DJ, Martinez-Lorenzo MJ, Sieira R, Gorvel JP, Ugalde RA. 2001. Essential role of the VirB machinery in the maturation of the *Brucella abortus*-containing vacuole. Cell Microbiol 3:159–168. https://doi.org/10.1046/j.1462-5822.2001.00102.x.
11. O'Callaghan D, Cazevieille C, Allardet-Servent A, Boschiroli ML, Bourg G, Foulongne V, Frutos P, Kulakov Y, Ramuz M. 1999. A homologue of the *Agrobacterium tumefaciens* VirB and *Bordetella pertussis* Ptl type IV secretion systems is essential for intracellular survival of *Brucella suis*. Mol Microbiol 33:1210–1220. https://doi.org/10.1046/j.1365-2958.1999.01569.x.
12. Kohler S, Foulongne V, Ouahrani-Bettache S, Bourg G, Teyssier J, Ramuz M, Liautard JP. 2002. The analysis of the intramacrophagic virulome of *Brucella suis* deciphers the environment encountered by the pathogen inside the macrophage host cell. Proc Natl Acad Sci U S A 99:15711–15716. https://doi.org/10.1073/pnas.232454299.
13. Abdo MR, Joseph P, Mortier J, Turtaut F, Montero JL, Masereel B, Kohler S, Winum JY. 2011. Anti-virulence strategy against *Brucella suis*: synthesis, biological evaluation and molecular modeling of selective histidinol dehydrogenase inhibitors. Org Biomol Chem 9:3681–3690. https://doi.org/10.1039/c1ob05149k.
14. Lestrate P, Delrue RM, Danese I, Didembourg C, Taminiau B, Mertens P, De Bolle X, Tibor A, Tang CM, Letesson JJ. 2000. Identification and characterization of in vivo attenuated mutants of *Brucella melitensis*. Mol Microbiol 38:543–551. https://doi.org/10.1046/j.1365-2958.2000.02150.x.
15. Christen B, Abeliuk E, Collier JM, Kalogeraki VS, Passarelli B, Coller JA,

Fero MJ, McAdams HH, Shapiro L. 2011. The essential genome of a bacterium. Mol Syst Biol 7:528. https://doi.org/10.1038/msb.2011.58.
16. Hallez R, Mignolet J, Van Mullem V, Wery M, Vandenhaute J, Letesson JJ, Jacobs-Wagner C, De Bolle X. 2007. The asymmetric distribution of the essential histidine kinase PdhS indicates a differentiation event in *Brucella abortus*. EMBO J 26:1444–1455. https://doi.org/10.1038/sj.emboj.7601577.
17. Laloux G, Deghelt M, de Barsy M, Letesson JJ, De Bolle X. 2010. Identification of the essential *Brucella melitensis* porin Omp2b as a suppressor of Bax-induced cell death in yeast in a genome-wide screening. PLoS One 5:e13274. https://doi.org/10.1371/journal.pone.0013274.
18. Robertson GT, Reisenauer A, Wright R, Jensen RB, Jensen A, Shapiro L, Roop RM, II. 2000. The *Brucella abortus* CcrM DNA methyltransferase is essential for viability, and its overexpression attenuates intracellular replication in murine macrophages. J Bacteriol 182:3482–3489. https://doi.org/10.1128/JB.182.12.3482-3489.2000.
19. Van der Henst C, Beaufay F, Mignolet J, Didembourg C, Colinet J, Hallet B, Letesson JJ, De Bolle X. 2012. The histidine kinase PdhS controls cell cycle progression of the pathogenic alphaproteobacterium *Brucella abortus*. J Bacteriol 194:5305–5314. https://doi.org/10.1128/JB.00699-12.
20. Willett JW, Herrou J, Briegel A, Rotskoff G, Crosson S. 2015. Structural asymmetry in a conserved signaling system that regulates division, replication, and virulence of an intracellular pathogen. Proc Natl Acad Sci U S A 112:E3709–E3718. https://doi.org/10.1073/pnas.1503118112.
21. Curtis PD, Brun YV. 2014. Identification of essential alphaproteobacterial genes reveals operational variability in conserved developmental and cell cycle systems. Mol Microbiol 93:713–735. https://doi.org/10.1111/mmi.12686.
22. Paulsen IT, Seshadri R, Nelson KE, Eisen JA, Heidelberg JF, Read TD, Dodson RJ, Umayam L, Brinkac LM, Beanan MJ, Daugherty SC, Deboy RT, Durkin AS, Kolonay JF, Madupu R, Nelson WC, Ayodeji B, Kraul M, Shetty J, Malek J, Van Aken SE, Riedmuller S, Tettelin H, Gill SR, White O, Salzberg SL, Hoover DL, Lindler LE, Halling SM, Boyle SM, Fraser CM. 2002. The *Brucella suis* genome reveals fundamental similarities between animal and plant pathogens and symbionts. Proc Natl Acad Sci U S A 99:13148–13153. https://doi.org/10.1073/pnas.192319099.
23. Aakre CD, Phung TN, Huang D, Laub MT. 2013. A bacterial toxin inhibits DNA replication elongation through a direct interaction with the beta sliding clamp. Mol Cell 52:617–628. https://doi.org/10.1016/j.molcel.2013.10.014.
24. Fontana C, Conde-Alvarez R, Stahle J, Holst O, Iriarte M, Zhao Y, Arce-Gorvel V, Hanniffy S, Gorvel JP, Moriyon I, Widmalm G. 2016. Structural studies of lipopolysaccharide defective mutants from *Brucella melitensis* identify a core oligosaccharide critical in virulence. J Biol Chem 291:7727–7741. https://doi.org/10.1074/jbc.M115.701540.
25. Brilli M, Fondi M, Fani R, Mengoni A, Ferri L, Bazzicalupo M, Biondi EG. 2010. The diversity and evolution of cell cycle regulation in alpha-proteobacteria: a comparative genomic analysis. BMC Syst Biol 4:52. https://doi.org/10.1186/1752-0509-4-52.
26. Delrue RM, Martinez-Lorenzo M, Lestrate P, Danese I, Bielarz V, Mertens P, De Bolle X, Tibor A, Gorvel JP, Letesson JJ. 2001. Identification of *Brucella* spp. genes involved in intracellular trafficking. Cell Microbiol 3:487–497. https://doi.org/10.1046/j.1462-5822.2001.00131.x.
27. Arocena GM, Sieira R, Comerci DJ, Ugalde RA. 2010. Identification of the quorum-sensing target DNA sequence and *N*-acyl homoserine lactone responsiveness of the *Brucella abortus virB* promoter. J Bacteriol 192:3434–3440. https://doi.org/10.1128/JB.00232-10.
28. Delrue RM, Deschamps C, Leonard S, Nijskens C, Danese I, Schaus JM, Bonnot S, Ferooz J, Tibor A, De Bolle X, Letesson JJ. 2005. A quorum-sensing regulator controls expression of both the type IV secretion system and the flagellar apparatus of *Brucella melitensis*. Cell Microbiol 7:1151–1161. https://doi.org/10.1111/j.1462-5822.2005.00543.x.
29. Detilleux PG, Deyoe BL, Cheville NF. 1990. Penetration and intracellular growth of *Brucella abortus* in nonphagocytic cells in vitro. Infect Immun 58:2320–2328.
30. Porte F, Naroeni A, Ouahrani-Bettache S, Liautard JP. 2003. Role of the *Brucella suis* lipopolysaccharide O antigen in phagosomal genesis and in inhibition of phagosome-lysosome fusion in murine macrophages. Infect Immun 71:1481–1490. https://doi.org/10.1128/IAI.71.3.1481-1490.2003.
31. Sheehan LM, Budnick JA, Blanchard C, Dunman PM, Caswell CC. 2015. A LysR-family transcriptional regulator required for virulence in *Brucella abortus* is highly conserved among the alpha-proteobacteria. Mol Microbiol 98:318–328. https://doi.org/10.1111/mmi.13123.
32. Endley S, McMurray D, Ficht TA. 2001. Interruption of the *cydB* locus in *Brucella abortus* attenuates intracellular survival and virulence in the mouse model of infection. J Bacteriol 183:2454–2462. https://doi.org/10.1128/JB.183.8.2454-2462.2001.
33. Cha SB, Rayamajhi N, Lee WJ, Shin MK, Jung MH, Shin SW, Kim JW, Yoo HS. 2012. Generation and envelope protein analysis of internalization defective *Brucella abortus* mutants in professional phagocytes, RAW 2647. FEMS Immunol Med Microbiol 64:244–254. https://doi.org/10.1111/j.1574-695X.2011.00896.x.
34. Delrue RM, Lestrate P, Tibor A, Letesson JJ, De Bolle X. 2004. *Brucella* pathogenesis, genes identified from random large-scale screens. FEMS Microbiol Lett 231:1–12. https://doi.org/10.1016/S0378-1097(03)00963-7.
35. Kim DH, Lim JJ, Lee JJ, Kim DG, Lee HJ, Min W, Kim KD, Chang HH, Rhee MH, Watarai M, Kim S. 2012. Identification of genes contributing to the intracellular replication of *Brucella abortus* within HeLa and RAW 264.7 cells. Vet Microbiol 158:322–328. https://doi.org/10.1016/j.vetmic.2012.02.019.
36. Liautard J, Ouahrani-Bettache S, Jubier-Maurin V, Lafont V, Kohler S, Liautard JP. 2007. Identification and isolation of *Brucella suis* virulence genes involved in resistance to the human innate immune system. Infect Immun 75:5167–5174. https://doi.org/10.1128/IAI.00690-07.
37. Wu Q, Pei J, Turse C, Ficht TA. 2006. Mariner mutagenesis of *Brucella melitensis* reveals genes with previously uncharacterized roles in virulence and survival. BMC Microbiol 6:102. https://doi.org/10.1186/1471-2180-6-102.
38. Sklar JG, Wu T, Gronenberg LS, Malinverni JC, Kahne D, Silhavy TJ. 2007. Lipoprotein SmpA is a component of the YaeT complex that assembles outer membrane proteins in *Escherichia coli*. Proc Natl Acad Sci U S A 104:6400–6405. https://doi.org/10.1073/pnas.0701579104.
39. Gora KG, Tsokos CG, Chen YE, Srinivasan BS, Perchuk BS, Laub MT. 2010. A cell-type-specific protein-protein interaction modulates transcriptional activity of a master regulator in *Caulobacter crescentus*. Mol Cell 39:455–467. https://doi.org/10.1016/j.molcel.2010.06.024.
40. Iniesta AA, McGrath PT, Reisenauer A, McAdams HH, Shapiro L. 2006. A phospho-signaling pathway controls the localization and activity of a protease complex critical for bacterial cell cycle progression. Proc Natl Acad Sci U S A 103:10935–10940. https://doi.org/10.1073/pnas.0604554103.
41. Holtzendorff J, Hung D, Brende P, Reisenauer A, Viollier PH, McAdams HH, Shapiro L. 2004. Oscillating global regulators control the genetic circuit driving a bacterial cell cycle. Science 304:983–987. https://doi.org/10.1126/science.1095191.
42. Wright R, Stephens C, Shapiro L. 1997. The CcrM DNA methyltransferase is widespread in the alpha subdivision of proteobacteria, and its essential functions are conserved in *Rhizobium meliloti* and *Caulobacter crescentus*. J Bacteriol 179:5869–5877. https://doi.org/10.1128/jb.179.18.5869-5877.1997.
43. Murray SM, Panis G, Fumeaux C, Viollier PH, Howard M. 2013. Computational and genetic reduction of a cell cycle to its simplest, primordial components. PLoS Biol 11:e1001749. https://doi.org/10.1371/journal.pbio.1001749.
44. Caswell CC, Elhassanny AE, Planchin EE, Roux CM, Weeks-Gorospe JN, Ficht TA, Dunman PM, Roop RM, II. 2013. Diverse genetic regulon of the virulence-associated transcriptional regulator MucR in *Brucella abortus* 2308. Infect Immun 81:1040–1051. https://doi.org/10.1128/IAI.01097-12.
45. Godfroid F, Cloeckaert A, Taminiau B, Danese I, Tibor A, de Bolle X, Mertens P, Letesson JJ. 2000. Genetic organisation of the lipopolysaccharide O-antigen biosynthesis region of *Brucella melitensis* 16M (*wbk*). Res Microbiol 151:655–668. https://doi.org/10.1016/S0923-2508(00)90130-X.
46. Martin DW, Baumgartner JE, Gee JM, Anderson ES, Roop RM, II. 2012. SodA is a major metabolic antioxidant in *Brucella abortus* 2308 that plays a significant, but limited, role in the virulence of this strain in the mouse model. Microbiology 158:1767–1774. https://doi.org/10.1099/mic.0.059584-0.
47. Mignolet J, Van der Henst C, Nicolas C, Deghelt M, Dotreppe D, Letesson JJ, De Bolle X. 2010. PdhS, an old-pole-localized histidine kinase, recruits the fumarase FumC in *Brucella abortus*. J Bacteriol 192:3235–3239. https://doi.org/10.1128/JB.00066-10.
48. Mirabella A, Terwagne M, Zygmunt MS, Cloeckaert A, De Bolle X, Letesson JJ. 2013. *Brucella melitensis* MucR, an orthologue of *Sinorhizobium meliloti* MucR, is involved in resistance to oxidative, detergent, and saline stresses and cell envelope modifications. J Bacteriol 195:453–465. https://doi.org/10.1128/JB.01336-12.
49. Ugalde JE, Czibener C, Feldman MF, Ugalde RA. 2000. Identification and characterization of the *Brucella abortus* phosphoglucomutase gene: role of lipopolysaccharide in virulence and intracellular multiplication. Infect Immun 68:5716–5723. https://doi.org/10.1128/IAI.68.10.5716-5723.2000.

50. Bukata L, Altabe S, de Mendoza D, Ugalde RA, Comerci DJ. 2008. Phosphatidylethanolamine synthesis is required for optimal virulence of *Brucella abortus*. J Bacteriol 190:8197–8203. https://doi.org/10.1128/JB.01069-08.
51. Hubbard TP, Chao MC, Abel S, Blondel CJ, Abel Zur Wiesch P, Zhou X, Davis BM, Waldor MK. 2016. Genetic analysis of *Vibrio parahaemolyticus* intestinal colonization. Proc Natl Acad Sci U S A 113:6283–6288. https://doi.org/10.1073/pnas.1601718113.
52. Ke Y, Wang Y, Li W, Chen Z. 2015. Type IV secretion system of *Brucella* spp. and its effectors. Front Cell Infect Microbiol 5:72. https://doi.org/10.3389/fcimb.2015.00072.
53. Nijskens C, Copin R, De Bolle X, Letesson JJ. 2008. Intracellular rescuing of a *B. melitensis* 16M *virB* mutant by co-infection with a wild type strain. Microb Pathog 45:134–141. https://doi.org/10.1016/j.micpath.2008.04.005.
54. Xavier MN, Winter MG, Spees AM, den Hartigh AB, Nguyen K, Roux CM, Silva TM, Atluri VL, Kerrinnes T, Keestra AM, Monack DM, Luciw PA, Eigenheer RA, Baumler AJ, Santos RL, Tsolis RM. 2013. PPARgamma-mediated increase in glucose availability sustains chronic *Brucella abortus* infection in alternatively activated macrophages. Cell Host Microbe 14:159–170. https://doi.org/10.1016/j.chom.2013.07.009.
55. Joseph P, Abdo MR, Boigegrain RA, Montero JL, Winum JY, Kohler S. 2007. Targeting of the *Brucella suis* virulence factor histidinol dehydrogenase by histidinol analogues results in inhibition of intramacrophagic multiplication of the pathogen. Antimicrob Agents Chemother 51:3752–3755. https://doi.org/10.1128/AAC.00572-07.
56. Kim S, Watarai M, Kondo Y, Erdenebaatar J, Makino S, Shirahata T. 2003. Isolation and characterization of mini-Tn*5*Km2 insertion mutants of *Brucella abortus* deficient in internalization and intracellular growth in HeLa cells. Infect Immun 71:3020–3027. https://doi.org/10.1128/IAI.71.6.3020-3027.2003.
57. LoVullo ED, Wright LF, Isabella V, Huntley JF, Pavelka MS, Jr. 2015. Revisiting the Gram-negative lipoprotein paradigm. J Bacteriol 197:1705–1715. https://doi.org/10.1128/JB.02414-14.
58. Selkrig J, Mosbahi K, Webb CT, Belousoff MJ, Perry AJ, Wells TJ, Morris F, Leyton DL, Totsika M, Phan MD, Celik N, Kelly M, Oates C, Hartland EL, Robins-Browne RM, Ramarathinam SH, Purcell AW, Schembri MA, Strugnell RA, Henderson IR, Walker D, Lithgow T. 2012. Discovery of an archetypal protein transport system in bacterial outer membranes. Nat Struct Mol Biol 19:506–510. https://doi.org/10.1038/nsmb.2261.
59. Salcedo SP, Chevrier N, Lacerda TL, Ben Amara A, Gerart S, Gorvel VA, de Chastellier C, Blasco JM, Mege JL, Gorvel JP. 2013. Pathogenic brucellae replicate in human trophoblasts. J Infect Dis 207:1075–1083. https://doi.org/10.1093/infdis/jit007.
60. Hanot Mambres D, Machelart A, Potemberg G, De Trez C, Ryffel B, Letesson JJ, Muraille E. 2016. Identification of immune effectors essential to the control of primary and secondary intranasal infection with *Brucella melitensis* in mice. J Immunol 196:3780–3793. https://doi.org/10.4049/jimmunol.1502265.
61. Christen M, Beusch C, Bosch Y, Cerletti D, Flores-Tinoco CE, Del Medico L, Tschan F, Christen B. 2016. Quantitative selection analysis of bacteriophage phiCbK susceptibility in *Caulobacter crescentus*. J Mol Biol 428:419–430. https://doi.org/10.1016/j.jmb.2015.11.018.
62. Haine V, Sinon A, Van Steen F, Rousseau S, Dozot M, Lestrate P, Lambert C, Letesson JJ, De Bolle X. 2005. Systematic targeted mutagenesis of *Brucella melitensis* 16M reveals a major role for GntR regulators in the control of virulence. Infect Immun 73:5578–5586. https://doi.org/10.1128/IAI.73.9.5578-5586.2005.
63. Anderson ES, Paulley JT, Gaines JM, Valderas MW, Martin DW, Menscher E, Brown TD, Burns CS, Roop RM, II. 2009. The manganese transporter MntH is a critical virulence determinant for *Brucella abortus* 2308 in experimentally infected mice. Infect Immun 77:3466–3474. https://doi.org/10.1128/IAI.00444-09.
64. Anderson ES, Paulley JT, Martinson DA, Gaines JM, Steele KH, Roop RM, II. 2011. The iron-responsive regulator Irr is required for wild-type expression of the gene encoding the heme transporter BhuA in *Brucella abortus* 2308. J Bacteriol 193:5359–5364. https://doi.org/10.1128/JB.00372-11.
65. Delory M, Hallez R, Letesson JJ, De Bolle X. 2006. An RpoH-like heat shock sigma factor is involved in stress response and virulence in *Brucella melitensis* 16M. J Bacteriol 188:7707–7710. https://doi.org/10.1128/JB.00644-06.
66. Gil-Ramirez Y, Conde-Alvarez R, Palacios-Chaves L, Zuniga-Ripa A, Grillo MJ, Arce-Gorvel V, Hanniffy S, Moriyon I, Iriarte M. 2014. The identification of wadB, a new glycosyltransferase gene, confirms the branched structure and the role in virulence of the lipopolysaccharide core of Brucella abortus. Microb Pathog 73:53–59. https://doi.org/10.1016/j.micpath.2014.06.002.
67. Himeno H, Kurita D, Muto A. 2014. tmRNA-mediated trans-translation as the major ribosome rescue system in a bacterial cell. Front Genet 5:66. https://doi.org/10.3389/fgene.2014.00066.